Enhancement of Charging Resource Utilization of Electric Vehicle Fast Charging Station with Heterogeneous EV Users

Konara Mudiyanselage Sandun Yasantha Konara

UiA University of Agder

Doctoral Dissertations at the University of Agder 416

Enhancement of Charging Resource Utilization of Electric Vehicle Fast Charging Station with Heterogeneous EV Users

Konara Mudiyanselage Sandun Yasantha Konara

Enhancement of Charging Resource Utilization of Electric Vehicle Fast Charging Station with Heterogeneous EV Users

Doctoral Dissertation for the Degree *Philosophiae Doctor (Ph.D.)*
at the Faculty of Engineering and Science, Specialisation in Renewable Energy Engineering

University of Agder
Faculty of Engineering and Science
2023

Doctoral Dissertations at the University of Agder 416
ISSN: 1504-9272
ISBN: 978-82-8427-131-6

Printed by Make!Graphics
Kristiansand

Dedicated to my beloved Amma and Appachchi (parents)

Mrs. Rathanayaka Mudiyanselage P.M. Rathanayaka
Mr. Konara Mudiyanselage Premarathna B. Konara

and my Ph.D. Supervisor

Prof. Mohan L. Kolhe

Preface

The dissertation is based on the research work done at the Department of Engineering Sciences, Faculty of Engineering and Science, University of Agder (UiA), in Grimstad, Norway from December 2018 to August 2022. Professor Mohan Lal Kolhe has been the principle supervisor and Associate Professor Nils Ulltveit-Moe has been the co-supervisor of this Ph.D work. This Ph.D. research work intends to develop, analyze and evaluate the performance of charging resource allocation and coordination strategies for an electric vehicle (EV) fast charging station (FCS). The uniqueness of this research work is that it enhances the utilization of limited charging resources at FCS with heterogeneous EV users while assuring a high-quality service to EV users. FCS allows opportunistic EV users to dynamically exploit unused limited charging resources at the FCS with proposed innovative charging resource allocation, admission control and charging coordination strategies. The research work presented in this dissertation has been funded by UiA.

Acknowledgments

I am very pleased to acknowledge the efforts of many people whose guidance, corporation, and support were vital to making my Ph.D carrier successful. Hereby, I take this opportunity to extend my heartfelt gratitude to my supervisors, resource persons, colleagues, friends and family who supported me during my Ph.D journey.

First and foremost, I need to express my heartfelt gratitude and a deep sense of appreciations to my principal supervisor, Professor Mohan Lal Kolhe for his incredible support, constant guidance and excellent supervision throughout my Ph.D journey. I strongly believe that I was very lucky to continue both of my Ph.D and M.Sc. research works under his supervision. Since the beginning of my M.Sc degree in Renewable Energy at the University of Agder, I have benefited enormously from his keen supervision, constant guidance, encouraging thoughts and great enthusiasm towards high-quality research. He was a great mentor for even my personal life during this long journey who looked after me with care and affection. I am really indebted to him for conceptualizing invaluable research ideas and revising my manuscripts with his broad knowledge and enormous research experience. Simply, I would not have gone so far, without his incredible support in all possible ways. It has been such an inspiration to work with him and more eagerly, I look forward to having more collaborations with him in the future.

Moreover, it is my great pleasure to gratefully acknowledge and express my sincere gratitude to my co-supervisor Associate Professor, Nils Ulltveit-Moe for his motivation and guidance in the successful completion of the research tasks. I must thankfully acknowledge him for sharing his insightful thoughts, comments and experience during my Ph.D works. I need to tribute my great sense of gratitude and a deep sense of appreciation to Dr. Indika Anuradha Mendis for sharing his broad knowledge and experience on stochastic modeling which contributes a lot for some of the work packages of my Ph.D research works. His insightful comments have significantly improved the quality of my work. It has been a great pleasure to collaborate with him during my Ph.D journey. Despite being a research collaborator, he has been such a nice friend who always took care of my well-being and supported in all possible ways during my stay in Norway.

I would like to extend my sincere thanks to Prof. Sunniva Whittaker, the Rector of UiA, Prof. Michael Rygaard Hansen, Dean of the Faculty of Engineering Science, Prof. Geir Grasmo and Prof. Paul Ragnar Svennevig, the former and current Head of the Department of Engineering Sciences and Prof. Henrik Kofoed Nielsen, Sectional Leader of Renewable Energy Engineering for their administrative support. Moreover, I whole-heatedly appreciate and would like to extend my sincere gratitude to Mrs. Emma Elisabeth Hornerman, Ph.D. Coordinator for her kind assistance and guidance in all administrative procedures. I wanted to especially acknowledge her kind cooperation throughout my Ph.D. journey in making all the practicalities run smoothly. I would like express my sincere thanks to all the resource persons who conduct and evaluate Ph.D courses by sharing their valuable knowledge at UiA and Aalborg University (AAU), Denmark. I must appreciate and tribute my gratitude to AAU, Denmark for providing the opportunity to participate in their PhD courses.

My deep sense of gratitude goes to Dr. Sarath Chandrasena, Dr. Rajitha Udawalpola, Dr. Udayanga Galappaththi, Dr. Chandana Perera, Dr. Keerthi Gunawickrame, Dr. Nisabha Jayasundere, Mr. Eranda Jayathunaga Senior Lecturers of University of Ruhuna, Sri Lanka for giving me the opportunity to study at UiA and their continuous support during my stay in Norway. I would like to extend my gratitude to Ms. Sunita M.L. Kolhe for her valuable advises, kind cooperation and delicious meals for me. My great sense of appreciations and gratitude need be extended to all my colleagues and friends I met in UiA, Grimstad especially including Arvind Sharma, Milad Golzar, Ahmed Salem, Basant Paudyal, Saba Alipour, Sissel Kristensesn, Nils Johannesen, Alex Ho and Antoine for their mutual support, amity and cooperation. In particular, I wish to thank Jagath Senanayake, Ranga Wijesekara, Wajira Senanayaka, Thilina Weerasinghe, Subhodha Ireshika, Pabasara Weeraman, Harsha Sandaruwan, Sasanka Ranasinghe, Madawa Jayathilake, Kalpanie Mendis for providing a sense of community, arranging gatherings and threw nice talks.

Last but not least, I would like to tribute my deepest gratitude and my great sense of appreciations to my parents Mrs. Rathnayaka Mudiyanselage Punchi Manike Rathnayaka and Mr. Konara Mudiyanselage Premarathna Banda Konara for their love, affection, outstanding support, continuous hear-felt prays and very valuable advises for the success in my Ph.D studies.

Konara Mudiyanselage Sandun Yasantha Konara
University of Agder, Grimstad

Abstrakt

Elektrisk transport får stadig mer oppmerksomhet fra alle interessenter innen transportsektoren på grunn av de mange miljø- og helsemessige fordelene ved e-mobilitet. Spredningen av elektriske kjøretøy (EV-er) utgjør derimot en enorm utfordring på grunn av problemer knyttet til lange ladetider, rekkeviddeangst og ladeautonomi. Den raske utplasseringen av hurtigladestasjoner(FCS-er) for elektriske kjøretøy (EV) kan lindre disse utfordringene. For å begrense belastningen på strømnettet må FCS-er for øyeblikket bygges som mikronett eller aktive generatorer (AG-er), noe som gir en mulighet til å introdusere flere fornybare energikilder (RE) i de distribuerte nettverkene. Kapasiteten til FCS-en og antallet ladere for EV-er/utstyr for EV-strømtilførsel (EVSE) kan betraktes som den begrensende ladingsressursen for FCS-en. FCS-en står overfor drifts- og tekniske utfordringer for å imøtekomme etterspørselen fra heterogene EV-brukere.

Denne avhandlingen presenterer innovative strategier for tildeling og koordinering av ladingsressurser som maksimerer de begrensede ladingsressursene ved FCS-en med heterogene EV-brukere. Det tillater at opportunistiske EV-brukere (OEV-er) utnytter tilgjengelige ladingsressurser med dynamiske hendelsesstyrte strategier for tildeling og koordinering av ladingsressurser, i tillegg til primære EV-brukere (PEV-er) (registrerte eller planlagte EV-brukere). Videre fokuserer utviklede strategier på de begrensede ladingsressursene som er tildelt primære/registrerte EV-brukere (PEV-er) ved FCS-en, som får tilgang til FCS-en med spesifikke privilegier i henhold til tidligere avtaler. Men tilgjengelige ressurser blir ikke optimalt utnyttet på grunn av ulike usikkerheter knyttet til EV-ladingsprosessen, som EV-mobilitetsrelaterte usikkerheter, feil på EVSE, usikkerhet i energipriser osv. Utviklede strategier tar hensyn til at ubrukte ladere og ledig plass for EV-er ved FCS-en er en mulighet for ytterligere utnyttelse med OEV-er ved hjelp av innovative strategier for koordinering av ladingsressurser. Denne avhandlingen utvikler et FCS-sentrert rammeverk for vurdering av ytelse som evaluerer ytelsen til utviklede strategier med hensyn til utnyttelse av ladingsressurser, fullføring av lading og kvalitetsaspekter ved tjenesten (QoS) for EV-brukere. For å evaluere QoS for EV-ladingsprosessen, blir forskjellige parametere som EV-blokking, forhåndsavbrudd i ladeprosessen, gjennomsnittlig ventetid, gjennomsnittlig ladetid, tilgjengelighet av FCS, lade pålitelighet osv. utledet og analysert. I tillegg forbedrer de utviklede innovative strategiene for tildeling og koordinering av ladingsressurser med ressursaggregering og etterspørselselastisitet utnyttelsen av ladingsressurser samtidig som de gir høy QoS for lading av EVs.

For de vurderte tilfellene har vi observert at selv om mer enn 80% av ressursutnyttelsen ikke kan oppnås bare med PEV-er, oppnår FCS-en nesten 100% ressursutnyttelse med ladningsressursaggregering og etterspørselselastisitet med heterogene EV-brukere. Ressursutnyttelsen er alltid over 50% uavhengig av ankomsttakten for PEV-er. Ladepåliteligheten til FCS-en forbedres med utviklede strategier for tildeling og koordinering av ladingsressurser sammen med en rekke mobile eksterne ladere (MOBCs). Analysen viser at økt antall ankomster av PEV-er og feil på EVSE-er påvirker ladepåliteligheten til OEV-er i stor grad. Imidlertid kan reservering av MOBC-en ved FCS-en betydelig forbedre ladepåliteligheten til OEV-er. De utviklede strategiene for koordinering av ladingsressurser har forbedret ladepåliteligheten til OEV-er med 56% og PEVer med 91% i scenariet der den betraktede ankomsttakten for PEV-er er maksimal, sammenlignet med FCS uten MOBC-er. For å skalere opp kapasiteten til FCS-en, er en fotovoltaisk (PV) basert aktiv generator (AG) integrert ved hjelp av en utviklet AC-koblet mikronettarkitektur. PV-AG-en bruker en innovativ kontrollmetode basert på en endelig tilstandsmaskin med tilstandsstrømkontroll og droop-karakteristikker for å håndtere den dynamiske kraftflyten innen FCS-en. Den sikrer frekvensstabiliteten påvirket av de raske endringene i kraftintensiv EV-etterspørsel ved FCS-en.

Det utviklede FCS-sentrerte rammeverket for vurdering av ytelse, sammen med strategier for tildeling og koordinering av ladingsressurser, er nyttige for å optimalt utnytte de begrensede ladingsressursene samtidig som en høy QoS opprettholdes for heterogene EV-brukere. I tillegg er dette arbeidet nyttig for å få en kvantitativ oversikt over hele ladeprosessen ved FCS-en.

Abstract

Electric transportation is gaining the increasing attention of all the stakeholders of the transportation sector due to the many environmental and health merits of e-mobility. However, the proliferation of electric vehicles (EVs) is an enormous challenge due to some issues related to long charging times, range anxiety and charging autonomy. The rapid deployment of electric vehicle (EV) fast charging stations (FCSs) can alleviate these challenges. To mitigate the impact on the power grid, currently, FCSs must be built as micro-grids or active generators (AGs) which provides an opportunity to penetrate more renewable energy (RE) sources within the distributed networks. The capacity of FCS and the number of EV chargers/ EV supply equipment (EVSE) can be considered as the limiting charging resource of the FCS. The FCS faces operational and technical challenges to fulfill the demand of heterogeneous EV users.

This thesis presents innovative charging resource allocation and coordination strategies that maximize the limited charging resources at FCS with heterogeneous EV users. It allows opportunistic EV users (OEVs) to exploit available charging resources with dynamic event-driven charging resource allocation and coordination strategies apart from primary EV users (PEVs) (registered or scheduled EV users). Moreover, developed strategies focus on the limited charging resources that are allocated for primary/ registered EV users (PEVs) of the FCS who access the FCS with specific privileges according to prior agreements. But the available resources are not optimally utilized due to various uncertainties associated with the EV charging process such as EV mobility-related uncertainties, EVSE failures, energy price uncertainties, etc. Developed strategies consider that idle chargers and vacant space for EVs at the FCS is an opportunity for further utilizing them with OEVs using innovative charging resource coordination strategies. This thesis develops an FCS-centric performance assessment framework that evaluates the performance of developed strategies in terms of charging resource utilization, charging completion and the quality of service (QoS) aspects of EV users. To evaluate QoS of EV charging process, various parameters such as EV blockage, charging process preemptage, mean waiting time, mean charging time, availability of FCS, charging reliability, etc are derived and analyzed. In addition, the developed innovative charging resource allocation and coordination strategies with resource aggregation and demand elasticity further enhance the charging resource utilization while providing a high QoS in EV charging for both PEVs and OEVs.

For the considered cases, we have observed that even though more than 80% of resource utilization can not be achieved only with PEVs, but FCS accomplishes all most all 100% of resource utilization with charging resource aggregation and demand elasticity with heterogeneous EV users. The resource utilization is always higher than 50% irrespective of the arrival rate of PEVs. The charging reliability of FCS is enhanced with developed charging resource allocation and coordination strategies along with a set of mobile off-board chargers (MOBCs). The analysis shows that increasing more arrivals of PEVs and EVSE failures severely affect the charging reliability of OEVs. However, reserving MOBCs at FCS can enhance the charging reliability of OEVs significantly. The developed charging resource coordination strategies have improved the charging reliability of OEVs by 56% and PEVs by 91% in the scenario where the considered PEV arrival rate is maximum, compared to that of FCS without MOBCs. To scale up the capacity of FCS, a photovoltaic (PV) based active generator(AG) is integrated using developed AC-coupled micro-grid architecture. The PV-AG uses an innovative finite state machine-based hierarchical control approach with state-flow control and droop characteristics to manage the dynamic power flow within FCS. It assures the frequency stability affected by the rapid changes in power-intensive EV demand of FCS.

The developed FCS-centric performance assessment framework along with charging resource allocation and coordination strategies are useful for optimally utilizing the limited charging resources while assuring a high QoS for heterogeneous EV users. In addition, this work is useful to get a quantitative overview of the whole charging process at FCS.

Publications

The following peer-reviewed published articles are based on the research work caried out during this Ph.D studies.

Peer Reviewed Journal Publications

- K.M.S.Y. Konara, M.L. Kolhe, N. Ulltveit-Moe, I.A.M. Balapuwaduge, "Reliability Enhancement of Fast Charging Station under Electric Vehicle Supply Equipment Failures and Repairs," *Energies (ISSN: 1996-1073)*, vol 16, 2933, 2023. doi : 10.3390/en16062933.

- K.M.S.Y. Konara, M.L. Kolhe, N. Ulltveit-Moe, I.A.M. Balapuwaduge, "Optimal Utilization of Charging Resources of Fast Charging Station with Opportunistic Electric Vehicle Users," *Batteries (ISSN: 2313-0105)*, vol 9, 140, 2023. doi : 10.3390/batteries9020140

- K.M.S.Y. Konara, M.L. Kolhe, "Queue Based Dynamic Charging Resource Allocation and Coordination for Heterogeneous Traffic in an Electrical Vehicle Charging Station," *Energy Sources, Part A: Recovery, Utilization, and Environmental Effects (ISSN: 1556-7230)*, 1–18, 2021.
doi : 10.1080/15567036.2021.1974983

- K.M.S.Y. Konara, M.L. Kolhe, A. Sharma, "Power Flow Management Controller within a Grid Connected Photovoltaic Based Active Generator as a Finite State Machine using Hierarchical Approach with Droop Characteristics," *Renewable Energy (ISSN 1879-0682)*, Vol 155, 1021–1031, 2020.
doi : 10.1016/j.renene.2020.03.138

- K.M.S.Y. Konara, M.L. Kolhe, A. Sharma, "Power Dispatching Techniques as a Finite State Machine for a Standalone Photovoltaic System with a Hybrid Energy Storage," *AIMS Energy (ISSN 2333-8334)*, vol 8, 214–230, 2020.
doi : 10.3934/energy.2020.2.214

- A. Sharma, M. Kolhe, K.M.S.Y. Konara, N. Ulltveit-Moe, K. Muddineni, A. Mudgal, S. Garud, "Performance Assessment of Institutional Photovoltaic based Energy System for Operating as a Micro-grid," *Sustainable Energy Technologies and Assessments (ISSN 2213-1396)*, vol. 37, pp. 1-13, 2020.
doi: 10.1016/j.seta.2019.100563

- K.M.S.Y. Konara, M.L. Kolhe, N. Ulltveit-Moe, I.A.M. Balapuwaduge, "Aggregation Based Charging Resource Coordination at Fast Charging Station for Heterogeneous Electric Vehicle Users," *IEEE Transactions on Industrial Informatics (ISSN 1941-0050)*, 2023 (Under Review)

- K.M.S.Y. Konara, M.L. Kolhe, N. Ulltveit-Moe, I.A.M. Balapuwaduge, "Maximal Utilization of Charging Resources of Fast Charging Station with Ultra-Fast Electric Vehicle Users," *eTransportation (ISSN 2590-1168)*, 2023, (Under Review)

Peer Reviewed Conference Proceeding Publications

- K.M.S.Y. Konara, M.L. Kolhe, "Charging Coordination of Opportunistic EV Users at Fast Charging Station with Adaptive Charging," In Proceedings of Transportation Electrification Conference (ITEC-India), IEEE, pp. 1–6, 2021. doi : 10.1109/ITEC-India53713.2021.9932507

- K.M.S.Y. Konara, M.L. Kolhe, "Priority Based Coordinated Electric Vehicle Charging System for Heterogeneous Traffic," In Proceedings of the 5th International Conference on Smart and Sustainable Technologies (SpliTech), IEEE, pp. 2020. doi : 10.23919/SpliTech49282.2020.9243782

- K.M.S.Y. Konara, M. Kolhe, A. Sharma, 'Load Compensator with an Energy Storage for a Grid Connected PV Based Active Generator', IOP Conference series- Materials Science and Engineering, vol. 605, no. 012009, pp. 1-8, 2019. doi:10.1088/1757-899X/605/1/012009.

- A. Sharma, M. Kolhe, K.M.S.Y. Konara, K. Muddineni, A. Mudgal, S. Garud and U. Nils, "Operational Analysis of Institutional Energy System for Developing a Micro-grid," IOP Conference Series- Materials Science and Engineering, vol. 605, pp. 1-8, 2019. doi:10.1088/1757-899X/605/1/012008

- A. Sharma, M. Kolhe, K.M.S.Y. Konara, K. Muddineni, A. Mudgal, S. Garudand U. Nils, "Performance Assessment of Building Integrated Photovoltaicand Battery Energy System: A Case Study of TERI-Retreat Faculty in India,"5th International Conference on Smart and Sustainable Technologies(SpliTech), IEEE, pp. 1-5, 2019. doi: 10.23919/SpliTech.2019.8783046.

- D. J. K. Dassanayake, H. M. A. P. Ruwanthi, K. K. D. I. Karunanayaka, K. M. S. Y. Konara, P. D. C. Perera, Mohan Lal Kolhe "Controller for the Power Injection from a Grid-Interfaced Energy Storage within an AC Micro Grid," International Conference on Smart Technologies for Energy, Environment and Sustainable Development (ICSTEESD), Springer Proceedings in Energy, vol 1, pp 337, 2022. doi : 10.1007/978-981-16-6875-328

Contents

List of Figures

List of Tables

Chapter 1

Introduction

This chapter presents the background information related to electric vehicle (EV) charging emphasizing the grid impact associated with EV charging. The state-of-art literature review is presented in this chapter to formulate the research goal along with research objectives. Finally, the outline of the report presenting the structure of the available chapters is given.

1.1 Background and Motivation

Growing concerns about climate change, global warming, and the rapid depletion of fossil fuels have boosted the attention of all the stakeholders of the transportation sector towards electric transportation in place of fossil-fueled transportation. Globally, reducing the contaminants in emissions according to yearly based targets has become a mandatory requirement to be achieved [1]. The proliferation of electric vehicles (EVs) contributes to the United Nations' sustainable development goals (SDGs) in terms of mobility to achieve an affordable, reliable, and sustainable mode of transportation [2]. The evaluation of the global EV stock by transport mode from 2010 to 2020 is illustrated in Figure 1.1.

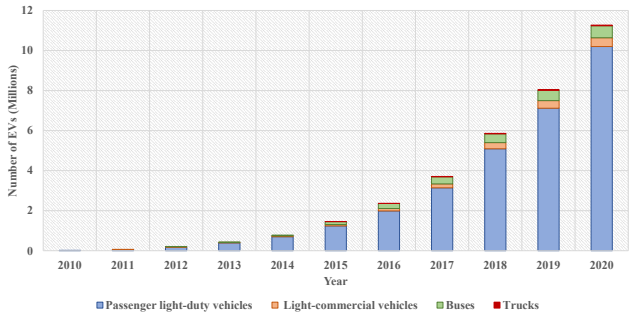

Figure 1.1: Global EV stock by transport mode in 2010-2020 [4]

Moreover, due to the scarcity of fossil fuels and the volatility of their prices, EVs are getting growing in popularity with the advancement of energy storage technologies. In this context, EVs create a more clean, sustainable and decarbonized future [1, 3].

Over the last decade, a variety of governmental policies for EVs have been instituted that support mass adoption of EVs. But still, the challenge in terms of required EVs on the world's roads remains enormous to make progress toward climate goals [4]. Due to perceptible advancements of EV battery, energy conversion and electric propulsion technologies over the last couple of years, the proliferation of EVs has become a cost efficient substitute in transportation sector as compared to escalating fuel prices [4–6]. The weighted average cost of EV batteries has been declined 13% in 2020 with respect to 2019, reaching USD 137/kWh at a pack level that attributes to the rapid adoption of EVs [4]. Despite the declining cost and performance advancement of EV batteries, battery degradation, charging constraints,thermal characteristics, limited energy densities still pose major challenges in terms of the long charging time and range anxiety of one charge to promote EVs [7, 8].

Apart from limitations associated with EV batteries, lack of quick and seamless charging facilities to extend the cruise range of an EV, just like in fuel-based counterparts poses another key challenge to proliferation of EVs. Currently, charging of EVs is done mostly with private chargers at residential places and parking lots. Residential charging is possible at detached houses only. Consequently, the charging autonomy affects the achievement of goals for rapid EV deployment [4]. Currently, high capacity EVs are used to increase the driving range with one charge but it increases the weight and cost of vehicle enormously. As overall, despite socio-economic, health and environmental merits associated with EVs, issues related with high vehicle cost, long charging time, range anxiety and charging autonomy pose key challenges to promote EVs [9, 10].

The battery charging modes can be basically classified as slow charging and fast charging based on the charging power level. The international standards for these different modes of EV charging from a power source are defined in IEC 61851-1:2017 [11]. The EV suply equipment (EVSE) that can provide these different charging modes are practically built with different protocols and couplers. The slow charging mode employs the AC power, where as the fast charging mode uses the DC power. Usually, the slow charging mode is built with AC Level 1 and AC Level 2 on board chargers that use 120 V and 240 V AC input, respectively[12]. The Society of Automotive Engineers (SAE) has defined a North American standard SAE J1772 (IEC 62196 Type 1) for EV conductive charge coupler that perform Level 1 or Level 2 charging [13]. This is the general industry standard for Level 1 and Level 2 slow charging that supports charging rates from 1.44 kW up to 19.2 kW [14]. This slow charging mode is widely employed in overnight charging at homes and parking lots where long charging time is acceptable. Consequently, due to limited power ratings of on board chargers, quick and seamless refueling process of EVs can not be achieved with slow charging mode. In the recent market, we can see different EVSE producers manufacture DC fast conductive chargers rated at 50 kW to 400 kW. And further efforts are on developing mega-chargers rated at 900 kW [15].

Table 1.1: Different Industrial Standards for DC Fast Charging Systems [17]

Industry Standard	International Standard	Maximum Output Parameters Voltage	Current	Power
CHAdeMo	IEC 62196-3 (Configuration AA) IEEE 2030.1.1	1000 V	400 A	400 kW
GB/T	IEC 62196-3 (Configuration BB) GB/T 2034.3	1000V	250 A	120 kW
CCS Type1	SAE J1772 IEC 62196-3 (Configuration EE)	600 V	200 A	150 kW
CCS Type 2	IEC 62196-3 (Configuration FF) SAE J1772	1000V	200 A	175 kW
Tesla	-	410 V	330 A	135 kW

The ICE62196-3 [16] standard has been formulated especially for DC fast charging (Level 3) and it defines four different vehicle coupler configurations for DC fast EVSE. These four configurations are built with four different industry standards with corresponding voltage, current and power ratings to assure compatibility. Tesla has their own DC fast EVSE with a own coupler inlet explicitly for Tesla vehicles. These five industry standard systems for DC fast charging are tabulated in Table 1.1 [17]. Configuration AA defined in the ICE62196-3 standard is proposed and built by CHAdeMO association. Correspondingly, configuration BB (GB/T) is only available in China. Combined charging system (CCS) type 1 is an extended version of the SAE J1772 standard and used in North America. CCS Type 2 is adopted in Europe and Australia. In EVSE, the cable size increases with the maximum power delivery [17].

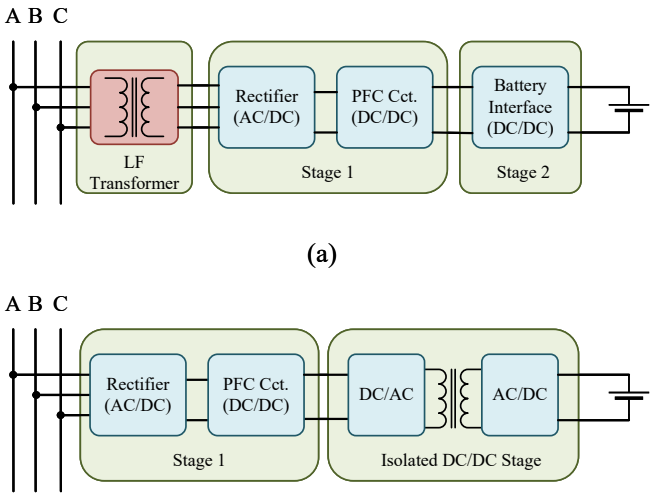

Figure 1.2: Building block of a typical DC fast EVSE energy conversion system [17]

The state-of-the-art of recently manufactured DC fast EVSE converts AC energy into DC through two energy conversion stages as illustrated in Figure 1.2. Therefore, it should be noted that a DC fast charger itself is a power electronic system. The three-phase AC input with a voltage up to 480 V is converted into DC with desired output voltage based on the employed standard [17]. In the EVSE, the grid facing-stage is an AC-DC rectifier with a power factor correction circuit that converts AC voltage into intermediate DC voltage. This intermediate DC voltage is again converted into regulated DC voltage that charges the EV.

As illustrated in Figure 1.2, the electrical isolation between power grid and EV can be accomplished by one of the following two means. Figure 1.2 (a) shows the first method in which a line frequency (LF) transformer is placed in between the grid and the AC-DC stage and in the other method, an isolated DC-DC converter can be used at the battery interfacing stage as depicted in Figure 1.2 (b). When the output power of the EVSE increases, a single module violates its ratings, hence, multiple identical Stage 1 and Stage 2 must be connected in parallel to meet high power requirements [17]. Therefore, the evolution of DC fast charging can be considered as a paradigm shift in EVs as it provides sort of similar refueling experience like gasoline counterparts.

Currently EVSE manufacturers produce modern EV chargers capable of variable rate charging (VRC) and constant rate charging (CRC) as illustrated in Figure 1.3. The charging power can be varied between specified limits continuously (Figure 1.3 (a)) or discretely (Figure 1.3 (b)) with VRC. CRCs come with simple on-off controllers to modulate the power [18].

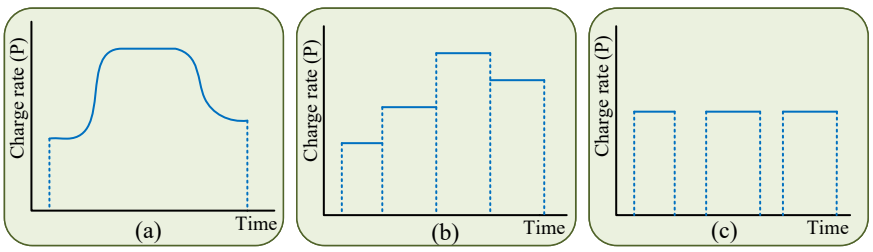

Figure 1.3: Variable rate and Discrete rate charging [18]

For continuous VRC, a sophisticated actuator is needed to moderate power with an infinite number of values between specific limits. By contrast, the charging power can be easily moderated with discrete VRC as it deals with only a finite number of levels within a specific limit. A CRC supplies constant power to EV depending on the respective EV battery constraints. If CRC is employed in a charging management scheme, a simple on-off controller can be used to modulate the power. Nevertheless, recharging time with a commonly available 50 kW fast charger is approximately three to six times longer than that of gasoline refueling. Charging time can be further reduced by a factor of two to four with higher charging rates [5].

Moreover, advancements in lithium-ion battery technology over the last decade leads to manufacturing EV batteries with high energy and power densities in addition to long-life time. Therefore, high energy and power-dense batteries and modern energy conversion technologies enable EV manufacturers to produce EVs with fast charging capabilities [19–21].

In this context, to cope with the challenges associated with the rapid adoption of EVs in place of gasoline counterparts, charging infrastructures that facilitate a similar refueling experience like fossil-fueled vehicles is essential. Consequently, publicly accessible fast charging stations (FCSs) must be deployed in a widespread manner, especially in urban areas where EV population is high and long driving trips are common. Therefore, as a promising approach to promote EVs, FCSs can be deployed with innovative operation management mechanisms in all major cities. Publicly accessible FCSs facilitate occasions where quick charging is inevitable. Consequently, rapid deployment of FCSs encourages long-trip drivers and those late adopters who do not have access to private charging to purchase an EV.

Although the sparse deployment of FCSs would alleviate charging time, range and autonomy concerns of EVs without requiring costly high-capacity EVs, high penetration of FCSs poses substantial impacts on the power grid in terms of network capacity, power system stability, and power quality [23, 24]. When FCS demand grows, rapid voltage changes and voltage flicker take place at the distribution grid. Due to rapid changes of charging demand frequency fluctuations within and outside the FCS can be taken place. An FCS is a significant harmonic emission source to the grid that results in both voltage and current harmonic distortion. As EVSE are power electronic-based systems, an FCS causes super harmonic distortion in the power grid [22]. Therefore, increasing penetration of FCSs into the distribution grid requires costly grid reinforcements or reconstructions to avoid issues related to power quality, network capacity, and energy market operation [25–28].

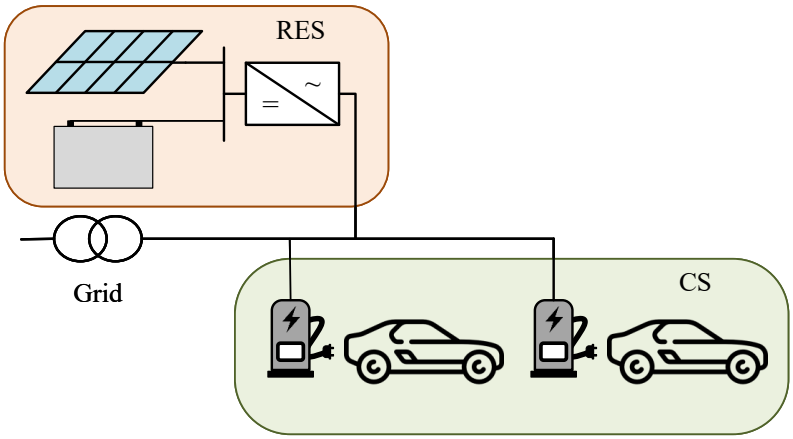

Figure 1.4: RE based EV FCS

However, these costly grid reinforcements and reconstructions can be mitigated by embedding a renewable energy system (RES) or energy storage (ES) into the FCS while employing a coordinated charging scheme [29–31]. RE based FCS is illustrated in Figure 1.4. Therefore, the contract demand, RES, or ES can be considered as the energy supply of the FCS that should ensure uninterruptible supply. These energy components must be techno-economically sized so that the FCS capacity is adequate to supply the EVSE available at FCS. Consequently, the total capacity of FCS is based on the capacity of RES or ES and the contract demand of the utility. To avoid grid stresses, the power supply of the FCS should strictly adhere to grid constraints while maximally utilizing the local energy supply. Therefore, energy resources and chargers/EVSE at FCS can be considered as the limited charging resources of FCS.

As far as commercially available EV models are concerned, most of them are equipped with battery packs with a size ranging from 10 kWh to 100 kWh, along with specific charging constraints. Consequently, the charging time of different EVs is also ranging from several minutes to a few hours. When we consider the basic EV user behavior, there is one category of EV users (eg. daytime workers) who plug-in their EVs overnight preferably after arriving home from work and plug-out when departing for work. Some people might charge their EVs at the curbside or in a parking lot more especially during the day time. As they plugged their EVs for plenty of time they can charge with slow charging. EVs can also be charged in EV charging stations (CSs) at occasions where quick charging becomes inevitable [18]. With the increasing population, in near future, a detached house for everyone or securing a charging point (CP) in a parking lot would not be possible at every time. Therefore, with the rapid adoption of EVs, charging autonomy would be a significant matter in EV charging. EV users may charge their EVs at lower prices at CSs as CS owners may purchase bulk energy from the energy market and the competition among CSs. Therefore, this wide range of charging demand has to be taken into consideration when developing FCSs and charging coordination schemes. Moreover, it should be clearly understood that an FCS is a power-intensive load to the power grid that should be properly designed, constructed and managed from the deployment stage. Limited charging resources must be optimally utilized to maximize the profit without exerting adverse impact to the power grid while assuring a high-quality service to its customers (EV users).

1.2 State-of-the-Art Literature Review

Comprehensive analysis is needed to design and operate an FCS sustainably. Authors have focused three major concerns on the design and operation of an FCS : (1) maximizing the revenue of FCS (2) Minimizing the impact of FCS to the power grid (3) Enhancing user satisfaction. An FCS can not be built by considering only land availability in an urban area.

FCS deployment analysis in the literature is a very important class of work related to DC fast charging. In FCS deployment problems, generally, authors put efforts to find the optimum location of the FCS in a particular area or region with an optimum number of charging piles. Deployment of an FCS is quite different compared to that of a gasoline station due to several aspects. Sparsely distributed FCSs help EV users to alleviate range anxiety [32]. EV user satisfaction in terms of waiting time and blockage significantly affects the sustainable operation of an FCS and therefore, congested FCSs are not often chosen by EV users [33, 34]. Driving distance to find a FCS is also a major factor in attracting customers to the FCS [35]. Innovative pricing schemes along with charging management strategies can maximize the profit of an FCS, but to counterbalance the EV user satisfaction and sustainable operation of the FCS while earning a good profit, it is very important to consider the optimal siting of the FCS with optimal units of EVSE.

Consequently, relevant spatiotemporal analysis is essential before deploying an FCS if one wants to earn maximized profit while providing a quality service to customers. FCS deployment problems are mainly based on FCS operator perspectives, EV user perspectives and grid operator perspectives. Moreover, in the literature related to the deployment of FCSs, we can observe that authors have mainly taken the following aspects into account to form the FCS deployment problems; (1) Deployment or construction cost (2) Charging profit (3) Service quality (4) Grid impact. In the EV paradigm, all the time we should strictly note that the charging time is significant in contrast to the gasoline counterparts although we have employed high-power DC fast charging. To avoid unnecessary blockages, an adequate number of charging piles must be built in the FCS to facilitate several parallel charging processes. Therefore, the upfront investment to build several units of EVSE in line with the standards discussed in Section 1.1 is significant [36]. Nevertheless, FCS is a significantly large and rapidly varying load to the distributed grid. Therefore, FCS is not recommended to be deployed in a location where the power grid is weak.

Enormous research efforts are made in the literature that intend to find the optimal location of FCS by considering EV traffics. Moreover, in the literature related to the deployment of FCSs, we can observe that authors have mainly taken construction cost aspects and service quality to formulate the problem. As for cost aspects, various types of costs are considered including grid stability and service quality violation penalties, etc. Authors in [37, 38] have presented a placement and sizing work related to a DC fast charging network that minimizes the deployment cost while ensuring acceptable waiting time, shorter travel distance to charge, etc. In their study, they have further analyzed the voltage stability by adding a minimum number of voltage stabilizers. Shukla *et al.* [39] have proposed a technique to find the optimal location and size of FCS by capturing maximal EV flow so that it reduces investment cost by minimizing the number of charging facilities required in the FCS. They have in-cooperated queuing analysis based on waiting time constrain in their model to find the optimal siting and sizing of the FCS.

Authors in [40] have proposed strategies to find a minimum number of FCSs in a particular area so that at least one FCS covers any route of the road network to minimize the construction cost of the FCS. Iqbal *et al.* has done a comprehensive review in [41] on the optimal placement of vehicle charging stations in an area and its impact on the grid.

In the literature related to FCS deployment problems, there is another category where the main objective function is defined considering the service quality aspects. At the same time, we have observed that some authors have taken cost aspects and/or grid impact aspects into consideration as constraints. Shukla *et al.* in [42], has formulated the optimization problem to minimize social cost by minimizing driving distance for charging EVs. They have used K-mean and fuzzy C-means clustering techniques to find the location of FCS. Ref.[43] has used a novel graph-automorphic approach to place and size FCSs by limiting vehicle waiting times at all stations below a desired threshold level. Moreover,in this study, the authors have presented strategies to the deployment of portable charging stations (PCSs) in selected areas to further reduce the overshooting of waiting times during peak traffic hours. Xiong *et al.* [44] have employed a game theory-based bi-level optimization model to minimize the traveling distance and waiting time of EV users with competitive charging behaviors. Monte Carlo analysis is used in [45] for three types of areas (urban, suburban, and rural) to quantify the effect of uncertain parameters on FCS loading and service quality and the placement strategy has been optimized to minimize charging duration and waiting time in the queue. Gan *et al.* have formulated a Genetic algorithm-based FCS deployment problem as a nonlinear integer problem to seek the optimal locations to build the FCS with the corresponding optimal number of charging piles so that it maximizes the FCS profit while minimizing driving distance and waiting time. We can observe that due to the limitations associated with queue-based models, authors have focused mainly on driving distance and waiting time as the quality of service (QoS) parameters. But EV blockage, charging preempting, mean charging time, mean charging completion would be more impacting QoS parameters regards to EV charging in a CS for which adequate research attention has not been given.

Once the best location and the optimum number of charging points are determined to build an FCS, then it is required to techno-economically size the different energy supply units of FCS including the RES and/or ES as elaborated in Section 1.1. Li *et al.* [47] have investigated the techno-economic feasibility of hybrid renewable energy (solar photovoltaic (PV) and wind turbine (WT) based environment-friendly CSs at five different locations in China. Moreover, the authors in [47] have shown through sensitivity analysis that the greater the load or number of EVs, lower the reliability of CS. Authors in [48] have investigated on determining the optimal size of the ES embedded with FCS such that the station energy cost and the storage cost are minimized. Ref. [48] has considered that the ES is a way to reduce the operational costs of the station.

As far as an already deployed FCS is concerned, the limited number of chargers, grid supply (with contract demand) and RES and/or ESS can be considered as limited charging resources at an FCS. The optimal utilization of these limited charging resources is dispensable to maximize the profit earned by the FCS. EVSE capable of variable rate charging can be employed to facilitate a wide range of EVs at the FCS [18]. Uncoordinated charging regimes may lead to underutilization of limited resources and EV user dissatisfaction. Therefore, the charging process at an FCS must be a coordinated process that encounters different parameters from all the stakeholders of the FCS such as EV users, aggregators, utility, power grid, energy market, etc.

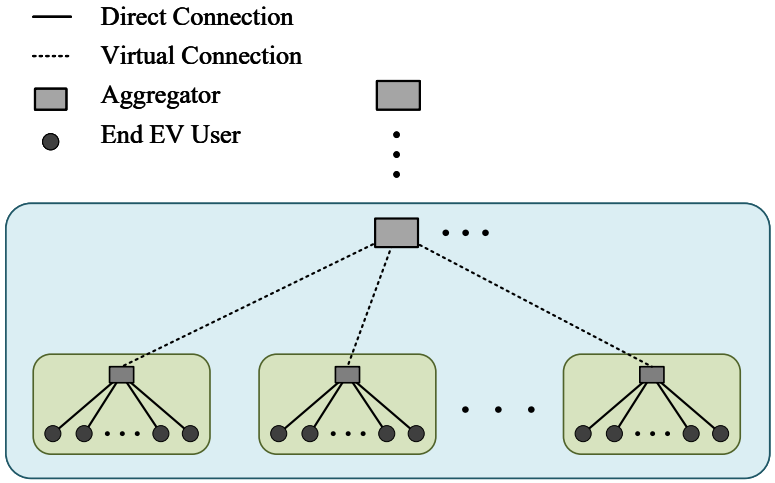

Figure 1.5: Hierachical approach of EV charging coordination .

In this context, attention must be given to distinct charging demands where charging time is varying from a few minutes to a few hours to propose charging management systems for FCSs. Then we can expand the scope of services given by an FCS so that the high throughput of potential customers/ EV users can be achieved while guaranteeing a high-quality service to EV users. Therefore, the limited charging resources available at FCS can be maximally utilized if time-consuming charging processes can be optimally scheduled in advance. We can see that significant research efforts have been devoted to the charging coordination and optimal scheduling of EVs at CSs in the literature. These review articles [18, 49–51] very clearly elaborate on the state-of-art EV charging scheduling and coordinating strategies proposed in the literature. We can see, most of the available charging coordination algorithms are developed in a hierarchical approach as depicted in Figure 1.5. It can be seen that different objectives such as economic aspects, operational aspects, service quality aspects, etc. are considered to formulate EV charging coordination schemes.

Overall, we can see some EV charging management schemes are proposed as time-advanced deterministic problems while others are real-time models. Although EV charging management systems developed as deterministic problems obtain the optimum charging schedule, they are not very feasible as they assume that the

required information for computations is well-known prior to the actual execution of the charging schedule. We should clearly understand that EV charging process at an FCS is a stochastic process. It is affected by various uncertain aspects illustrated in Figure 6.1 [18].

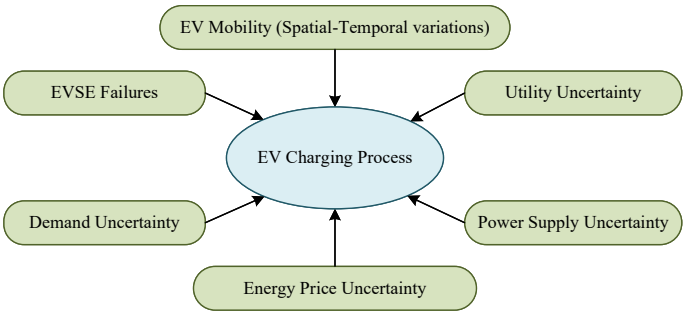

Figure 1.6: Uncertain aspects for EV charging process [18].

Even though an offline strategy obtains the optimum charging schedule, due to various uncertainties associated with EV charging illustrated in Figure.6.1, the expected revenue might not be accomplished in real-time operation and the obtained solution would not be a feasible or practical one. In order to cope with these uncertainties, authors have in-cooperated several techniques to optimally schedule EVs at the CS with this hierarchical approach. In some cases [52, 53], intermediate or upper layers schedule charging processes with a static approach as an offline schedule and the CS executes this schedule in real-time using a straight-forward heuristic algorithm with less computational overhead to cope with the dynamic environment. Xu *et al.* in [52] have presented a hierarchical coordinated charging scheme to optimize system load profile and charging costs while satisfying customer charging requirements with necessary interactions between different levels. Authors in [52] have considered three levels (e.g., provincial level, municipal level, and CS level) at multiple timescales (i.e., day-ahead and real-time) in their proposed strategies to jointly optimize system load profile and charging costs while adhering distinct EV user requirements. At the CS layer, they have in-cooperated a heuristic algorithm to distribute the allocated power among connected EVs to achieve high charging completeness at departure.

In [53], a hierarchical charging coordination framework is presented to maximize the profit of the central aggregator by minimizing the energy purchase cost under the time-of-use tariff system. In the proposed system, the central aggregator is informed by the sub-aggregators with expected aggregated EV demand to calculate the optimum power share of each sub-aggregator. Zhao *et al.* in [54] have modeled the operation of FCS as a leader–followers game where FCS operator acts as the leader while EVs are considered as the followers to manages local sources and sets energy prices for EVs to increase its revenue. EVs participate in the game to obtain a tradeoff between the benefits from energy consumption and reserves provision. Usually, CS aggregator purchases energy at wholesale price from the day-ahead market

based on the forecasted aggregate EV demand and sells to individual EV users at retail price seeking a profit. Consequently, authors of [55, 56] have formulated their charging coordination strategies through the aforementioned optimum energy trade. Authors of [57] have formulated their charging coordination strategies as a bi-level programming model. Yao *et al.* [58] have presented a real-time single-stage charging coordination scheme formulated as a binary optimization problem to maximize the revenue of CS. Authors in [58] have employed convex relaxation in the proposed strategies to avoid computational complexity and dimensionality in real-time operation. However, with limited charging resources, FCS with the described strategies may lose potential customers due to unadmitted overlapping demand as it is not very flexible to shift demand requests in real-time without putting a queue.

In some other set of works presented in [59–61], the proposed static algorithm is executed iteratively to deal with the stochastic nature of EV charging process. Vandael *et al.* have proposed their demand management strategies in three steps : (1)aggregation, (2)optimization, and (3) control and executed iteratively to obtain optimal, centrally computed charging plans, while significantly improving scalability. In Ref. [60], an iterative, agent-based control concept is presented in a hierarchical structure. Because of this iterative nature at each time slot computational complexity is high and hence, it poses some challenges in real-time operation. To minimize the revenue loss due to cancellations of scheduled charging and unexpected departures, authors have proposed multi-aggregator collaborative scheduling. As the EV demand can be shared among multiple aggregators in these strategies, the peak load caused by the high penetration of EVs can be smoothened at the power grid level.

Mukherjee and Gupta present in [62] multi-aggregator collaborative scheduling that intends to maximize the aggregator profits and charged vehicle throughput in both offline and online. However, authors have found that, even though a larger number of EVs were scheduled, a significant difference in the profit was not observed through multi-aggregator collaboration when compared with the noncollaborative scenario. Rahbari *et al.* [63] have proposed a global optimal power allocation under all local and global constraints through peer-to-peer coordination of charging stations. A multi-aggregator collaboration-based coordinated charging scheme is proposed in a [64, 65] that optimizes the benefits of all the stakeholders (EV users and aggregators). In Ref. [65] , we study the problem of scheduling EV charging with ES from an electricity market perspective with joint consideration for the aggregator energy trading in the day-ahead and real-time markets.

However, the computational overhead associated with this approach is significantly high due to its iterative nature. Apart from mentioned directions, the authors have paid attention towards stochastic programming in formulating charging scheduling problems to address the inherent volatility and uncertainty of the EV charging process. In ref. [66–69], authors have given the focus on stochastic parameters such as arrival time, departure time, waiting time, charging time, demand

uncertainty, renewable energy supply uncertainty etc. to enhance the feasibility of proposed strategies in the execution phase. Chung et al [66] have proposed charging coordination as a stochastic game in which they have given focused attention on modeling EV user behaviors. Authors of [66] have considered the quality of service aspects of EV users.

As the overall operation of an FCS, there are EV traffic inflows into the station and outflows from the station after service completion or interruption. Depending on the availability of charging resources, the only portion of arrived EVs at the FCS are admitted for charging and the rest has to wait in a queue or be blocked. Admitted EVs are served with EVSE at the FCS. In some of the reported works related to the charging coordination of EVs at CSs, authors have employed queue-based models. The premise of these queue-based studies focuses not only on the plugged-in EVs but also on uncertainties associated with EV mobility to the FCS. Operation of the FCS is modeled as a multi-server queue system with Poisson arrival and exponential charging time distribution [10]. As an example, the authors in [71] have proposed an admission control strategy with different tandem queuing disciplines to maximize the profit of the FCS while minimizing the waiting time and the blockage of EVs. Moghaddam *et al.* [72] has proposed a smart charging strategy to find a FCS that ensures minimum charging time, travel time and charging cost. They have modeled the CS operation as an M/M/s/C queue and incorporated ant colony optimization in their analysis.

Furthermore, to cope with the dynamics and uncertainty associated with EV charging process, recently, significant research efforts have been devoted to reinforcement learning based approaches. Authors in [73–76] have proposed their EV charging coordination schemes with model-free data-driven approaches using reinforcement learning. Recently we can see that there has been increasing attention to data-driven approaches in EV charging coordination to avoid the high computational overhead associated with model-based approaches. Ref.[73] provides a comprehensive review of proposed charging coordination systems based on reinforcement learning.

Regardless of offline or online charging coordination strategies, the most of reported EV charging coordination schemes have considered scheduling EV charging processes or adjusting the charge rate to achieve required objectives while adhering to necessary constraints. Usually, we tend to schedule an EV charging process if it takes significant time only. Just like gasoline counterparts, scheduling ultra-fast charging processes is not very practical as it takes only a few minutes. Most of the RE-based FCSs are AC or DC microgrids where load demand should be properly managed in line with the intermittent renewable energy generation. Therefore, energy resources at such an FCS can be optimally utilized if we can allow ultra-fast charging users as opportunistic secondary users (OEVs) to get their EVs charged at lower prices with defined liabilities.

1.3 Research Goal

The capacity of FCS and the number of EV chargers/ EVSE can be considered as the limiting charging resource of the FCS. The primary/ registered EV users (PEVs) of the FCS access the FCS with specific privileges according to prior agreements. However, these limited charging resources would not be fully utilized due to uncertainties associated with the EV charging process. The capacity of the FCS including the generated energy from FCS integrated distributed sources is wasted if the FCS does not optimally utilize it. Moreover, due to the charging schedules and uncertainties associated with the EV charging process, there can be idle chargers and vacant spaces for EVs at the FCS even for short durations. However, such idle chargers and vacant space for EVs at the FCS is an opportunity for further enhancing the charging resource utilization while assuring high QoS for EV users. Therefore, how to exploit such unused limited charging resources with secondary opportunistic EV users (OEVs) with defined liabilities to enhance the charging resource utilization assuring high QoS to heterogeneous EV users is analyzed in this thesis. As there are basic two types of user categories, we evaluate the QoS of both EV user types. Therefore, we develop, analyze and assess the performance of dynamic charging resource allocation and coordination strategies that allow OEVs to exploit unused limited charging resources of an FCS. And also we develop and analyze innovative architecture and dynamic control strategies for the FCS integrated PV based active generator that can effectively manage the power flow while maintaining the frequency stability within FCS.

1.4 Research Objectives

The research goal is formulated based on the identified research gaps through the state-of-art literature review. In line with the reaerch goal defined in Section 1.3, the followings are the key objectives of the thesis.

1. To develop strategies for dynamic charging resource allocation and coordination for EV users to enhance the charging resource utilization considering available resources at FCS. To analyze how opportunistic secondary users can exploit unused limited charging resources allocated for prioritized EV users. And to evaluate the performance of developed strategies in terms of charging resource utilization, charging completion, and quality of service aspects.

2. To research the effectiveness of aggregating available charging resources at the FCS to dynamically adjust the charging rate of opportunistic users to get their EVs charged at higher charging rate. And to evaluate how dynamic charging resource aggregation and demand elasticity help to enhance the utilization of limited charging resources while providing quality service to heterogeneous EV users.

3. To evaluate the reliability of FCS under EVSE failures and repairs and to develop dynamic charging resource allocation and coordination strategies for heterogeneous EV users to enhance the reliability of FCS.

4. To develop hierarchical control strategies for grid connected EV FCS integrated with PV-based active generator and operating as an AC micro-grid for maintaining frequency stability.

1.5 Thesis Organization

Chapter 1 gives the overall introduction to the whole work elaborating on the background and motivation of this research topic. The state-of-art literature review is carried out to formulate the research goal along with research objectives. The subsequent seven chapters of this thesis elaborate the achievement of research objectives.

Chapter 2 : This chapter presents proposed dynamic charging resource allocation and coordination strategies modeled as event-driven Monte-Carlo simulation that allows OEVs to exploit unused limited charging resources. And also this chapter presents a performance assessment framework to evaluate charging resource utilization, charging completion, and the QoS of EV users.

Chapter 3 : In this chapter, a continuous time Markov chain (CTMC)-based analytical model is developed in generic nature to investigate, how effectively dynamic charging resource aggregation can be employed to enhance the utilization of limited charging resources while providing quality service to both types of EV users. Moreover, this chapter describes FCS centric performance assessment framework for QoS aspects of EV users.

Chapter 4 : This chapter describes developed charging resource allocation and coordination strategies that allow dynamic charging resource aggregation and demand elasticity to enhance the utilization of limited charging resources while providing high QoS to both types of EV users. The presented case study is validated with the Monte-Carlo simulation-based model.

Chapter 5 : This chapter elaborates on developed queue-based dynamic charging resource allocation and coordination strategies for both slow and fast-charging EV users to enhance the charging resource utilization of FCS. The presented strategies are analyzed with a case study modeled as a discrete simulation.

Chapter 6 : In this chapter, we have discussed the developed dynamic charging resource allocation and coordination strategies employing MOBCs to enhance the reliability of FCS under EVSE failures. An analytical model is presented with a CTMC to analyze the performance of developed strategies.

Chapter 7 : This chapter presents the details of the proposed photovoltaic-based active generator architecture for the FCS as the embedded local energy source. This chapter elaborates on the complete control architecture developed in a hierarchical approach with a finite-state machine.

Chapter 8 concludes the completed work by providing contributions, key research findings and future works.

Chapter 2

Enhancement of Charging Resource Utilization with Opportunistic Electric Vehicle Users

[2] *The rapid deployment of fast-charging stations provides a viable solution to the high charging time, potential driving range anxiety and charging autonomy. FCS-integrated renewable energy system avoids costly grid reinforcements due to extra load caused by fast charging. The energy supply and fixed number of EV supply equipment (EVSE) are considered as the limited charging resources of FCS. Amidst various uncertainties associated with the EV charging process, how to optimally utilize limited charging resources with opportunistic EV users (OEVs) is studied in this chapter. This chapter proposes resource allocation and charging coordination strategies that facilitate OEVs to dynamically exploit these limited charging resources with defined liabilities when pre-scheduled users (PEVs) do not occupy them. Moreover, the proposed dynamic charging coordination strategies are analyzed with a Monte Carlo simulation (MCS). The presented numerical results reveal that the major drawbacks of under-utilization of limited charging resources by PEVs can be significantly improved through dynamic charging resource allocation and coordination along with OEVs. With the proposed charging coordination strategies in this study, the maximum charging resource utilization of considered FCS with 10 EVSE has been improved to 90%, which bounds to 78% only with PEVs.*

2.1 Introduction

Usually, we tend to schedule an EV charging process if it takes significant time only. Just like gasoline counterparts, scheduling ultra-fast charging processes is not very practical as it takes only a few minutes.

Most of the renewable energy (RE)-based fast charging stations (FCSs) are AC

[2] This chapter is based on the peer-reviewed journal paper, K. M. S. Y. Konara *et. al* "Optimal Utilization of Charging Resources of Fast Charging Station with Opportunistic Electric Vehicle Users," *Batteries (ISSN: 2313-0105)*, vol 9, 140, 2023. doi : 10.3390/batteries9020140

or DC micro-grids where load demand should be properly managed in line with the intermittent renewable energy generation. Therefore, energy resources at such an FCS can be optimally utilized if we can allow ultra-fast charging users as opportunistic secondary users (OEVs) to get their EVs charged at lower prices with defined liabilities when scheduled users (PEVs) do not utilize the charging resources.

In an FCS, the energy is wasted if the FCS does not fully utilize its capacity. Moreover, due to the charging schedule as well as uncertainties associated with the EV charging process discussed in Chapter 1, there can be idle chargers and vacant spaces for EVs at the FCS even for short durations. However, these idle chargers and vacant space for EVs at the FCS are also a waste. In this context, OEVs are very indispensable as they can utilize a significant amount of electrical energy that would otherwise be wasted if the charging resources are not fully utilized. If we can employ OEVs as a flexible load, we can utilize more intermittent renewable energy at an FCS as well.

In this Chapter, we consider a commercial FCS where the prime objective is to schedule and execute EV charging. For the aforementioned FCS, we propose and analyze charging coordination strategies for OEVs to exploit unused charging resources to enhance the charging resource utilization at the FCS. By allowing OEVs to the FCS, on the one hand, the charging process of PEVs might be affected and on the other hand, there could be service dissatisfaction of OEVs. Therefore, as overall, we propose event-based dynamic charging resource allocation and charging coordination strategies so that OEVs are allowed with different access privileges to exploit unused limited charging resources when registered PEVs are not very active within the FCS. In this research work, we employ the Monte Carlo simulation approach to assess the performance of the FCS in terms of charging resource utilization, charging completion, and quality of service (QoS) aspects.

The novel technical contributions from this work can be summarized as follows:

1. Dynamic charging resource coordination strategies are proposed so that OEVs can exploit unused limited charging resources to enhance the charging resource utilization at the FCS while assuring high-quality service for both types of users.

2. Resource allocation and charging coordination is performed in a manner that the system changes its state when an event occurs and it remains until the next event occurs. This alleviates more practical issues of frequent on-off or modulating charging coordination strategies.

3. Performance evaluation parameters are defined and analyzed in a generic nature to evaluate the QoS of charging processes of PEVs and OEVs.

2.2 Dynamic Charging Coordination Strategies

An FCS is built with a limited number of off-board chargers/EVSE and energy supply units with limited capacity. Therefore, a commercial FCS intends to maximize the profit by scheduling EVs optimally with the effective use of available limited resources. However, due to various uncertainties associated with the scheduled charging process, charging resources may not be optimally utilized even though the EV schedule obtains the maximized profit with PEVs. In order to get the advantage of very short charging time associated with ultra-fast charging technology, this work intends to evaluate the overall performance of an FCS that serves both PEVs and OEVs, as illustrated in Figure 2.1.

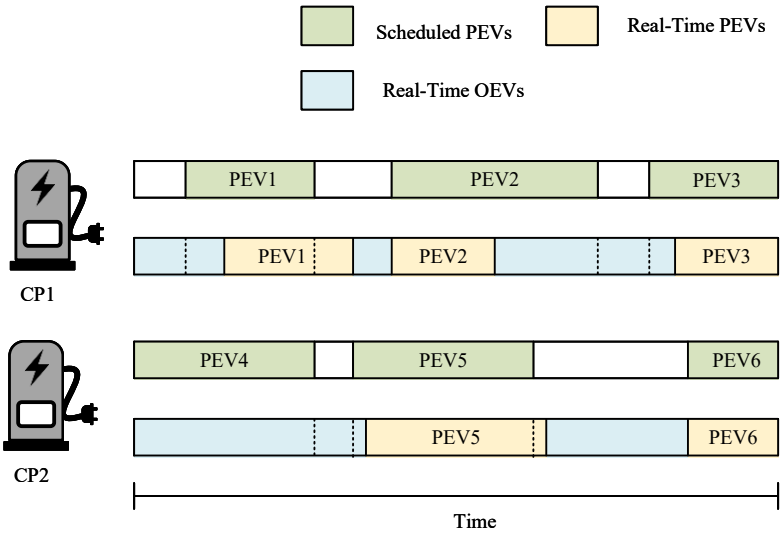

Figure 2.1: Utilization of charging resources by OEVs.

When we consider the operation of FCS, there are basically two types of EV users, as tabulated in Table 2.1: (1) PEVs and (2) OEVs with distinct privileges and constraints in accessing the FCS.

Table 2.1: Access Privileges and Constraints of EV users

PEVs	**OEVs**
• Access according to a prior agreement	• Access opportunistically
• Charged at specified charge rate $P_p;\ P_p \in [P_p^{min}, P_p^{max}]$	• Charged at specified higher charge rate $P_o = nP_p; (n \in \mathbb{Z}^+)\ ,\ P_o \in [P_o^{min}, P_o^{max}]$
• Charger is guaranteed during scheduled time.	• Charger is assigned if charging resources are available only.
• Do not subject to blockages	• Subject to blockages
• Charging process regularly finishes.	• Charging process is liable to be preempted before regularly finishes.
• Expect uninterruptible EV charging	• Expect to charge as quickly as possible

The prime objective of FCS is to provide uninterruptible EV charging to PEVs who have prior agreements with the FCS. The operating model of the considered FCS is illustrated in Figure 2.2.

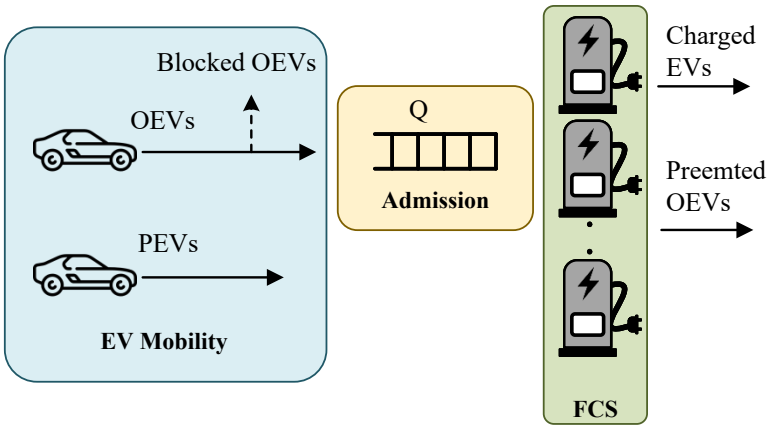

Figure 2.2: Proposed operation mechanism of the FCS

In this work, we have considered an already deployed FCS with M; $(M \in \mathbb{Z}^+)$ number of off-board chargers (OBCs), and it is assumed that the charging power of each charger can be adjustable. A queue space (Q) with q number of queue points (QPs) is allocated so that newly arrived OEVs are queued if charging resources are not available. In the meantime, FCS admits opportunistic OEVs to compensate for under-utilization of limited charging resources. PEVs are charged at a specified charge rate of P_p; $P_p \in [P_p^{min}, P_p^{max}]$. Consequently, the capacity of FCS is limited to MP_p^{max} throughout the operating horizon. Therefore, depending on the availability of charging resources, OEVs can be charged at high charge rate. Based on the day-to-day life activities of EV users and the charging constraints of EV batteries, some EV users may need undisturbed and prioritized EV charging (i.e., PEVs). At the same time, some other EV users just want to enhance their cruise range by refilling their high-capacity EV batteries up to the maximum possible level quickly during their journey. Consequently, they can be considered as OEVs. Therefore, FCSs should have a charging pricing mechanism for PEVs and OEVs based on charging priorities. Moreover, EVs capable of ultra-fast charging with high charging power rates can request to be an OEV so that they can charge their EVs with an economical pricing scheme. In this work, we assume that the charging rate of OEVs is nP_p and the value n is selected such that nP_p is less than the maximum capacity of an OBC (P_c^{max}). Therefore, it is considered that $P_c^{max} = nP_p^{max}$.

Although the OBC capacity is nP_p^{max}, we consider that the initial capacity of the FCS is MP_p^{max}. In this work, we intend to analyze the possibility of enhancing capacity utilization with the help of heterogeneous EV users. However, with regard to M OBCs, the maximum capacity of FCS is nMP_p^{max}. Depending on the progressing charging demand, the capacity of the FCS can be scaled up to nMP_p^{max} from MP_p^{max}.

This work intends to develop a Monte Carlo simulation-based performance assessment framework to analyze proposed charging resource coordination strategies. When we consider the whole charging management at the FCS, there are two stages: (1) scheduling PEVs in an optimal way to maximize the profit; (2) admitting OEVs as secondary users to further enhance the utilization of limited charging resources. In this work, we focus on the impact of opportunistic users over PEVs and themselves. Monte Carlo simulation is used to analyze system dynamics and uncertainties associated with the EV charging process.

2.2.1 Stochastic EV Mobility Model

Monte Carlo simulation is developed to analyze proposed charging coordination strategies. Therefore, the following assumptions are made to develop this MCS model.

- The arrivals of PEVs and OEVs are Poisson processes with mean arrival rates of λ_p and λ_o, respectively (λ denotes the average number of charging requests made by the respective category of EVs per unit time).
- All OBCs are homogeneous and the charging time of an OBC is exponentially distributed with the service rate of μ_c (μ_c rate denotes the average number of charged EVs per OBC per unit time).
- Admission delays associated with EVs at the FCS are negligible as compared to charging times.

The EV mobility model is developed as a continuous-time discrete-space stochastic model. The arrival rate and service rate are considered as time-dependent data to cater system dynamics. Let T be the planning horizon and thus, we consider δt intervals over T. Consequently, the planning horizon can be denoted as $(0, \delta t, 2\delta t, \ldots, t, t+\delta t, t+2\delta t, \ldots, T)$. It is considered that the number of arrivals within time interval t follows a Poisson distribution under the following conditions. If the average arrival rate of EVs is λ_t ($\lambda_t > 0$) over the $[t,\ t+\delta t]$, the probability of one arrival of EV during $[t,\ t+\delta t]$ is $\lambda_t t + O(\delta t)$; $O(\delta t)$: order of δt. The probability of more than one arrival of EVs during $[t,\ t+\delta t]$ is $O(\delta t)$. The occurrence of EV arrivals in non-overlapping intervals are mutually independent. Then, the number of EV arrivals ($N_t,\ t \geq 0$) occurring during $[t,\ \delta t]$ can be modeled as a Poisson process with parameter λ_t as expressed in (2.1) [77–79].

$$P\{N_t\} = \frac{\exp(\lambda_t)(\lambda_t)^{N_t}}{N_t!} \tag{2.1}$$

2.2.2 Dynamic Charging Coordination Model

To develop the MCS model with proposed event-based dynamic charging coordination strategies, the following events are considered: PEV or OEV arrivals at FCS and PEV or OEV departures from FCS. Each plugged-in EV and each queued EV are sequentially indexed and placed in dynamic arrays $\left(\boldsymbol{A^{ev}_{j_{ev}(t)\times l}};\ j_{ev}(t) \leq M\right)$ and $\left(\boldsymbol{A^{q}_{j_q(t)\times l}};\ j_q(t) \leq Q\right)$, respectively, to analyze system dynamics. Let t^a_k, t^p_k, t^c_k, t^r_k, α_k, and β_k be the arrival time, plugged-in time, required charging time, remaining charging time, EV user type, and index of the kth $(k \in \mathbb{Z}^+)$ plugged-in EV, an element of $\boldsymbol{A^{ev}_{j_{ev}(t_k)}}$ associated with the kth PEV or OEV arrival at time t_k can be expressed as (2.2). Similarly, an $\boldsymbol{A^{ev}_{j_{ev}(\tau_m)}}$ element is derived for an PEV or OEV departure at time τ_m. If t_c follows the exponential distribution, it is expressed in (2.3).

$$\boldsymbol{A^{ev}_{j_{ev}(t_k)}} = \{t^a_k,\ t^p_k,\ t^c_k,\ t^r_k,\ \alpha_k,\ \beta_k\} \tag{2.2}$$

$$P(t_c, \mu_c) = \frac{1}{\mu_c} \exp\left(\frac{-t_c}{\mu_c}\right) \tag{2.3}$$

The MCS model keeps its current state in terms of allocated resources, the number of plugged-in EVs, and their charging power unchanged until the next event occurs. Information pertaining to all possible events is kept in matrix $\boldsymbol{A^{ev}_{M\times l\times T}}$. Therefore, $\boldsymbol{A^{ev}}$ that accounts for all possible x events taken place at t_1, t_2, ... ,t_x within 0 to T can be expressed as (2.4). Similarly, all the information of queued EVs at each event is kept in $\boldsymbol{A^q}$ expressed in (2.5).

$$\boldsymbol{A^{ev}} = \left[\boldsymbol{A^{ev}_{j_{ev}(t_1)}},\ \boldsymbol{A^{ev}_{j_{ev}(t_2)}},\ \ldots\ , \boldsymbol{A^{ev}_{j_{ev}(t_k)}},\ \boldsymbol{A^{ev}_{j_{ev}(t_{k+1})}},\ \ldots\ , \boldsymbol{A^{ev}_{j_{ev}(t_x)}},\ \right] \tag{2.4}$$

$$\boldsymbol{A^{q}} = \left[\boldsymbol{A^{q}_{j_q(t_1)}},\ \boldsymbol{A^{q}_{j_q(t_2)}},\ \ldots\ , \boldsymbol{A^{q}_{j_q(t_k)}},\ \boldsymbol{A^{q}_{j_q(t_{k+1})}},\ \ldots\ , \boldsymbol{A^{q}_{j_q(t_x)}},\ \right] \tag{2.5}$$

The FCS is obliged to admit PEVs if they arrive within the scheduled time period. For charging resource allocation, M number of OBCs and a queue with Q number of QPs $(M, Q \in \mathbb{Z}^+)$ are considered. The queue is reserved only for OEVs at the arrival if charging resources are not adequate to admit them. To update system matrix $\boldsymbol{A^{ev}}$ and $\boldsymbol{A^q}$, the following events are considered.

Arrival of PEVs at FCS: Charging resource allocation for PEVs is illustrated in Algorithm 2.1. When an PEV arrives at the FCS at time t_k, if there is at least one idle CP, it is plugged into the FCS without disturbing any ongoing OEV charging process. Otherwise, one charging process of OEV has to be preempted to admit the newly arrived PEV, as they are liable to do so.

Departure of PEVs from FCS: Algorithm 2.2 explains how charging resources are coordinated upon a departure of PEV at time t_k. Once an PEVs' charging process regularly finishes, it departs the FCS, resulting in an idle OBC. For this OBC, the chance is given to queued OEVs if any. Otherwise, the OBC will be idle.

Algorithm 2.1: Pseudo code (PC) for updating $\boldsymbol{A}^{ev}_{j_{ev}(t_k)}$ at PEV arrivals.

Input : $j_s(t_k)$: Number of plugged-in PEVs at time t_k
Input : $j_u(t_k)$: Number of plugged-in OEVs at time t_k
Input : $j_{sa}(t_k)$: Total number of arrived PEVs at time t_k
Input : $j_{ev}(t_k)$: Total number of plugged-in EVs by time t_k
Output: $\boldsymbol{A}^{ev}_{j_{ev}(t_k)}$: Plugged-in EVs matrix at time t_k
Output: $\boldsymbol{A}^{q}_{j_q(t_k)}$: Queued EVs matrix at time t_k

if $j_s(t_k) + nj_u(t_k) < M$ **then**
  $j_s(t_{k+1}) = j_s(t_k) + 1,\ j_u(t_{k+1}) = j_u(t_k)$
  $j_{sa}(t_{k+1}) = j_{sa}(t_k) + 1,\ j_{ev}(t_{k+1}) = j_{ev}(t_k) + 1$
  PEV is plugged-into an idle OBC.
  $\boldsymbol{A^{ev}_{j_{ev}(t_{k+1})}}(i; \alpha_k \sim idle) = \left\{t^a_{k+1},\ t^p_{k+1},\ t^c_{k+1},\ t^r_{k+1},\ \alpha_{k+1},\ \beta_{k+1}\right\}$
else if $j_s(t_k) + nj_u(t_k) == M\ AND\ j_u(t) > 0$ **then**
  $j_s(t_{k+1}) = j_s(t_k) + 1,\ j_u(t_{k+1}) = j_u(t_k) - 1$
  $j_{sa}(t_{k+1}) = j_{sa}(t_k) + 1,\ j_{ev}(t_{k+1}) = j_{ev}(t_k)$
  PEV is plugged-into the vacated OBC by OEV.
  $\boldsymbol{A^{ev}_{j_{ev}(t_{k+1})}}(i; \alpha_k \sim oev) = \left\{t^a_{k+1},\ t^p_{k+1},\ t^c_{k+1},\ t^r_{k+1},\ \alpha_{k+1},\ \beta_{k+1}\right\}$
else
  Block the PEV
end

Algorithm 2.2: PC for updating $\boldsymbol{A}^{ev}_{j_{ev}(t_k)}$ and $\boldsymbol{A}^{q}_{j_q(t_k)}$ at PEV departures.

Input : $j_s(t_k)$: Number of plugged-in PEVs at time t_k
Input : $j_u(t_k)$: Number of plugged-in OEVs at time t_m
Input : $j_q(t_k)$: Total number of queued OEVs at time t_k
Input : $j_{ev}(t_k)$: Total number of plugged-in EVs at time t_k
Input : $\boldsymbol{A}^{q}_{j_q(t_k)}$: Queued EVs matrix at time t_k
Output: $\boldsymbol{A}^{ev}_{j_{ev}(t_k)}$: Plugged-in EVs matrix at time t_k

$j_s(t_{k+1}) = j_s(t_k) - 1$
if $(0 < j_q(t_k) \leq Q)\ AND\ (M - (j_s(t_{k+1}) + nj_u(t_k)) \geq n)$ **then**
  $j_u(t_{k+1}) = j_u(t_k) + 1$
  $j_q(t_{k+1}) = j_q(t_k) - 1,\ j_{ev}(t_{k+1}) = j_{ev}(t_k)$
  Queued OEV is plugged-in.
  $\boldsymbol{A^{ev}_{j_{ev}(t_{k+1})}}(i; t^r_k == 0) = \boldsymbol{A^{q}_{j_q(t_k)}}(1)$
else
  $j_s(t_{k+1}) = j_s(t_k) - 1,\ j_u(t_{k+1}) = j_u(t_k)$
  $j_q(t_{k+1}) = j_q(t_k),\ j_{ev}(t_{k+1}) = j_{ev}(t_k) - 1$
  OBC is idle.
  $\boldsymbol{A^{ev}_{j_{ev}(t_{k+1})}}(i; t^r_k == 0) = \boldsymbol{0}$
end

Arrival of OEVs at FCS: The FCS accepts OEVs if PEVs do not occupy all the OBCs. The charging process of plugged-in OEVs are not preempted upon the arrival of a new OEV. When a new OEV arrives at the FCS, it is plugged in if at least an OBC and enough energy resources are available to provide a charge rate of P_o^{max}. Otherwise, the OEV is blocked. Charging resource allocation for newly arrived OEVs is illustrated in Algorithm 2.3.

Departure of OEVs from FCS: Unlike for PEVs, an OEV departure leaves one OBC and energy resources associated with n OBCs. The idle OBC(s) that appeared in the FCS due to the departure of an OEV will be offered to EVs waiting in the queue. If the queue is empty, then the vacant OBC(s) become idle. The charging resource coordination upon an OEV departure is performed according to Algorithm 2.4.

Algorithm 2.3: PC for updating $\boldsymbol{A}^{ev}_{j_{ev}(t_k)}$ and $\boldsymbol{A}^{q}_{j_q(t_k)}$ at OEV arrivals.

Input : $j_s(t_k)$: Number of plugged-in PEVs at time t_k
Input : $j_u(t_k)$: Number of plugged-in OEVs at time t_k
Input : $j_{ua}(t_k)$: Total number of arrived PEVs at time t_k
Input : $j_{ev}(t_k)$: Total number of plugged-in EVs by time t_k
Output: $\boldsymbol{A}^{ev}_{j_{ev}(t_k)}$: Plugged-in EVs matrix at time t_k
Output: $\boldsymbol{A}^{q}_{j_q(t_k)}$: Queued EVs matrix at time t_k

if $M - (j_s(t_k) + nj_u(t_k)) \geq n$ **then**
  $j_s(t_{k+1}) = j_s(t_k),\ j_u(t_{k+1}) = j_u(t_k) + 1$
  $j_{ua}(t_{k+1}) = j_{ua}(t_k) + 1,\ j_{ev}(t_{k+1}) = j_{ev}(t_k) + 1$
  OEV is plugged-into an idle OBC.
  $\boldsymbol{A}^{\boldsymbol{ev}}_{\boldsymbol{j_{ev}(t_{k+1})}}(i; \alpha_k \sim idle) = \left\{t^a_{k+1},\ t^p_{k+1},\ t^c_{k+1},\ t^r_{k+1},\ \alpha_{k+1},\ \beta_{k+1}\right\}$
else if $j_q(t_k) < Q$ **then**
  $j_s(t_{k+1}) = j_s(t_k),\ j_u(t_{k+1}) = j_u(t_k) + 1$
  $j_{sa}(t_{k+1}) = j_{sa}(t_k) + 1,\ j_{ev}(t_{k+1}) = j_{ev}(t_k)$
  OEV is queued.
  $\boldsymbol{A}^{\boldsymbol{q}}_{\boldsymbol{j_q(t_{k+1})}}(i; \alpha_k \sim vacant) = \left\{t^a_{k+1},\ t^p_{k+1},\ t^c_{k+1},\ t^r_{k+1},\ \alpha_{k+1},\ \beta_{k+1}\right\}$
else
  Block the PEV
end

Figure 2.3 shows how these algorithms work together in the MCS to determine the system matrix $\boldsymbol{A}^{ev}$ and $\boldsymbol{A}^{q}$ at considered events. These algorithms (2.1 - 2.4) calculate the system parameters defined in eq. 2.2 at the events of arrival and departure of EVs. Specifically, Algorithm 2.1 and 2.2 determine the system marix $\boldsymbol{A}^{ev}$ and $\boldsymbol{A}^{q}$ upon arrival and departure of PEVs. Similarly, Algorithm 2.3 and 2.4 perform with the arrival and departure of OEVs.

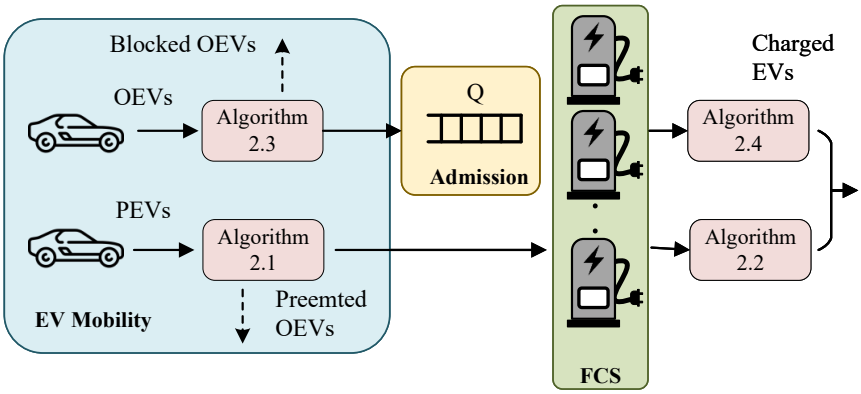

Figure 2.3: The structure of MCS with defined algorithms

Algorithm 2.4: PC for updating $\boldsymbol{A}^{ev}_{j_{ev}(t_k)}$ and $\boldsymbol{A}^{q}_{j_q(t_k)}$ at OEV departures.

Input : $j_s(t_k)$: Number of plugged-in PEVs at time t_k
Input : $j_u(t_k)$: Number of plugged-in OEVs at time t_k
Input : $j_q(t_k)$: Total number of queued OEVs at time t_k
Input : $j_{ev}(t_k)$: Total number of plugged-in EVs at time t_k
Input : $\boldsymbol{A}^{q}_{j_q(t_k)}$: Queued EVs matrix at time t_k
Output: $\boldsymbol{A}^{ev}_{j_{ev}(t_k)}$: Plugged-in EVs matrix at time t_k

if $(0 < j_q(t_k) \leq Q)$ **then**
  $j_s(t_{k+1}) = j_s(t_k),\ j_u(t_{k+1}) = j_u(t_k)$
  $j_q(t_{k+1}) = j_q(t_k) - 1,\ j_{ev}(t_{k+1}) = j_{ev}(t_k)$
  Queued OEV is plugged-in.
  $\boldsymbol{A}^{\boldsymbol{ev}}_{\boldsymbol{j_{ev}(t_{k+1})}}(i; t^r_k == 0) = \boldsymbol{A}^{\boldsymbol{q}}_{\boldsymbol{j_q(t_k)}}(1)$
else
  $j_s(t_{k+1}) = j_s(t_k),\ j_u(t_{k+1}) = j_u(t_k) - 1$
  $j_q(t_{k+1}) = j_q(t_k),\ j_{ev}(t_{k+1}) = j_{ev}(t_k) - 1$
  OBC is idle.
  $\boldsymbol{A}^{\boldsymbol{ev}}_{\boldsymbol{j_{ev}(t_{k+1})}}(i; t^r_k == 0) = \boldsymbol{0}$
end

2.3 FCS Centric Performance Evaluation Parameters

At an FCS, the optimum resource allocation for EVs is very indispensable for sustainable operation. When there are two EV categories, it is necessary to analyze the blockages and waiting of inferior users. However, high charging resource utilization may affect the charging completion rates of both plugged-in PEVs and OEVs. Upon the arrival of PEVs, some charging processes of OEVs might be preempted. Analyzing all these aspects is very essential for the FCS to provide high QoS.

In this Chapter, we develop an MCS model with proposed resource allocation and charging coordination strategies as an event-driven model and simulate for a large time horizon until the model comes to its equilibrium. From the system matrices ($\boldsymbol{A^{ev}}$, $\boldsymbol{A^{q}}$), we have analyzed the performance of developed strategies in terms of charging resource utilization and charging service quality.

2.3.1 Blocking Probability of OEVs ($P_{b,oev}$)

Although the FCS accepts OEVs to enhance the utilization of limited charging resources, there may be occasions where a charging request from an OEV has to be dropped due to limited or unavailable charging resources. Therefore, upon arrival of an OEV at the FCS, there is a probability that the charging request is denied. This EV blockage is a crucial factor to be analyzed from a service quality perspective. A charging request from an OEV is denied when the following conditions are met at the same time: (1) all OBCs are occupied; (2) energy resources are not adequate to admit the new OEV; (3) the allocated space for the queue is full. The blocking probability of OEVs can be obtained with (2.6).

$$P_{b,oev} = \frac{j_{ua}(t_x) - \sum_{k=1,\ j_u(t_k)>j_u(t_{k-1})}^{x} [j_u(t_k) - j_u(t_{k-1})]}{j_{ua}(t_x)} \ ; \ \forall \boldsymbol{A}^{ev}_{j_{ev}(t_k)|t\in[0\ T]} \tag{2.6}$$

2.3.2 Preempting Probability of OEVs ($P_{p,oev}$)

According to the defined admission control and charging coordination strategies, the charging process of OEVs are liable to be preempted if charging resources are not adequate to admit PEVs. This action is defined as the preempting of OEVs. Therefore, the probability at which an ongoing charging process of a OEV is forcibly terminated before being regularly finished is termed as the preempting probability of OEVs. If there are limitations for certain user types to utilize limited charging resources, the charging quality of such users is a crucial factor to be analyzed for long-term benefits. By considering derived system matrix ($\boldsymbol{A^{ev}}$), $P_{p,oev}$ can be derived as expressed in (2.7).

$$P_{p,oev} = \frac{\sum_{k=1,\ j_s(t_k)>j_s(t_{k-1}),\ j_u(t_k)<j_u(t_{k-1})}^{x} [j_u(t_{k-1}) - j_u(t_k)]}{\sum_{k=1,\ j_u(t_k)>j_u(t_{k-1})}^{x} [j_u(t_k) - j_u(t_{k-1})]} \ ; \ \forall \boldsymbol{A}^{ev}_{j_{ev}(t_k)|t\in[0\ T]} \tag{2.7}$$

2.3.3 Mean Charging Time at FCS ($\bar{t}_c$)

Amidst busy schedules, users prefer to get their EVs recharged as fast as possible, hence, the total time spent at the FCS is going to be a crucial measure for evaluating the service quality provided by the FCS. Total time of charging is not only essential for operation management but also for finding the optimum location and the size of the FCS within a certain area/region. Specifically, analyzing the mean time spent by an opportunistic OEV at the FCS is indispensable for assuring quality service for secondary users.

The total time spent by PEVs at FCS is nothing but the required charging time to attain the requested SoC. However, as some of OEVs have to wait at the queue and terminate their charging process forcibly before being regularly finished, this $\bar{t}_c$ provides very essential QoS measurement for opportunistic users. Mean charging time of PEVs can be obtained from ($\boldsymbol{A^{ev}}$) as expressed in (2.8).

$$\bar{t}_{c,pev} = \frac{\substack{\sum_{k=1,}^{x} \sum_{i=1,}^{j_{ev}(t_k)} t_i^c \\ \beta_k \neq \beta_{k-1},\ \alpha_i \sim pev}}{\substack{\sum_{k=1,}^{x} [j_s(t_{k-1}) - j_s(t_k)] \\ j_u(t_k) == j_u(t_{k-1}),\ j_s(t_k) < j_s(t_{k-1})}} \ ;\ \forall \boldsymbol{A}^{ev}_{j_{ev}(t_k)|t\in[0\ T]} \tag{2.8}$$

$$\bar{t}_{c,oev} = \frac{\substack{\sum_{k=1,}^{x} \sum_{i=1,}^{j_{ev}(t_k)} t_i^c \\ \beta_k \neq \beta_{k-1},\ \alpha_i \sim oev,\ t_i^r == 0}}{\substack{\sum_{k=1,}^{x} [j_u(t_{k-1}) - j_u(t_k)] \\ j_s(t_k) == j_s(t_{k-1}),\ j_u(t_k) < j_u(t_{k-1})}} \ ;\ \forall \boldsymbol{A}^{ev}_{j_{ev}(t_k)|t\in[0\ T]} \tag{2.9}$$

In order to analyze the total time spent by OEVs at the FCS, we consider both mean charging time ($\bar{t}_c$) and mean waiting time ($\bar{t}_q$) at the queue. Therefore, the total waiting time of OEVs over total queued OEVs gives the mean waiting time of OEVs ($\bar{t}_{q,oev}$) as expressed in (2.10).

$$\bar{t}_{q,oev} = \frac{\substack{\sum_{k=1,}^{x} \sum_{i=1,}^{j_{ev}(t_k)} t_i^a - t_i^p \\ \beta_k \neq \beta_{k-1},\ \alpha_i \sim oev}}{\substack{\sum_{k=1,}^{x} [j_u(t_k) - j_u(t_{k-1})] \\ j_u(t_k) > j_u(t_{k-1})}} \ \begin{matrix} ;\ \forall \boldsymbol{A}^{ev}_{j_{ev}(t_k)|t\in[0\ T]} \\ ;\ \forall \boldsymbol{A}^{q}_{j_q(t_k)|t\in[0\ T]} \end{matrix} \tag{2.10}$$

The total mean time spent by an EV user type (PEV or OEV) can be found by calculating the summation of ($\bar{t}_c$) and ($\bar{t}_q$).

2.3.4 Mean Charging Completion Rate ($\dot{c}$)

Mean charging completion rate ($\dot{c}$) of a particular EV user type implies the corresponding number of charging processes that finish regularly attaining the requested SoC within unit time. As we have employed secondary users over scheduled or registered users in the proposed strategies, it is very essential to evaluate the impact on one another in the charging process. Therefore, $\dot{c}_{pev}$ and $\dot{c}_{oev}$ are expressed in (2.11) and (2.12), respectively.

$$\dot{c}_{pev} = \frac{\sum_{k=2,}^{x} [j_s(t_{k-1}) - j_s(t_k)]/T}{j_u(t_k) == j_u(t_{k-1}),\ j_s(t_k) < j_s(t_{k-1})};\ \forall \boldsymbol{A}^{ev}_{j_{ev}(t_k)|t\in[0\ T]} \tag{2.11}$$

$$\dot{c}_{oev} = \frac{\sum_{k=2,}^{x} [j_u(t_{k-1}) - j_u(t_k)]/T}{j_s(t_k) == j_s(t_{k-1}),\ j_u(t_k) < j_u(t_{k-1})};\ \forall \boldsymbol{A}^{ev}_{j_{ev}(t_k)|t\in[0\ T]} \tag{2.12}$$

2.3.5 Charging Resource Utilization of FCS (U)

The main objective of this work is to further maximize the utilization of limited charging resources with opportunistic OEVs providing a compensation to underutilization of limited charging resources due to various uncertainties associated with EV charging process. Therefore, charging resource utilization is an important parameter to present the overall performance of the FCSs' operation. In this work, as we have considered the total capacity of the FCS along with the number of OBCs instead of employing a separate demand limit.

The charging resource utilization (U) is defined as the steady state value of utilized OBCs over the total number of OBCs. Therefore, U can be expressed as in (2.13).

$$U = \sum_{k=1}^{x} \left[j_s(t_k) + n j_u(t_k) \right] / Mx; \; \forall \boldsymbol{A}^{ev}_{j_{ev}(t_k)|t\in[0\ T]} \tag{2.13}$$

The presented MCS based analytical model assesses the performance of proposed dynamic charging resource coordination strategies for selected categories of EV users depending on their charging priorities.

2.4 Results and Discussion

How to compensate under-utilization of limited charging resources of an FCS due to uncertainties associated with PEV charging process is analyzed in this work. This Section elaborates the behavior of FCS for variation of EV arrivals. In this Section, we have in-cooperated derived performance assessment parameters in Section 2.3 to evaluate the ability of developed charging resource coordination strategies in enhancing the charging resource utilization whilst a satisfactory service quality for EV users. In the considered scenario, the FCS is equipped with 10 CPs (i.e, $M = 10$) that can adjust the charging power within a specified range in steps. The MCS parameter n is set to 2.

2.4.1 Charging Resource Utilization

We intend to analyze how OEVs can enhance the utilization of limited charging resources by quickly exploiting charging resources when PEVs do not occupy. In this analysis, we consider the variation of charging resource utilization with and without OEVs.

Therefore, we have considered three cases where λ_o is set to 18 h^{-1}, 24 h^{-1} and 30 h^{-1} while λ_p varies from 0 to 60 h^{-1} . The variation of U against λ_p is shown in Figure 2.4. Figure 2.4 depicts that unexploited charging resources by PEVs can be effectively utilized with OEVs. It is evident that proposed strategies have improved the U with opportunistic OEVs. Limited charging resources are not optimally utilized at higher values of λ_p due to high blockages of EVs. For the considered case in Figure 2.4, the U can not be enhanced beyond 78%. But by allowing opportunistic OEVs to exploit unused charging resources to attain high power charging, the U has been improved up to 90%.

Figure 2.5 plots the variation of U against λ_p and λ_o. From Figure 2.5, it can be seen that the U can not be improved more than 78% only with PEVs even at high arrival rates. But by letting OEVs to exploit available charging resources when PEVs are not very much active within the FCS, limited charging resources can be maximally (92%) utilized.

Even for lower values of λ_p, U is significantly enhanced with opportunistic OEVs. U against λ_p and λ_o shows continuous ascent with positively decreeing slope due to high blockages of EVs and preemptions of OEVs at high arrival rates.

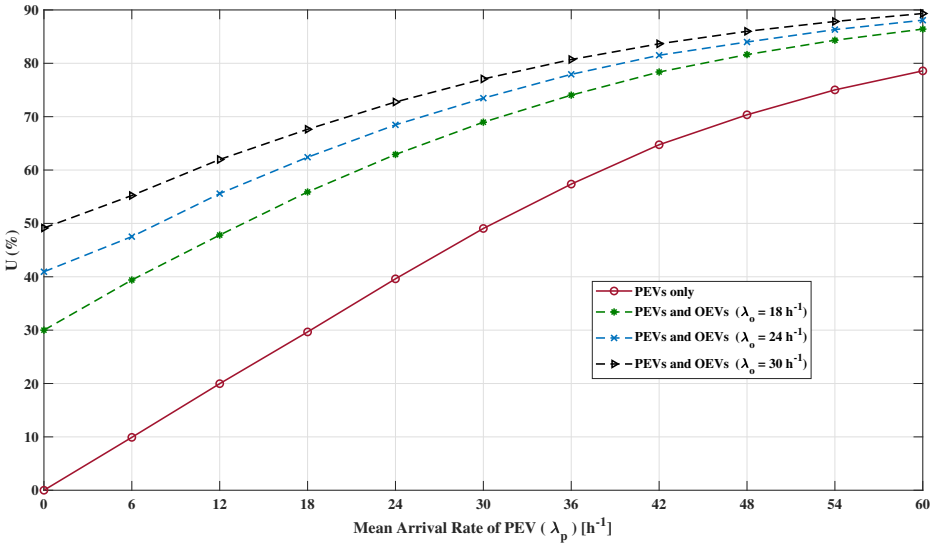

Figure 2.4: Charging resource utilization with λ_p

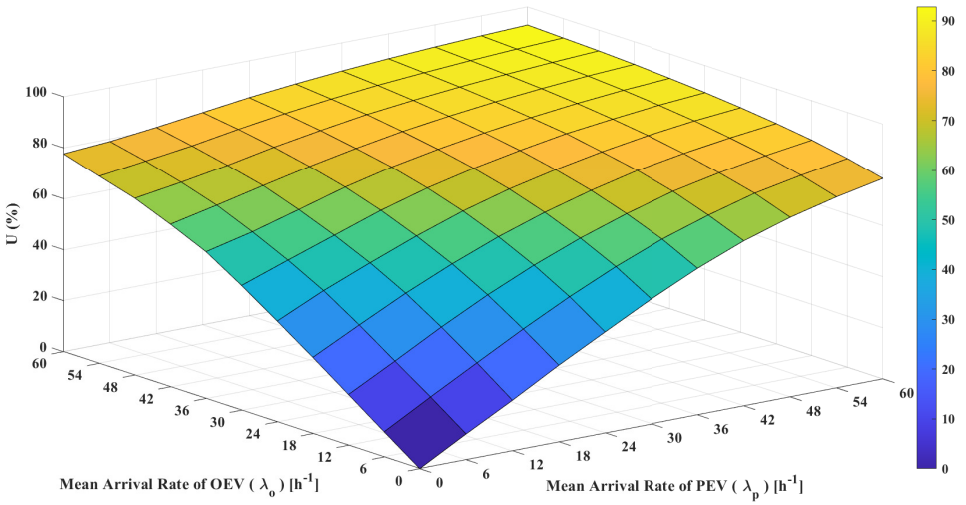

Figure 2.5: Charging resource utilization with λ_p and λ_o

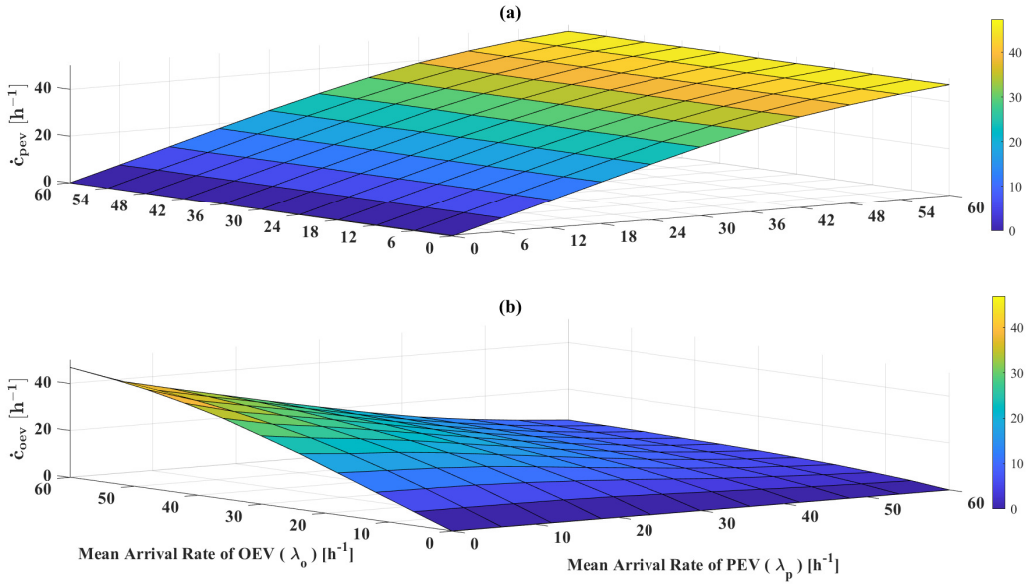

Figure 2.6: Mean charging completion rate of EVs with λ_p and λ_o

2.4.2 Mean Charging Completion Rate

To analyze the impact of opportunistic OEVs on the charging process of PEVs, the mean charging completion rate of particular EV user type is used. The mean charging completion rate ($\dot{c}$) implies the number of completed charging processes of concerned EV user category within unit time. Assuring a high quality service for PEVs is dispensable as they have prior agreements for an uninterruptible charging process. Derived expressions for the mean charging completion rates of PEVs ($\dot{c}_{pev}$) and OEVs ($\dot{c}_{oev}$) (equations (2.11) and (2.12)) are considered for the analysis in this subsection. Figure 2.6 (a) and (b) illustrate the variation of mean completion rates of PEVs and OEVs as a function of λ_p and λ_o , respectively. Increment of PEV arrivals at FCS deteriorates the mean charging completion rate of OEVs but it does not happen in vise versa. $\dot{c}_{pev}$ shows continuous ascent against the λ_p with positively decreasing slope due to possible blockages of PEVs at high arrival rates. More importantly, resource coordination strategy with aggregation shows better performance in terms of the charging completion of PEVs. In order to analyze the mutual impact of EV charging completion, we have plotted $\dot{c}$ against both λ_p and λ_o within a range starting from 0 to 60 h^{-1} . As Figure 2.6 (a) depicts, obviously, increment of λ_o does not make any impact on PEVs. Nevertheless, although $\dot{c}_{oev}$ shows a continuous ascent with λ_o, the rate of change of increment gradually decrease when λ_p is increased.

2.4.3 Blocking and Preempting Probability of OEVs

When there are different user categories with defined privileges, assessing user satisfaction in terms of accessing and utilizing limited charging resources is vital. Especially, as OEVs are liable to terminate their charging process forcibly if charging

resources are not adequate to admit the newly arrived PEV, evaluating the likelihood of such preemptages is indispensable for long-term operation of the FCS. Therefore, we have analyzed the blocking and preempting probability of Figure 2.7 (a) and (b) depict the variation of blocking and preempting probabilities of OEVs as a function of both λ_p and λ_o. From Figure 2.7, we can observe that both blocking and preempting probabilities of OEVs show continuous ascent with λ_p. It can be seen that the blockage and preemptage of OEVs become significant when PEVs are more active. In the considered scenario (Figure 2.7), for the available EV charging resources, the blocking probability gradually increases to 0.6 when λ_p increases from 0 to 60 h^{-1}.

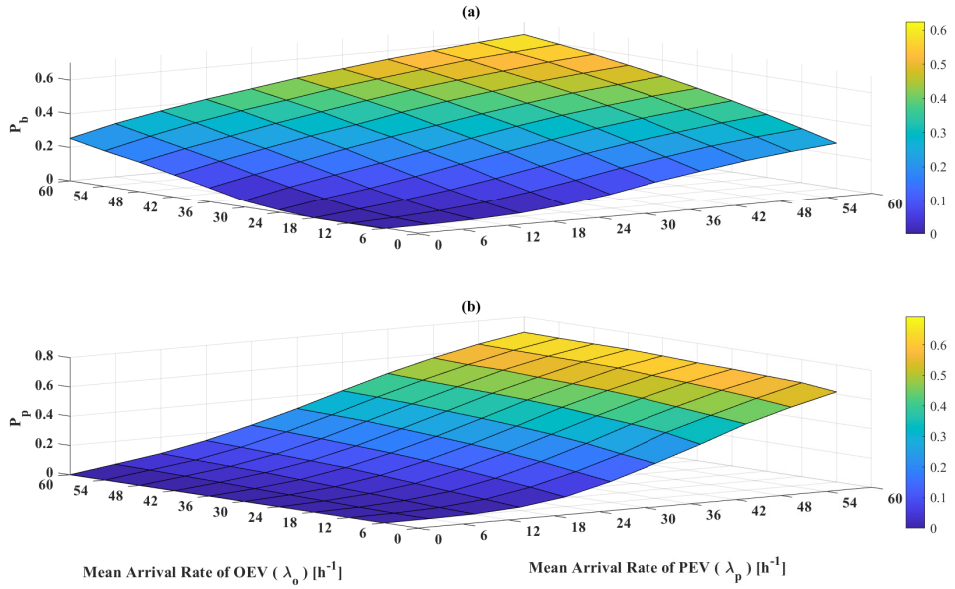

Figure 2.7: (a) Blocking and (b) Preempting probability of OEVs with λ_p and λ_o

Nevertheless, we can observe that the blockage of OEVs is influenced by themselves. Moreover, at the same arrival rate of PEVs, the preempting probability is also around 0.6 which is a bit higher value from a service quality point of view. To provide satisfactory service to OEVs, the FCS would schedule PEVs so that it does not exceed the mean arrival rate 30 h^{-1} for a considered time horizon.

All these parameters should be taken into account to evaluate the FCS centric performance.

2.5 Conclusion

In this chapter, we have analyzed how opportunistic EV users can be in-cooperated to maximize the utilization of limited charging resources. The proposed strategy enables OEVs to exploit unused charging resources by scheduled EV users at FCS to enhance charging resource utilization. Developed event-based dynamic charging resource allocation and coordination strategies are analyzed with Monte-Carlo simulation.

The presented results prove that coordination strategy to optimally utilize the limited charging resources of FCS with OEVs considering uncertainties associated with EV charging process. In this chapter, the presented results prove that the developed charging resource coordination strategy significantly improves the charging resource utilization of the FCS at any arrival rate of PEVs. At higher arrival rates of EVs, FCS accomplishes more than 90% of resource utilization which is bounded to 78% only with PEVs.

Along with the proposed strategies, we have derived a framework in generic nature using MCS to assess the FCS-centric performance in terms of charging resource utilization, charging completion rates of EV users, blocking probability, preempting probability, waiting time, charging time, etc. This FCS-centric performance assessment framework can be in-cooperated at the planning and deployment stage to find the optimum siting and sizing of FCS. At the operating stage of an FCS, the developed framework can be used to ensure high-quality service to both PEVs and OEVs as it provides a quantitative overview of the whole charging process. The proposed work will be extended for analysis with charging resource aggregation and different OEV categories in Chapter 3. Charging coordination strategies will be further improved to reduce the preempting probability of OEVs with mobile chargers in Chapter 6.

Chapter 3

Maximization of Charging Resource Utilization with Resource Aggregation for Opportunistic Electric Vehicle Users

[3] *Widespread deployment of electric vehicle (EV) fast-charging stations (FCSs) can provide better solutions for challenges of EV charging pertaining to charging time, potential driving range anxiety and charging autonomy. However, the extra power demand caused by the fast charging of EVs at FCS must be coordinated with innovative charging management strategies. Even optimum utilization of limited charging resources can not be achieved owing to various uncertainties associated with the coordinated EV charging process. Therefore, this chapter focuses on charging resource coordination strategies so that opportunistic EV users (OEVs) can dynamically exploit these limited charging resources when registered users do not use them. Furthermore, proposed strategies enable OEVs to aggregate charging resources depending on their availability to achieve faster-charging rates. Moreover, the proposed dynamic charging resource coordination scheme is analyzed with a continuous-time Markovian (CTMC) process. Furthermore, an analytical model is developed to evaluate the overall performance of the FCS. Numerical results from the developed CTMC model demonstrate that the proposed strategies can achieve high resource utilization while guaranteeing a satisfactory quality of service to EV users.*

3.1 Introduction

The required number of electric vehicles (EVs) should be enormously high to meet the net-zero emission targets defined by International Energy Agency (IEA) with respect to what is available now [4].

[3] This chapter is based on the peer-reviewed journal paper, K. M. S. Y. Konara *et. al* "Maximal Utilization of Charging Resources of Fast Charging Station with Ultra-Fast Electric Vehicle Users," *eTransportation (ISSN 2590-1168)*, 2023, (Under Review)

The power-intensive load demand should be properly managed to optimally utilize the limited charging resources in an FCS. However, the energy is wasted if the FCS does not fully utilize its capacity. With the rapid growth of EVs, they tend to reach fast charging stations (FCSs) opportunistically rather than following charge schedule programs. At the same time, we should note that scheduling EV charging processes with sophisticated models is not very practical and feasible in a real-time dynamic environment. However, as described in Chapter 1, some commercial EV models with certain charging constraints have to participate in charge scheduling schemes as their charging time is comparatively high.

In Chapter 2, we analyze the possibility of employing opportunistic ultra-fast secondary EV users (OEVs) as a flexible load to utilize the limited charging resources including the generated renewable energy power. We understood that the limited charging resources including energy resources of FCS can be maximally utilized if we can allow ultra-fast charging users as opportunistic secondary users to get their EVs charged at lower prices with defined liabilities when scheduled users do not utilize the charging resources. Although the charging completion of OEVs is not affected by OEVs, the tendency of OEVs to participate in the proposed charging resource coordination scheme might be affected by the quality of service (QoS) of OEVs expressed in terms EV blockage, preemptage, waiting time, charging time, etc. As the charging resource aggregation level is fixed in the proposed strategies in Chapter 2, the demand flexibility of OEVs is limited.

In this Chapter 3, we consider a commercial FCS whose prime objective is to charge EVs registered at FCS. Such scheduled charging processes at the FCS are considered as primary EVs (PEVs). For the aforementioned FCS, we propose and analyze charging coordination strategies for OEVs to exploit unused charging resources to enhance the charging resource utilization at the FCS. We analyze the effectiveness of aggregating available charging resources at the FCS to dynamically adjust the charging rate of OEVs to get their EVs charged as fast as possible. Therefore, in this Chapter 3, we investigate, how dynamic charging resource aggregation helps to enhance the utilization of limited charging resources while providing quality service to both PEVs and OEVs. From the QoS perspective, more focus has been given to OEVs.

The novel technical contributions from this chapter can be summarized as follows,

1. Dynamic charging resource coordination strategies are proposed so that OEVs can exploit unused charging resources when PEVs do not fully utilize the capacity to enhance the utilization of limited charging resources at the FCS. The charging performance of OEVs is improved with resource aggregation.

2. Charging coordination strategies are proposed as an event-driven continuous-time model where an event is defined as either EV arrival or departure. At any time, when an event occurs, the system performs resource allocation and charging coordination but it keeps this schedule until the next event occurs.

In this manner, the charging coordination system can respond to more system dynamics compared that of with conventional time-slotted models with fixed intervals.

3. High QoS is guaranteed for PEV charging process so that PEVs are charged at a constant charge rate and without getting any disturbance from OEVs at any time. Nevertheless, in the proposed strategies, QoS of PEVs is improved by adjusting their charge rate depending on the available charging resources when an event occurs. As opposed to frequent on-off or modulating charging coordination strategies, proposed event-driven charging coordination strategies are more practical and feasible.

3.2 Dynamic Charging Coordination Strategies

The prime objective of FCS is to provide a reliable EV charging service to its registered customers (PEVs) who have registered with FCS to follow a charging schedule determined by a charging management scheme. Therefore, with the proposed strategies, FCS admits OEVs when PEVs are not very much active within the FCS to exploit unused charging resources to maximally utilize the limited charging resources. An illustration of opportunities where OEVs can exploit unused charging resources is depicted in Figure 3.1.

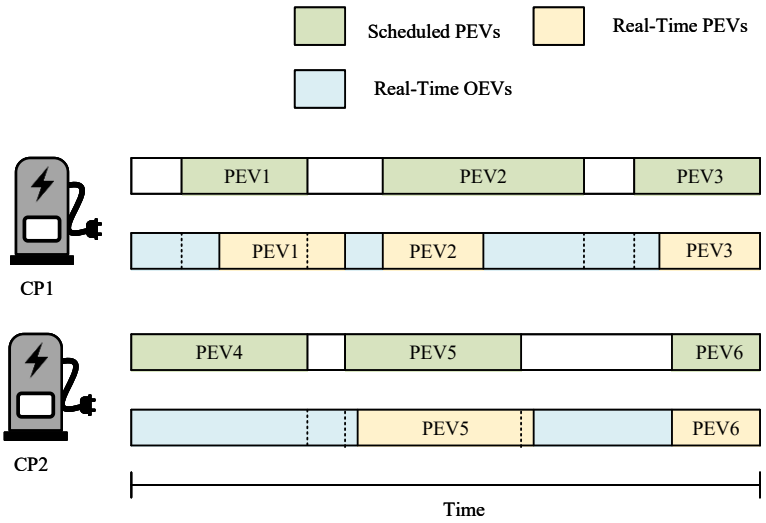

Figure 3.1: Charging resource utilization for PEVs and OEVs

However, charging processes of OEVs are liable to be preempted before being regularly finished, if charging resources are not adequate to admit newly arrived PEVs. In this work, we have considered an already deployed FCS with M ; ($M \in \mathbb{Z}^+$) number of charging points (CPs) which can facilitate variable rate EV charging. A queue space (Q) with q number of queue points (QPs) is allocated only for OEVs.

The proposed operating mechanism of the FCS is illustrated in Figure 3.2.

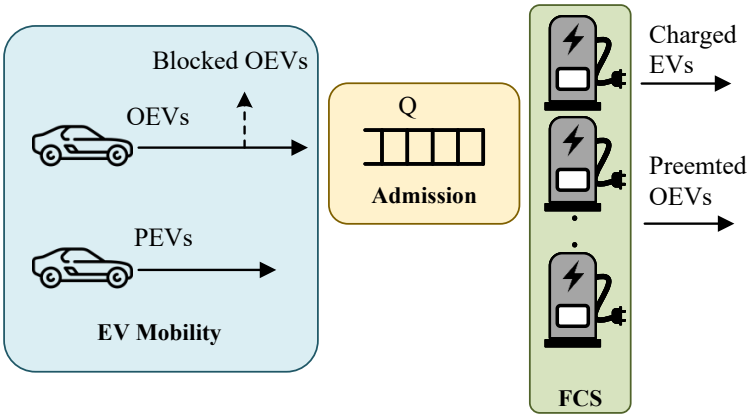

Figure 3.2: Proposed operation mechanism of the FCS

When we consider the operation of FCS, there are basically two types of EV users, as tabulated in Table 3.1: (1) PEVs and (2) OEVs with distinct privileges and constraints in accessing the FCS.

Table 3.1: Access Privileges and Constraints of EV users

PEVs	**OEVs**
• Access according to a prior agreement	• Access opportunistically
• Charged at specified charge rate P_p; $P_p \in [P_p^{min}, P_p^{max}]$	• Charged at variable charge rate $P_o = P_p \sim nP_p$ in steps; $(n \in \mathbb{Z}^+)$, $P_o \in [P_c^{min}, P_c^{max}]$
• Charger is guaranteed during scheduled time.	• Charger is assigned if charging resources are available only.
• Do not subject to blockages	• Subject to blockages
• Charging process regularly finishes.	• Charging process is liable to be preempted before regularly finishes.
• Expect uninterruptible EV charging	• Expect to charge quickly

Therefore, those who need undisturbed charging at FCS may go as PEVs. Usually, OEVs expect to charge their EVs as quickly as possible. Consequently, depending on the availability of charging resources, OEVs can aggregate more charging resources to attain a high charge rate. Consequently, EVs capable of fast charging with high charging power rates can request to be an OEV so that they can charge their EVs at a low cost. Therefore, in the proposed strategies, OEVs are able to adapt their charging power from P_p to $nP_p; (n \in \mathbb{Z}^+)$ in steps based on the availability of charging resources. The value n is selected so that nP_p is less than the maximum capacity of a CP (P_c^{max}).

Therefore, it is considered that $P_c^{max} = nP_p^{max}$.Therefore, considering M CPs, the maximum capacity of FCS is nMP_p^{max}. Depending on the progress of charging demand, the contract demand of the FCS can be lifted from MP_p^{max} to nMP_p^{max}. But with the uncertainties associated with EV charging process, even the MP_p^{max} is not optimally utilized. Therefore, in this work, we propose strategies to maximally utilize the charging resources with regard to the contract demand of MP_p^{max}.

In this study, we analyze the impact of charging OEVs at the FCS opportunistically when charging resources are not fully utilized by PEVs. Moreover, how charging resource aggregation of OEVs affect the overall charging process of the FCS is also analyzed. Depending on the resource availability, as OEVs adapt their charging rate in P_p steps, the charging resource aggregation of OEVs is analogous to the aggregation of CPs from 1 to n. Herein after, CP aggregation means the aggregation of charging resources associated with a CP. It is vital to analyze system dynamics along with uncertainties associated with EV charging process to achieve effective charging coordination.

3.3 Event Driven Continuous Time Markov Chain (CTMC) Model

Proposed charging coordination strategies are analyzed with the continuous-time Markov chain (CTMC) in this work. Therefore, to develop this CTMC, the following assumptions are made.

- The arrivals of PEVs and OEVs are Poisson processes with mean arrival rates of λ_p and λ_o, respectively. (λ denotes the average number of charging requests made by the respective category of EVs per unit time)
- All CPs are homogeneous and the service time of a CP is exponentially distributed with the service rate of μ_c. (μ_c rate denotes the average number of charged EVs per CP per unit time)
- Admission delays associated with EVs at the FCS are negligible as compared to charging times.

The CTMC developed with proposed dynamic charging coordination strategy is denoted as $DRC(n,q)$, where, first $'n'$ denotes the CP aggregation limits and $'q'$ is the maximum queue size of Q, respectively. In $DRC(n,q)$, following events are considered for state transitions; (1) PEV Arrivals at FCS (2) PEV Departures from FCS (3) OEV Arrivals at FCS (4) OEV Departures from FCS. In $DRC(n,q)$, we define a generic state $\mathbf{x}$; $\mathbf{x} = \{x_r, x_{s1}, .., x_{sk}, .., x_{sn}, x_q\}$ to model system dynamics at each event. In a generic state $\mathbf{x}$, x_r denotes the number of PEVs plugged-in at FCS and the number of OEVs with respective aggregated CPs are denoted by $[x_{s1}, .., x_{sk}, .., x_{sn}]$. Furthermore, x_q indicates the number of queued OEVs at FCS.

To develop $DRC(n,q)$, initial step is to find the set of feasible states of the system ($\mathbf{\Omega}$) from the whole state space. $\mathbf{\Omega} = \{\mathbf{x}|x_r, x_{s1}, .., x_{sk}, .., x_{sn}, x_q \geq 0;\ x_r \leq M, x_{sk}|\forall k \in [1, ..., n] \leq \lfloor (M/k) \rfloor,\ x_q \leq q,\ ; x_q = 0 \text{ if } a(\mathbf{x}) < M \text{ OR if } a(\mathbf{x}) = M, \sum_{i=2}^{n} x_{si} = 0, c(\mathbf{x}) > 0;\ \sum_{i=1}^{n-1} x_{si} = 0, x_{sn} \leq \lfloor (b(\mathbf{x})/n) \rfloor \text{ if } a(\mathbf{x}) < M, c(\mathbf{x}) > 0;\ \sum_{i=2}^{n} x_{si} = 0, \text{ if }, a(\mathbf{x}) = M, c(\mathbf{x}) > 0\}$. Where, $a(\mathbf{x})$, $b(\mathbf{x})$ and $c(\mathbf{x})$ are the total number of CPs utilized by plugged-in EVs, available CPs for OEVs and CPs utilized by plugged-in OEVs and expressed in $a(\mathbf{x}) = x_r + \sum_{k=1}^{n} k.x_{sk}$, $b(\mathbf{x}) = M - x_r$ and $c(\mathbf{x}) = \sum_{k=1}^{n} k.x_{sk}$ respectively. The level of charging resource aggregation is dynamically varied in n steps as per the charging resource availability. The state transitions (ST) of $DRC(n,q)$ owing to different events at the FCS are described in the subsequent subsections.

3.3.1 PEV Arrivals at FCS

STs triggered by the PEV arrivals are tabulated in ST Table 3.2. Generally, upon an arrival of a PEV, FCS is obliged to allocate resources immediately as they have prior-agreements. Consequently, when a PEV arrive at the FCS, if at least one idle CP, the PEV is plugged into CP without disrupting others. Otherwise, any ongoing OEV charging process must be interrupted. When a new PEV arrives at FCS while all CPs are being occupied (not necessarily be all physical CPs but the available total capacity of the FCS is fully utilized due to resource aggregation), if OEVs with aggregated $k; (\forall\ k \in [1, ..., n])$ CPs, the one with maximum number of aggregated CPs has to donate a CP to the newly arrived PEV. If there are no any OEVs with aggregated resources, one OEV charging process must be preempted to admit the newly arrived PEV. The destination states related to STs triggered by PEV arrivals from a generic state $\mathbf{x}$ of $DRC(n,q)$ at λ_p transition rate (TR) are tabulated in Table 3.2.

Table 3.2: STs from $\mathbf{x}$ of $DRC(n,q)$ at λ_p TR triggered by PEV Arrivals

Conditions		**Destination State**
At least an idle CP	$M - a(\mathbf{x}) > 0$	$\{x_r + 1, x_{s1}, \cdots, x_{sk}, \cdots, x_{sn}, x_q\}$
FCS is full. OEVs with aggregated CPs exist	$M - a(\mathbf{x}) = 0;\ x_{sk} > 0,$ $m = \max\{k \| x_{sk} > 0\}, 2 \leq k \leq n$	$\{x_r + 1, x_{s1}, \cdots, x_{s(m-1)} + 1,$ $x_{sm} - 1, \cdots, x_{sn}, x_q\}$
FCS is full. No OEVs with aggregated CPs	$M - a(\mathbf{x}) = 0;\ x_{s1} > 0;$ $x_{sk} = 0, 2 \leq k \leq n$	$\{x_r + 1, x_{s1} - 1, \cdots, x_{sk},$ $\cdots, x_{rn}, x_q\}$
FCS is full. No OEVs	$M - a(\mathbf{x}) = 0;\ c(\mathbf{x}) = 0$	$\{x_r, x_{s1}, \cdots, x_{sk}, \cdots, x_{sn}, x_q\}$

3.3.2 PEV Departures from FCS

When an idle CP appears in the FCS due to the departure of a PEV, it can be assigned to an OEV waiting in Q if any. If the queue is empty, the OEV who has minimum resource aggregation can increase its charge rate by aggregating the charging resources utilized. Otherwise, the CP will be idle.

The corresponding STs from $\mathbf{x}$ of $DRC(n,q)$, each with the TR of $x_r\mu_c$ upon departure of PEV under the conditions aforementioned is tabulated in Table 3.3.

Table 3.3: STs from $\mathbf{x}$ of $DRC(n,q)$ at $x_r\mu_c$ TR triggered by PEV Departures

Conditions		**Destination State**
There are OEVs in Q.	$0 < x_q \leq q$	$\{x_r - 1, x_{s1} + 1, \cdots, x_{sk}, \cdots, x_{sn}, x_q - 1\}$
Q is empty. There are OEVs.	$x_q = 0$; $l = \min\{k \mid x_{sk} > 0, 1 \leq k < n\}$	$\{x_r - 1, x_{s1}, \cdots, x_{sl} + 1, x_{s(l+1)}, \cdots, x_{sn}, x_q\}$
Q is empty. No OEVs.	$x_q = 0$; $c(\mathbf{x}) = 0$	$\{x_r, x_{s1}, \cdots, x_{sk}, \cdots, x_{sn}, x_q\}$

3.3.3 OEV Arrivals at FCS

FCS admits OEVs to the FCS when PEVs do not occupy all the CPs. Upon receipt of a charging request from an OEV, FCS seeks the maximum possible $k; (\forall\ k \in\ [1, ..., n])$ CPs that are idle at the moment to allocate resources. If all CPs are utilized, the OEV with maximum aggregated CPs has to donate one CP to admit the newly arrived charging request from OEV. However, if there are no ongoing OEV charging processes with aggregated resources, the newly arrived OEV will be queued if it is not full. Otherwise, the newly arrived charging request will be blocked. The corresponding STs triggered by aforementioned situations are tabulated in Table 3.4. Moreover, ST table Table 3.4 tabulates the destination states related to OEV arrivals with respect to a generic state $\mathbf{x}$ of $DRC(n,q)$ at λ_p TR.

Table 3.4: STs from $\mathbf{x}$ of $DRC(n,q)$ at λ_o TR triggered by OEV Arrivals

Conditions		**Destination State**
Sufficient idle CPs exist	$M - a(\mathbf{x}) \geq k, 1 \leq k \leq n$	$\{x_r, x_{s1}, \cdots, x_{sk} + 1, x_{s(k+1)}, \cdots, x_{sn}, x_q\}$
FCS is full. OEVs with aggregated CPs exist	$M - a(\mathbf{x}) = 0$; $x_{sk} > 0$, $m = \max\{k \mid x_{sk} > 0\}, 2 \leq k \leq n$	$\{x_r, x_{s1} + 1, \cdots, x_{s(m-1)} + 1, x_{sm} - 1, \cdots, x_{sn}, x_q\}$
FCS is full. Q is not full. No OEVs with aggre. CPs	$M - a(\mathbf{x}) = 0$; $x_q < q$; $x_{sk} = 0, 2 \leq k \leq n$	$\{x_r, x_{s1} - 1, \cdots, x_{sk}, \cdots, x_{rn}, x_q + 1\}$
FCS is full. No OEVs	$M - a(\mathbf{x}) = 0$; $c(\mathbf{x}) = 0$	$\{x_r, x_{s1}, \cdots, x_{sk}, \cdots, x_{sn}, x_q\}$

3.3.4 OEV Departures from FCS

Depending on the aggregation level, OEV may release one or more CPs. However, if there are queued vehicles, OEV leaves only one idle CP according to the defined admission control strategies. That idle CP will be allocated initially to the queue. If the vehicle queue is empty, multiple CPs could appear at the departure of OEV depending on its resources aggregation level.

Those CP(s) will be offered to OEVs to get their charging power level increased. Otherwise, the CP(s) will be idle. Corresponding STs are set out in Table 3.5.

Table 3.5: STs from $\mathbf{x}$ of $DRC(n,q)$ at $kx_s\mu_c$ TR triggered by OEV Departures

Conditions		**Destination State**
There are OEVs in Q.	$0 < x_q \leq q$	$\{x_r, x_{s1}, \cdots, x_{sk}, x_{s(k+1)}, \cdots, x_{sn}, x_q - 1\}$
Q is empty. There are OEVs.	$x_q = 0$; $x_{sl} > k$ $l = \min\{k \mid x_{sk} > 0, 1 \leq k < n\}$	$\{x_r, x_{s1}, \cdots, x_{sl} - k, x_{s(l+1)} + k \cdots, x_{sk} - 1, \cdots, x_{sn}, x_q\}$
Q is empty. There are OEVs.	$x_q = 0$; $x_{sl} < k$ $x_{s(l+1)} > (k - 2x_{sl})$ $l = \min\{k \mid x_{sk} > 0, 1 \leq k < n\}$	$\{x_r, x_{s1}, \cdots, x_{sl} - x_{sl}, x_{s(l+1)} + 2x_{sl} - k, x_{s(l+2)} + k - x_{sl} \cdots, x_{sk} - 1, \cdots, x_{sn}, x_q\}$
Q is empty. There are OEVs.	$x_q = 0$; $x_{sl} < k$ $x_{s(l+1)} < k - 2x_{sl}$ $x_{s(l+2)} > k - 2x_{sl} - 2x_{s(l+1)}$ $l = \min\{k \mid x_{sk} > 0, 1 \leq k < n\}$	$\{x_r, x_{s1}, \cdots, x_{sl} - x_{sl}, 0, x_{s(l+2)} + 2x_{s(l+1)} + 2x_{sl} - k, x_{s(l+3)} + k - x_{sl} - x_{s(l+1)} \cdots, x_{sk} - 1, \cdots, x_{sn}, x_q\}$
...	...	...
Q is empty. No OEVs.	$x_q = 0$; $c(\mathbf{x}) = 0$	$\{x_r, x_{s1}, \cdots, x_{sk}, \cdots, x_{sn}, x_q\}$

3.4 FCS Centric Performance Parameters

In this work, we model the proposed charging coordination strategies as an event-driven model using CTMC. In order to analyze the performance FCS's operation mechanism in terms of resource utilization and charging service quality, an analytical model with set of equations are derived.

System dynamics are studied considering the steady-state probability vector ($\pi(\mathbf{x})$) of the system that gives the corresponding steady-state probability of being in each and every state $\mathbf{x}$. To derive the ($\pi(\mathbf{x})$), we use the global balance equation and the normalization equation expressed in (3.2). In (3.2), $\mathbf{\Phi}$ is the TR matrix.

Non-diagonal elements ($\varphi_{x_i x_j}$; $x_i, x_j \in \mathbf{\Omega}$) of $\mathbf{\Phi}$ are calculated by getting the summation of TRs that are corresponding to all possible STs from x_i to x_j tabulated in STT 3.3 to 3.5 . Diagonal elements ($\varphi_{x_i x_i}$) of $\mathbf{\Phi}$ are found using (3.1).

$$\varphi_{x_i x_i} = - \sum_{x_j \in \mathbf{\Omega}, j \neq i} \varphi_{x_i x_j \ ; \ x_i, x_j \in \mathbf{\Omega}} \quad (3.1) \qquad \pi\mathbf{\Phi} = 0, \sum_{\mathbf{x} \in \mathbf{\Omega}} \pi(\mathbf{x}) = 1 \quad (3.2)$$

To analyze the performance of the long-term sustainable operation of the FCS, the optimum resource allocation for EVs is very indispensable. However, high charging resource utilization may affect the charging completion rates of both plugged-in PEVs and OEVs.

Upon the arrival of PEVs, some charging processes of OEVs might be preempted. Analyzing all these aspects are very essential for the FCU to provide high-quality service to EV users. Once $\pi(\mathbf{x})$ is determined using (3.2), the following performance parameters are derived in terms of $\pi(\mathbf{x})$ from the first principles.

3.4.1 Blocking Probability of OEVs ($P_{b,oev}$)

Upon the arrival of an OEV at the FCS, there is a probability that the charging request is denied for charging owing to the unavailability of charging resources. This EV blockage is a crucial factor to be analyzed at the charging station level from the sustainable operation perspective. The EV blockage generally happens with OEVs when they make a charging request from the FCS while it is fully occupied. A charging request from an OEV is blocked when the following conditions are met at the same time : (1) All CPs are occupied. (2) There is no any ongoing OEV charging processes with aggregated CPs. (3) The allocated space for queue is full. The blocking probability of OEVs are expressed in (3.3).

$$P_{b,oev} = \sum_{\substack{\mathbf{x}\in\mathbf{\Omega},\\ a(\mathbf{x})=M,\ \sum_{s=2}^{n} x_{si}=0,\\ x_q=q}} \pi(\mathbf{x}) \tag{3.3}$$

3.4.2 Preempting Probability of OEVs ($P_{p,oev}$)

In this study, OEVs are liable to terminate their charging process upon arrival of PEV if the charging resources are not adequate to admit the newly arrived PEV. This work defines this situation as preempting of OEVs. Therefore, the probability at which an ongoing charging process of OEV is preempted before being regularly finished is termed as the preempting probability of OEVs ($P_{p,oev}$).

From the overall performance of the FCS point of view, the preempting probability is a crucial factor in the quality of service assessments. Furthermore, an ongoing charging process of OEV has to be preempted if these three situations happen at the same time : (1) All CPs are occupied. (2) There is at least one ongoing OEV charging process. (3) There is no any ongoing OEV charging processes with aggregated CPs. Therefore, the mean preempting rate of OEVs ($\dot{\alpha}_{oev}$) is derived as expressed in (3.4). A portion of plugged-in OEVs might be subjected to termination of their charging process before reaching the requested SoC. Nevertheless, unlike PEVs, arrived all OEVs are not plugged into FCS. Therefore, the mean plugging rate of OEVs at FCS ($\dot{\beta}_{oev}$) as expressed in (3.5) is also very essential to find the $P_{p,oev}$.

$$\dot{\alpha}_{oev} = \sum_{\substack{\mathbf{x}\in\mathbf{\Omega},\\ a(\mathbf{x})=M,\ \sum_{i=1}^{n} x_{si}>0,\\ \sum_{j=2}^{n} x_{si}=0}} \lambda_p \pi(\mathbf{x}) \tag{3.4}$$

$$\dot{\beta}_{oev} = \lambda_o \left(1 - \sum_{\substack{\mathbf{x}\in\mathbf{\Omega}, \\ a(\mathbf{x})=M,\ \sum_{s=2}^{n} x_{si}=0, \\ x_q=q}} \pi(\mathbf{x}) \right) \tag{3.5}$$

By considering (3.4) and (3.5), $P_{p,oev}$ can be derived as (3.6).

$$P_{p,oev} = \sum_{\substack{\mathbf{x}\in\mathbf{\Omega}, \\ a(\mathbf{x})=M, \\ \sum_{i=1}^{n} x_{si}>0, \\ \sum_{j=2}^{n} x_{si}=0}} \frac{\lambda_p \pi(\mathbf{x})}{\lambda_o \left(1 - \sum_{\substack{\mathbf{x}\in\mathbf{\Omega}, \\ a(\mathbf{x})=M,\ \sum_{k=2}^{n} x_{sk}=0, \\ x_q=q}} \pi(\mathbf{x}) \right)} \tag{3.6}$$

3.4.3 Mean Time Spent at FCS (T)

For EV users, the total time spent at the FCS is a crucial measure to evaluate the service quality provided by the FCS. Researchers have given significant attention to the total time spent at the FCS in both deployment and operation management-based analysis related to FCSs.

In order to analyze the total time spent by an EV user at the FCS, we consider both mean charging time (T_c) and mean queuing time (T_q). Let γ and $\dot{\beta}$ be the mean value of ongoing charging processes and the mean plugged-in rate of a particular EV traffic type (PEV or OEV) then γ over $\dot{\beta}$ gives the mean charging time of the respective EV category. Consequently, ($T_{c,pev}$) and ($T_{c,oev}$) are expressed in (3.7) and (3.8), respectively.

$$T_{c.pev} = \sum_{\mathbf{x}\in\mathbf{\Omega}} \frac{x_r \pi(\mathbf{x})}{\lambda_p} \tag{3.7}$$

$$T_{c,oev} = \sum_{\mathbf{x}\in\mathbf{\Omega}} \sum_{k=1}^{n} \frac{k x_{sk} \pi(\mathbf{x})}{\lambda_o \left(1 - \sum_{\substack{\mathbf{x}\in\mathbf{\Omega}, \\ a(\mathbf{x})=M,\ \sum_{k=2}^{n} x_{sk}=0, \\ x_q=q}} \pi(\mathbf{x}) \right)} \tag{3.8}$$

Similarly, T_q can be derived from dividing the mean queue length ($\bar{l}$) by mean plugged-in rate ($\dot{\beta}$) for a particular EV category. However, according to the proposed strategies, PEVs are not supposed to wait in a queue, mean queuing delay is defined only for OEVs ($T_{q,oev}$).

$$T_{q,oev} = \sum_{\mathbf{x}\in\mathbf{\Omega}} \frac{x_q \pi(\mathbf{x})}{\lambda_o \left(1 - \sum_{\substack{\mathbf{x}\in\mathbf{\Omega}, \\ a(\mathbf{x})=M,\ \sum_{k=2}^{n} x_{sk}=0, \\ x_q=q}} \pi(\mathbf{x}) \right)} \tag{3.9}$$

According to Little's Law, T can be derived by adding corresponding T_c and T_q. Therefore, T_{pev} and T_{oev} are expressed in (3.10) and (3.11), respectively.

$$T_{pev} = \sum_{\mathbf{x}\in\mathbf{\Omega}} \frac{x_r \pi(\mathbf{x})}{\lambda_p} \tag{3.10}$$

$$T_{oev} = \sum_{\mathbf{x}\in\mathbf{\Omega}} \frac{\left(\sum_{k=1}^{n} k x_{sk} + x_q\right) \pi(\mathbf{x})}{\lambda_o \left(1 - \sum_{\substack{\mathbf{x}\in\mathbf{\Omega}, \\ a(\mathbf{x})=M,\ \sum_{k=2}^{n} x_{sk}=0, \\ x_q=q}} \pi(\mathbf{x})\right)} \tag{3.11}$$

3.4.4 Mean Charging Completion Rate ($\bar{c}$)

Mean charging completion rate ($\bar{c}$) of a particular EV category implies the corresponding number of charging processes that finish regularly attaining the requested SoC within a unit time. In fast charging, the prime objective of an EV user is to charge the EV as soon as possible. As we have proposed dynamic resource allocation strategies for two EV categories, it is very important to analyze the impact of charging resource distribution on each other. Therefore, $\bar{c}_{pev}$ and $\bar{c}_{oev}$ are expressed in (3.12) and (3.13), respectively.

$$\bar{c}_{pev} = \sum_{\mathbf{x}\in\mathbf{\Omega}} x_r \mu_p \pi(\mathbf{x}) \tag{3.12}$$

$$\bar{c}_{oev} = \sum_{\mathbf{x}\in\mathbf{\Omega}} \sum_{k=1}^{n} k x_{sk} \mu_o \pi(\mathbf{x}) \tag{3.13}$$

As equation (3.12) and (3.13) are derived in generic nature, each EV category can have its own service rate (μ). But in this work, $\mu_p = \mu_o = \mu_c$.

3.4.5 Charging Resource Utilization of FCS (U)

In this work, the main objective is to maximize the charging resource utilization by allowing opportunistic FCUs to charge their EVs when the registered users are not very active within the FCS.

Therefore, charging resource utilization is an important parameter for measuring the overall performance of the charging process at the FCS level. In our analysis, we define the charging resource utilization (U) as the steady state value of utilized CPs over the total number of CPs. Therefore, U can be expressed as (3.14).

$$U = \sum_{\mathbf{x}\in\mathbf{\Omega}} \pi(\mathbf{x}) \frac{a(\mathbf{x})}{M} \tag{3.14}$$

Charging resource utilization of each EV user category separately is also important in analyzing the performance of proposed charging coordination strategies. Therefore, U_{pev} and U_{oev} are expressed in (3.15) and (3.16), respectively.

$$U_{pev} = \sum_{\mathbf{x}\in\mathbf{\Omega}} \frac{x_r \pi(\mathbf{x})}{M} \tag{3.15}$$

$$U_{oev} = \sum_{\mathbf{x}\in\mathbf{\Omega}} \sum_{k=1}^{n} \frac{k x_{sk} \pi(\mathbf{x})}{M} \tag{3.16}$$

Presented CTMC-based analytical model assesses the performance of proposed dynamic charging resource coordination strategies for selected categories of EV users depending on their charging priorities.

3.5 Results and Discussion

The Effectiveness of managing the uncertainties associated with PEV charging process using opportunistic OEVs is analyzed in this Section. And how charging resource aggregation can further improve the performance of FCS is also analyzed. To analyze the performance of developed charging coordination strategies, we have considered derived performance evaluation indexes in Section 3.4. The proposed resource allocation and charging coordination strategies coordinate limited charging resources of the FCS optimally. To obtain results, it is considered that the FCS is equipped with 10 CPs (i.e, $M = 10$) capable of varible rate charging.

3.5.1 Validation of the CTMC Model

In this work, the preciseness of the CTMC analytical model is validated using Monte-Carlo simulation (MCS). We have developed a MCS considering the proposed dynamic charging resource allocation and coordination strategies to analyze the blocking probability and charging completion rates of OEVs.

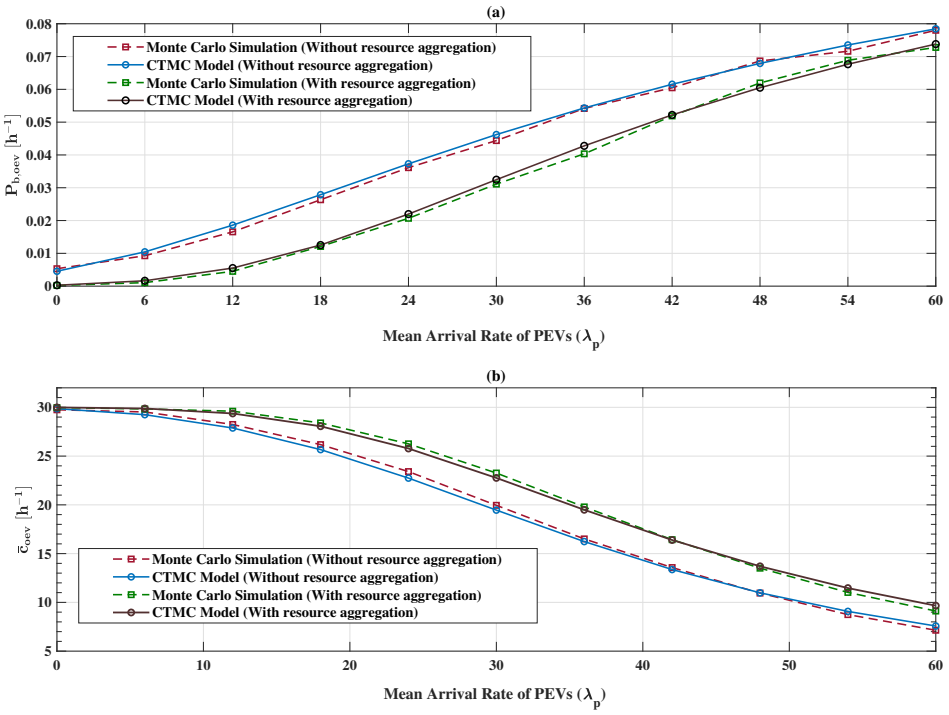

Figure 3.3: (a) Blocking probability and (b) Mean charging completion rate of OEVs with λ_p

The corresponding set of results obtained from the developed CTMC model is compared with the simulation. In the validation process, CTMC parameters are set as $\lambda_o = 30\,h^{-1}$ and $\mu_{\text{CP}} = 6\,h^{-1}$. Figure 3.3 (a) illustrates the variation of blocking probability of OEV against λ_p. The mean charging completion rate of OEVs against λ_p is depicted in Figure 3.3 (b). From these two figures (Figure 3.3 (a)and (b)), we can clearly observe that the presented CTMC model results are in close proximity with Montecarlo simulation results. Therefore, the presented model performs precisely.

3.5.2 Performance Evaluation of the CTMC Analytical Model

To evaluate the performance of proposed dynamic EV charging resource coordination strategies for both PEVs and OEVs, the behaviors of derived EV charging performance evaluation parameters against the variation of EV arrival rates are analyzed.

Charging Resource Utilization

We intend to analyze how OEVs can optimally utilize limited charging resources by exploiting unused charging resources by PEVs. Furthermore, we need to analyze how the utilization of limited charging resources is improved by charging resource aggregation. In this analysis, we consider the variation of charging resource utilization with and without OEVs.

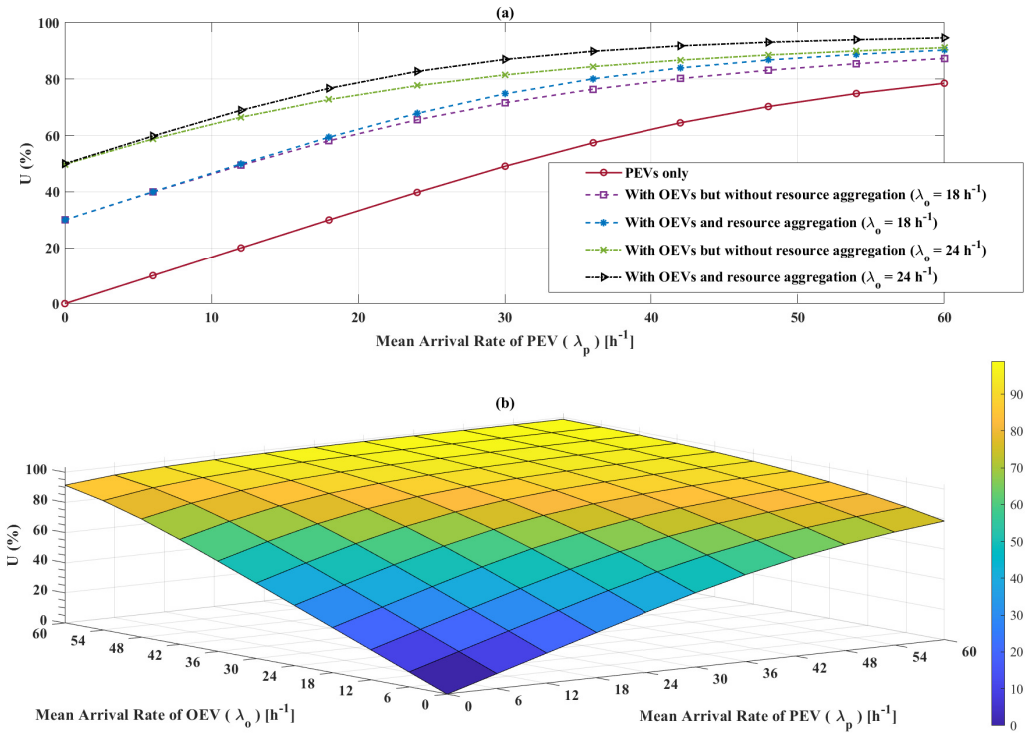

Figure 3.4: Charging resource utilization with (a) λ_p and (b) both λ_p and λ_o

CTMC model parameters are set to $\lambda_o = 18\ h^{-1}$ and $24\ h^{-1}$ while λ_p varies from 0 to $60\ h^{-1}$. The variation of U against λ_p is depicted in Figure 3.4 (a) and it shows that proposed strategies have improved the U with OEVs. At higher values of λ_p, charging resources are not optimally utilized due to the high blockages of EVs. But U can be maximized by allowing OEVs to exploit unused charging resources. Moreover, U is further enhanced with charging resource aggregation. Figure 3.4 (b) shows that no matter how much the arrival rate is increased, U can not be improved more than 80% only with PEVs. But with OEVs, these unused limited charging resources can be fully utilized. Even for lower values of λ_p, U is significantly improved by allowing opportunistic OEVs to exploit the unused charging resources through charging resource aggregation. U against λ_p shows continuous ascent with a positively decreeing slope due to high blockages of EVs and preemptions of OEVs.

Mean Charging Completion Rate

Mean charging completion rate denotes the number of completed charging processes associated with a particular EV user category within a unit time. The impact of OEVs on the charging process of PEVs is analyzed. Derived expressions for the mean charging completion rates of PEVs and OEVs (equations (3.12) and (3.13)) are considered for the analysis in this subsection. Figure 3.5 (a) and (b) illustrates the variation of mean completion rates of PEVs and OEVs as a function of λ_p and λ_o , respectively.

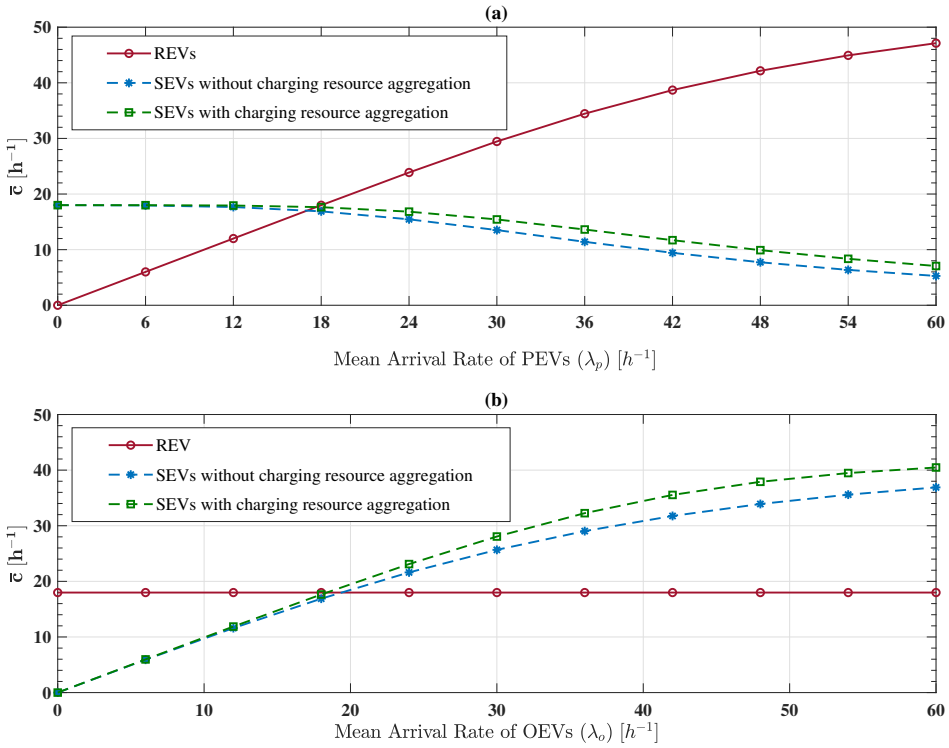

Figure 3.5: Mean charging completion rate of EVs (a) with λ_p and (b) with λ_o

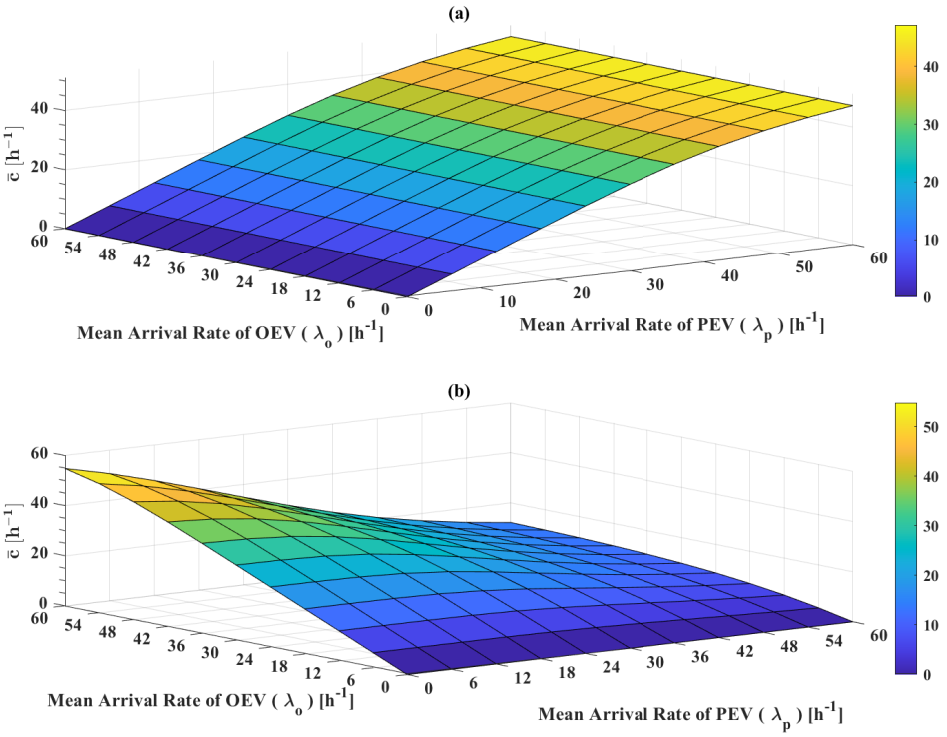

Figure 3.6: Mean charging completion rate of EVs with λ_p and λ_o

We consider the variation of $\bar{c}$ against λ_p over the range from 0 to 60 h^{-1} by letting the λ_o to be 18 h^{-1}. It can be seen that higher arrivals of PEVs deteriorate the mean charging completion rate of OEVs ($\bar{c}$) but it does not happen in vise versa. $\bar{c}_p$ shows continuous ascent against the λ_p with positively decreasing slope. The gradual declination of $\bar{c}_p$ with the λ_p is due to high blockages of PEVs. More importantly, the resource coordination strategy with aggregation shows better performance in terms of the charging completion of OEVs. In order to analyze the impact of OEVs on PEV's charging completion, we have considered a range of λ_o from 0 to 60 h^{-1} while keeping $\lambda_p = 18\ h^{-1}$. As Figure 3.5 (b) illustrates, obviously, increment of λ_o does not make any impact on PEVs. Similarly, in the case of $\bar{c}_{pev}$, $\bar{c}_{oev}$ shows a continuous ascent with λ_o but the rate of change of increment is lower than that of PEV. Nevertheless, with charging resource aggregation, the mean charging completion rate of OEVs shows higher values in contrast with the constant charging rate. To further analyze the performance of charging resource coordination strategy with aggregation, we consider the variation of $\bar{c}$ against both λ_p and λ_p over the range from 0 to 60 h^{-1} . Figure 3.6 (a) and (b) depicts the variation of mean completion rates of PEVs and OEVs as a function of both λ_p and λ_o. According to the Figure 3.6, it can be observed that there is no any impact of OEVs on the charging process of PEVs over the considered space. High mean charging completion rate of OEVs is present when they are very much active within the FCS and it gradually declines with the λ_p. It can be seen that even though the blockage of OEVs is considerably lower, their preemptage becomes significant when PEVs are more active.

Blocking and Preempting Probability of OEVs

In this section, we analyze the behavior of blocking and preempting probabilities of OEVs. Figure 3.7 (a) and (b) depict the variation of blocking and preempting probabilities of OEVs as a function of λ_p when $\lambda_o = 24\ h^{-1}$. Figure 3.8 clearly depicts that both blocking and preempting probabilities of OEVs show continuous ascent with λ_p.

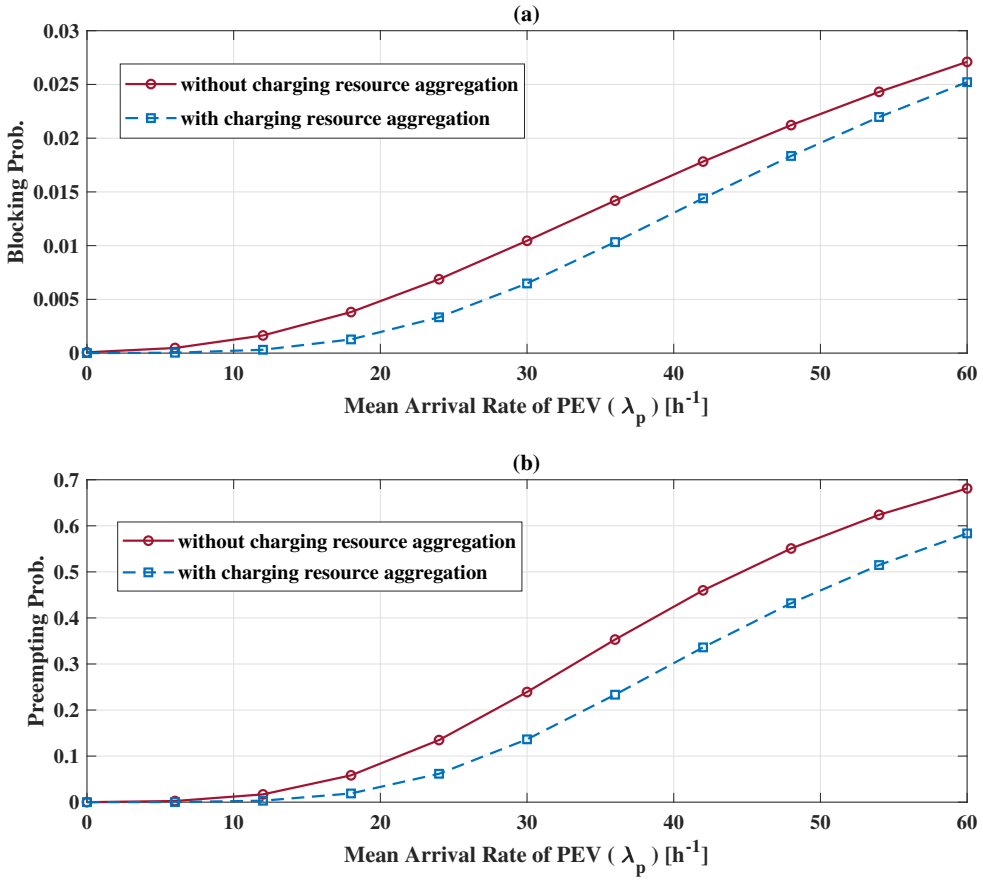

Figure 3.7: (a) Blocking and (b) Preempting probability of OEVs with λ_p

Moreover, we can observe that the resource coordination strategy with aggregation shows better performance in terms of the blockage and preemptage of OEVs. In the considered scenario (Figure 3.7), for the available EV charging resources, proposed strategies with resource aggregation keep the blocking probability less than 0.03 even at $\lambda_o = 60\ h^{-1}$. But at the same arrival rate of PEVs, the preempting probability is around 0.6 which is a bit higher value from a service quality point of view. Therefore, to keep the balance between OEV blockage and forced terminations in this case, $\lambda_p = 30\ h^{-1}$ would be a better choice. Figure 3.8 (a) and (b) depict the blocking and preempting probability of OEVs as a function of both λ_p and λ_o over the range from 0 to 60 h^{-1}. To operate the FCS with optimum resource utilization in line with service quality aspects, it is very important to visualize the blocking and preempting probability of OEVs over a space of λ_p and λ_o.

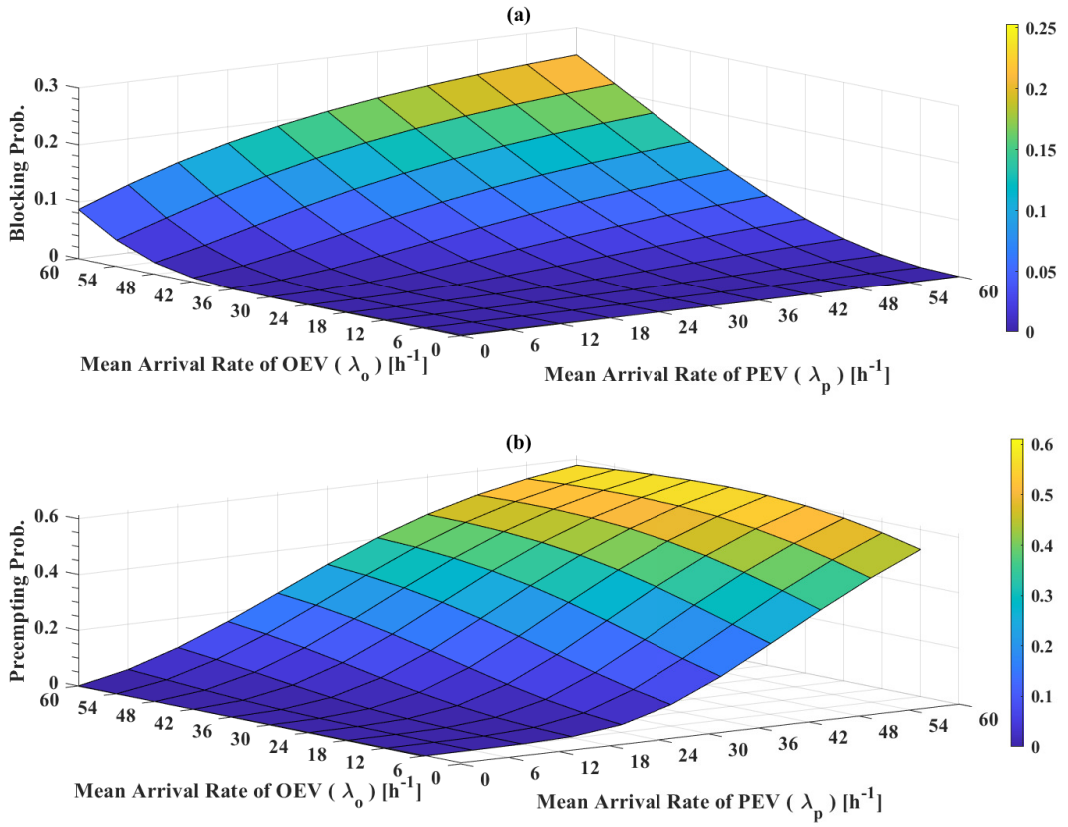

Figure 3.8: (a) Blocking and (b) Preempting probability of OEVs with λ_p and λ_o

Proposed aggregation-based charging resource coordination strategies maintain the OEV blockage below 0.3 for the considered range. However, it can be seen that when both λ_o and λ_p are less than 30 h^{-1}, blocking probability of OEVs is below 0.1. We can observe that the preempting probability is bounded to 0.6 maximum value with proposed aggregation-based charging resource coordination strategies. When operating the FCS, the station controller should take these blocking and preempting probability values into account along with the corresponding arrival rates to ensure satisfactory service to both PEVs and OEVs.

All these parameters should be taken into account to evaluate the FCS centric performance.

3.6 Conclusion

In this Chapter, we have developed an aggregation based dynamic EV charging resource coordination strategy to optimally utilize the limited charging resources of FCS with OEVs considering uncertainties associated with EV charging process. Proposed strategy enables OEVs to exploit unused charging resources at FCS to enhance the charging resource utilization.

Optimum resource utilization is achieved using dynamic charging resource coordination with aggregation. Along with the proposed strategies, we have derived an analytical framework using CTMC to evaluate the performance of an FCS in terms of charging resource utilization, charging completion rates of EV users, blocking probability, preempting probability, waiting time, charging time, etc. The analytical model is validated with Monte-Carlo simulation by considering the charging completion rate and blocking probability of OEVs.

Proposed charging coordination strategies ensure an undisturbed charging process for PEVs while providing a high-quality service to OEVs. In this chapter, we have proven with the presented results that the aggregation-based charging resource coordination strategy significantly improves the charging resource utilization of the FCS at any arrival rate of PEVs. At higher arrival rates of EVs, FCS accomplishes more than 90% of resource utilization that can not be achieved only with PEVs. Even for the considered case, the resource utilization is always higher than 50% irrespective of the arrival rate of PEVs. Presented results show that the aggregation-based strategies outperform the quality of service parameters such as charging completion rate, blocking probability, preempting probability, etc. contrast to the constant rate strategy. The blocking probability of real-time OEVs can be further reduced by increasing the queue size at the cost of waiting time. The proposed strategies, along with the analytical framework assist the FCS to visualize its EV charging behavior in maintaining long-term sustainable operation. The proposed work will be extended for analysis with different OEV categories enabling demand elasticity to enhance the charging resource utilization in Chapter 4.

Chapter 4

Maximization of Charging Resource Utilization with Resource Aggregation and Demand Elasticity for Heterogeneous EV Users

[4] *This chapter presents how heterogeneous opportunistic fast-charging users (OEVs) can dynamically exploit unused limited charging resources allocated for registered users (primary/prioritized users) (PEVs) with resource aggregation and demand elasticity to utilize the limited charging resources of an FCS maximally. Aggregation-based charging resource allocation strategy is used for OEVs in this scheme, and it enables the FCS to achieve faster charging rates for OEVs. Moreover, the proposed dynamic charging resource coordination scheme is analyzed with a continuous-time Markovian (CTMC) process in which charging coordination strategies are proposed as an event-driven model in place of the conventional time-slotted model. Furthermore, an analytical model is developed to evaluate the overall performance of the charging process of the FCS. Numerical results obtained from the developed CTMC model demonstrate that the proposed strategies can achieve high resource utilization while guaranteeing a satisfactory quality of service to EV users.*

4.1 Introduction

Deployment of electric vehicle (EV) fast charging stations (FCSs) alleviates the potential driving range anxiety and long charging time associated with EV charging. A flexible load demand is required to maximally utilize the limited charging resources of an FCS. EVs capable of ultra-fast charging would more prefer to reach FCSs opportunistically rather than following EV charging schedules.

[4]This chapter is based on the peer-reviewed journal paper, K. M. S. Y. Konara *et. al* "Aggregation Based Charging Resource Coordination at Fast Charging Station for Heterogeneous Electric Vehicle Users," *IEEE Trans. on Indust. Informat.(ISSN 1941-0050)*, 2023 (Under Review)

The FCS capacity including the energy generated from renewable sources is wasted if the FCS does not fully utilize it. For an EV-FCS, there are basically two types of traffic : (1) EV users who are living in close proximity to the FCS (2) long-trip drivers who are accessing an FCS opportunistically in the middle of their journey. Usually, depending on their current situation, EV users consider several aspects/ parameters such as economic aspects, driving distance, urgency, waiting time, plugging time, charging time, quality of service (QoS) etc. to get charged their EVs in a commercial FCS. Consequently, we can categorize EV users into different EV user categories with certain access privileges and constraints and hence, can investigate how these heterogeneous EV users can maximally utilize limited charging resources available at FCS.

We analyze the possibility of employing ultra-fast secondary EV users as a flexible load to maximally utilize the limited charging resources including the generated renewable energy power. In Chapter 2, We understood that the energy generated from intermittent renewable energy sources at FCS can be maximally utilized if we can allow ultra-fast charging users as opportunistic secondary users to get their EVs charged at lower prices with defined liabilities when scheduled users do not utilize the charging resources. Chapter 3 concludes that the utilization of limited charging resources can be further enhanced if OEVs can dynamically aggregate charging resources based on their availability depending on the activeness of PEVs and OEVs. The tendency of OEVs to participate proposed charging resource coordination scheme depends on mainly the economic benefits and the QoS expressed in terms EV blockage, preemptage, waiting time, charging time etc. Furthermore, Chapter 3 shows that QoS associated with OEVs can be effectively improved with dynamic charging resource aggregation.

In this Chapter 4, we consider a commercial FCS that admits heterogeneous EV users to charge their EVs. Here we have considered two types of OEVs (1) elastic OEVs ($\mathrm{OEV_E}$) that can wait to plugged-in to FCS till charging resources will be adequately available (2) real-time OEVs ($\mathrm{OEV_R}$) who would mostly be long-trip drivers. EVs located around an FCS can access the FCS as $\mathrm{OEV_E}$ when charging resources are available upon notification from the FCS. With the wide spread of FCSs, usually, long-trip drivers prefer to charge their EVs quickly and economically if possible to increase their cruise range. If they can charge their EVs throughout the journey quickly and economically, they may not want to get their EVs fully charged at one FCS at a high cost. Therefore, such sort of EV users can participate as $\mathrm{OEV_R}$ in this charging coordination scheme. We analyze the effectiveness of aggregating available charging resources to dynamically adjust the charging rate of $\mathrm{OEV_R}$ to get their EVs charged as fast as possible and also we employ another type of OEV as $\mathrm{OEV_E}$ to further enhance charging resources with the demand elasticity. Therefore, in this Chapter 4, we investigate, how dynamic charging resource aggregation and demand elasticity help to enhance the utilization of limited charging resources while providing quality service to both PEVs and OEVs.

In brief, the technical novelty and contributions from this work can be summarized as follows,

1. Aggregation and demand elasticity-based novel real-time charging resource coordination scheme is presented for an FCS where both PEVs (with scheduled charging processes) and OEVs can be charged to enhance the utilization of limited charging resources at the FCS while achieving distinct service needs of heterogeneous EV users.

2. An event-driven continuous-time model in which an event is defined as either EV arrival or departure is used in proposed strategies. In contrast to the time-slotted models with fixed intervals, more system dynamics can be treated with adaptive EV charging in steps.

3. Charging coordination strategies are proposed so that PEVs are charged at a constant charge rate and without getting any disturbance from OEVs at any time. Nevertheless, OEVs continue to be charged at a specified fixed rate till an event occurs at the FCS but it adjusts the charge rate depending on the resource availability at an event. Doing so can prolong the EV battery life as compared to that of frequent on-off or modulating charging coordination strategy. Hence, it is more practical and feasible to scale up the capacity of the FCS.

4. Multiple charging options with prescribed service priorities are introduced to attract more OEVs in the proposed Charging resource coordination strategies. In addition, two queuing schemes, including a virtual queue, are used along with novel queue management strategies to enhance the service quality of OEVs.

5. An analytical framework is developed to evaluate the overall performance of the proposed dynamic charging resource coordination strategies using a continuous-time Markov chain (CTMC).

4.2 Operating Mechanism of FCS

We consider an FCS with M number of charging points (CPs) ($M \in \mathbb{Z}^+$) that can facilitate variable-rate EV charging. As per the preference of EV users, they can register at the FCS with prescribed priorities in advance, subject to an optimum schedule.

These registered users are considered as the PEVs in the FCS. We have considered two types of OEVs : (1) Real-time OEVs (OEV_R) (2) Elastic OEVs (OEV_E). OEVs who need to get their EVs charged up to a maximum possible level quickly are considered as as OEV_R. On the other hand, OEV_E are OEVs who stay in close proximity with the FCS and can adjust the plugged-in time.

As described in Chapter 3, both types of OEVs opportunistically access the FCS and exploit unused charging resources to enhance the charging resource utilization. A schematic illustration of opportunities where OEVs can exploit unused charging resources is depicted in Figure 4.1.

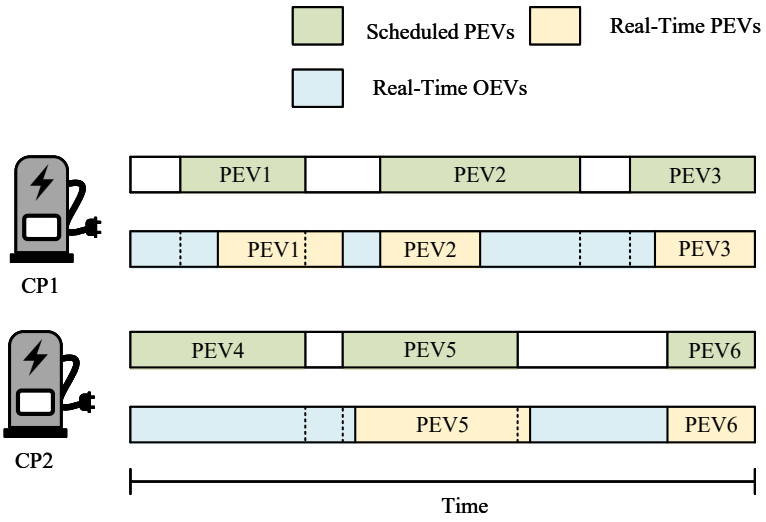

Figure 4.1: Charging resource utilization with OEVs

In this work, it is considered that PEVs are charged at a specified charge rate of P_p. As depicted in Figure 4.1, FCS admits OEVs opportunistically other than PEVs subject to that OEVs are liable to vacate their plugged-in-CP upon arrival of a PEV, depending on the availability of charging resources. The aforementioned operating mechanism of the FCS is illustrated in Figure 4.2.

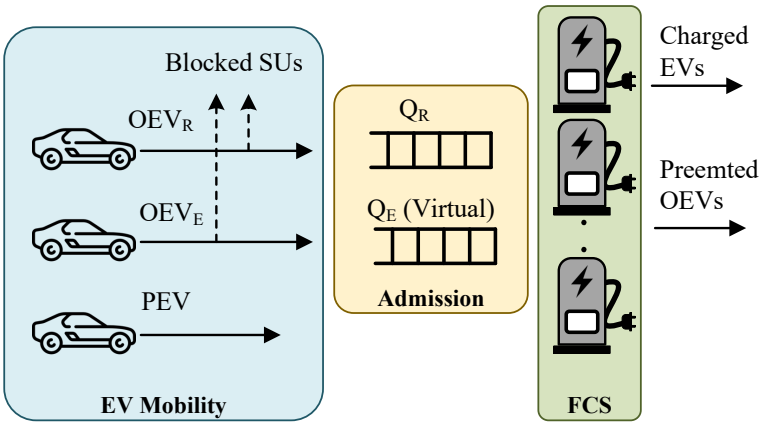

Figure 4.2: Proposed operation mechanism of the FCS

FCS should have a charging pricing mechanism for PEVs and OEVs based on charging priorities. Even though PEVs and OEV_E are charged at a constant rate of P_p, OEV_R can adapt their charge rate from P_p up to nP_p in steps based on the availability of charging resources without exceeding the contracted capacity (MP_p) of the FCS.

Therefore, it is considered that the maximum capacity of a CP is $nP_p; (n \in \mathbb{Z}^+)$. Consequently, considering M CPs, the maximum capacity of FCS is nMP_p. This P_p aggregation associated with OEV_R is analogous to the aggregation of CPs from 1 to n. Herein after, as described above, CP aggregation means the aggregation of charging resources associated with a CP. However, the contract demand of the FCS can be scaled up from MP_p to nMP_p , depending on the demand.

As depicted in Figure 4.2, two separate queues are employed in this work to cope with heterogeneous traffic according to different admission control strategies. Furthermore, a physical queue (QR) at the FCS with Q_R number of queue points (QPs) and a virtual queue (QE) with Q_E number of QPs are considered to introduce these novel dynamic charging resource allocations and admission control techniques in the proposed strategies. QR is reserved only for OEV_R. The station controller uses the QE only for OEV_E to access the FCS. With QE, there is no physical EV queue at the FCS as it mainly maintains the plugged-in time elasticity of OEV_E. To admit a PEV or an OEV_E to the FCS, at least one idle physical CP is required. Apart from that, P_p power out of the contracted demand should be available to feed the CP. OEV_R are charged at P_p power when all CPs (M) are occupied by EVs but depending on the availability of idle CPs, OEV_R can increase their charging power up to nP_p in P_p steps so that the total power demand of the FCS does not exceed its contracted capacity (MP_p) . This P_p aggregation associated with OEV_R is analogous to the aggregation of CPs from 1 to n. Herein after, as described above, CP aggregation means the aggregation of charging resources associated with a CP.

4.3 Dynamic Charging Resource Coordination

This work uses the continuous-time Markov chain (CTMC) to develop dynamic charging coordination strategies. Therefore, the following assumptions are considered in CTMC analysis.

- The arrivals of PEVs, OEV_E and OEV_R are Poisson processes with mean arrival rates of λ_p, λ_{oe} and λ_{or}, respectively. (Here mean arrival rate denotes the average number of charging requests made by EVs per unit time).

- The service times of plugged-in EVs are exponentially distributed with the service rate of μ_{CP}. (Here service rate denotes the average number of charged EVs per CP per unit time).

- All CPs are homogeneous.

The proposed dynamic charging coordination strategy is denoted as $DRA(n, Q_E, Q_R)$, where, first $'n'$ denotes the highest CP aggregation limits for OEV_R. Q_E and Q_R are the maximum queue sizes of the QE and QR, respectively.

A generic state x; $x = \{j_p, j_e, j_{r1}, .., j_{rk}, .., j_{rn}, j_{eq}, j_{rq}\}$ is defined to model system dynamics according to different events. Here, for a particular state of the FCS, j_p and j_e denote the number of plugged-in PEVs and OEV_Es, respectively. $[j_{r1}, .., j_{rk}, .., j_{rn}]$ represents the number of OEV_Rs corresponding to their aggregated CPs. In the state x, number of queued EVs are denoted by $[j_{eq}, j_{rq}]$.

In the developed CTMC model, a state transition is triggered by one of the following four events.(1)Arrival of PEVs at FCS (2)Departure of PEVs from FCS (3)Arrival of OEVs at FCS (4)Departure of OEVs from FCS. he state transitions associated with aforementioned events with different conditions are tabulated in state transition tables (STTs) I-IV. Each row in these STTs corresponds to a state transition from a state i to another state j, where $i, j \in \mathbf{S}$. The set of feasible states of the system is obtained as $\mathbf{S} = \{\mathbf{x}|j_p, j_e, j_{r1}, .., j_{rk}, .., j_{rn}, j_{eq}, j_{rq} \geq 0;\ j_p \leq M,\ j_e \leq M, j_{rk}|\forall k \in [1, ..., n] \leq \lfloor (M/k) \rfloor,\ j_{eq} \leq Q_E,\ j_{rq} \leq Q_R; j_{eq} = 0, j_{rq} = 0 \text{ if } p(\mathbf{x}) < M;\ \sum_{i=1}^{n-1} j_{ri} = 0, j_{rn} \leq \lfloor (b(\mathbf{x})/n) \rfloor \text{ if } \sum_{i=1}^{n} j_{ri} > 0, p(\mathbf{x}) < M\ \sum_{i=2}^{n} j_{ri} = 0,\ \text{if } \sum_{i=1}^{n} j_{ri} > 0, p(\mathbf{x}) = M\}$.

Where, $p(\mathbf{x})$ is the total number of CPs utilized by plugged-in EVs; $p(\mathbf{x}) = j_p + j_e + \sum_{i=1}^{n} k.j_{rk}$ and $b(\mathbf{x})$ is the available CPs for OEV_R $b(\mathbf{x}) = M - (j_p + j_e)$.

4.3.1 State transitions (STs) of the CTMC model

Arrival of PEVs at FCS : STs associated with the PEV arrivals are tabulated in ST-Table 4.1. When a PEV arrives at the FCS, it is plugged into the FCS if at least one idle CP without disturbing any ongoing OEV charging processes. Otherwise, OEVs have to either donate aggregated CRs or preempt their charging process to admit the newly arrived PEV as they are liable to do so. When a PEV arrives to the fully crowded FCS, if OEV_Rs with aggregated CRs present, the OEV_R with maximum number of aggregated CPs has to donate a CP. Unless, an OEV_R has to forcibly terminate its charging process to admit the PEV. If there are no OEV_R, the charging process of OEV_E is preempted.

Departure of PEVs from FCS : ST-Table 4.2 tabulates STs associated with the PEV departures. Once a PEV is charged, it departs the FCS resulting in an idle CP. Then, the first priority goes to the QE if it is fully occupied.
If the QE is not full, the chance is given to the QR. If the QR is empty, the vacant CP will be given to the QE, even though it is not full. If both the queues are empty, the vacant CP will be aggregated by an OEV_R with the minimum number of aggregated CPs ($k_{min}; \forall\, k_{min} \in\ [1, ..., (n-1)]$). Otherwise, the CP will be idle.

Arrival of OEVs at FCS : OEVs are accepted to the FCS if PEVs do not occupy all the CPs. The charging process of plugged-in OEVs are not preempted upon the arrival of a new OEV. When a new OEV arrives at the FCS, only the charging processes of OEVs with aggregated resources will be affected.

Table 4.1: STs of $DRA(n, Q_E, Q_R)$ from state x with λ_p transition rate upon arrival of PEVs

Conditions	**Destination State**
An idle CP exist	$\{j_p+1, j_e, j_{r1}, \cdots, j_{rk}, \cdots, j_{rn}, j_{eq}, j_{rq}\}$; $(M - p(x) > 0)$
FCS is fully utilized. There are OEV_R with aggregated CPs	$\{j_p+1, j_e, j_{r1}, \cdots, j_{r(m-1)}+1, j_{rm}-1, \cdots, j_{rn}, j_{eq}, j_{rq}\}$; $(M - p(x) = 0\ j_{rk} > 0, 1 < k \leq n;$ $m = \max\{k \vert j_{rk} > 0, 1 < k \leq n\})$
FCS is fully utilized. There are no OEV_R with aggregated CPs	$\{j_p+1, j_e, j_{r1}-1, \cdots, j_{rk}, \cdots, j_{rn}, j_{eq}, j_{rq}\}$; $(M - p(x) = 0;\ j_{r1} > 0;$ $j_{rk} = 0, 2 \leq k \leq n)$
FCS is fully utilized. There are only OEV_E as OEVs	$\{j_p+1, j_e-1, j_{r1}, \cdots, j_{rk}, \cdots, j_{rn}, j_{eq}, j_{rq}\}$; $M - p(x) = 0;\ j_e > 0;$ $j_{rk} = 0, 1 \leq k \leq n$
FCS is fully utilized. There are no OEVs	$\{j_p, j_e, j_{r1}, \cdots, j_{rk}, \cdots, j_{rn}, j_{eq}, j_{rq}\}$; $M - p(x) = 0;\ j_e = 0;$ $j_{rk} = 0, 1 \leq k \leq n$

Table 4.2: STs from the generic state x with $j_p\mu_{cp}$ transition rate on departure of PEVs

Conditions	**Destination State**
QE is full.	$\{j_p-1, j_e+1, j_{r1}, \cdots, j_{rk}, \cdots, j_{rn}, j_{eq}-1, j_{rq}\}$; $j_{eq} = Q_E$
QE is not fully occupied. There are OEV_R in QR.	$\{j_p-1, j_e, j_{r1}+1, \cdots, j_{rk}, \cdots, j_{rn}, j_{eq}, j_{rq}-1\}$; $j_{eq} < Q_E;\ j_{rq} > 0$
QR is empty. There are OEV_E in QE.	$\{j_p-1, j_e+1, j_{r1}, \cdots, j_{rk}, \cdots, j_{rn}, j_{eq}-1, j_{rq}\}$; $j_{eq} > 0;\ j_{rq} = 0$
Both QE and QR are empty.	$\{j_p-1, j_e, j_{r1}, \cdots, j_{rl}+1, j_{r(l+1)}, \cdots, j_{rn}, j_{eq}, j_{rq}\}$; $j_{eq} = 0;\ j_{rq} = 0$ $l < n,\ l = \min\{k \vert j_{rk} > 0, 1 \leq k \leq n\}$
Both QE and QR are empty. There are no OEV_R.	$\{j_p-1, j_e, j_{r1}, \cdots, j_{rk}, \cdots, j_{rn}, j_{eq}, j_{rq}\}$; $j_{eq} = 0;\ j_{rq} = 0$ $j_{rk} = 0, 1 \leq k \leq n$

Specific resource allocation and admission control for OEV_E and OEV_R are discussed with the corresponding state transitions in the following subsections.

Arrival of $\mathbf{OEV_E}$: ST associated with the $\mathrm{OEV_E}$ arrivals are tabulated in ST Table 4.3. An $\mathrm{OEV_E}$ can be plugged-in to the FCS, if at least one idle CP. Otherwise, the charging request will be queued as long as the QE is not full. But if the QE is full, FCS seeks for the $\mathrm{OEV_R}$ with maximum number of aggregated CPs if any to get a CP. But the CP is given to a queued $\mathrm{OEV_E}$ and the newly arrived charging request will be queued in QE. If still it can not find a CP, it has to be blocked.

Arrival of $\mathbf{OEV_R}$: ST associated with the $\mathrm{OEV_R}$ arrivals are tabulated in Table 4.4 When an $\mathrm{OEV_R}$ arrives to the FCS, CS controller assigns $k; (\forall\ k \in\ [1, ..., n])$ CPs , if k CPs or more are idle (*i.e.* One physical CP and the charging resources allocated for k CPs). Similar to $\mathrm{OEV_E}$ arrivals, only $\mathrm{OEV_R}$ with aggregated resources will have to donate a CP upon arrival of a new $\mathrm{OEV_R}$ at the fully occupancy. Otherwise, it will be queued in QR if it is not full. If the new $\mathrm{OEV_R}$ can not find a chance with any means described above, it has to be blocked.

Departure of OEVs from FCS : Unlike in PEVs, an OEV may result in more than one CP at its departure depending on the aggregated resources (*i.e.* charging resources allocated for multiple CPs). The idle CP(s) that appeared in the FCS due to the departure of an OEV will be initially offered to the same type of OEVs waiting at the corresponding queue. If the corresponding queue is empty, then the vacant CP(s) will be given to the other queue. Upon a departure of an OEV, if both the queues are empty, the vacant CP(s) will be aggregated by an $\mathrm{OEV_R}$. Otherwise, the CP(s) will be idle. The corresponding STs associated with the departures of $\mathrm{OEV_E}$ and $\mathrm{OEV_R}$ are tabulated in Table 4.5 and Table 4.6, respectively.

Table 4.3: STs from the generic state x with λ_{oe} transition rate upon arrival of $\mathrm{OEV_E}$

Conditions	**Destination State**
An idle CP exist	$\{j_p, j_e + 1, j_{r1}, \cdots, j_{rk}, \cdots, j_{rn}, j_{eq}, j_{rq}\}$; $M - p(x) > 0$
FCS is fully utilized. But QE is not full.	$\{j_p, j_e, j_{r1}, \cdots, \cdots, j_{rk}, \cdots, j_{rn} j_{eq} + 1, j_{rq}\}$; $M - p(x) = 0$; $j_{eq} < Q_E$
FCS is fully utilized. There are $\mathrm{OEV_R}$ with aggregated CPs	$\{j_p, j_e + 1, j_{r1}, \cdots, j_{r(m-1)} + 1, j_{rm} - 1, \cdots, j_{rn}, j_{eq}, j_{rq}\}$; $M - p(x) = 0$; $j_{eq} = Q_E$; $j_{rk} > 0, 1 < k \leq n$; $m = \max\{k \vert j_{rk} > 0, 1 < k \leq n\}$
FCS is fully utilized. There are no $\mathrm{OEV_R}$	$\{j_p, j_e, j_{r1}, \cdots, j_{rk}, \cdots, j_{rn}, j_{eq}, j_{rq}\}$; $M - p(x) = 0$; $j_{eq} = Q_E$; $j_{rk} = 0, 1 \leq k \leq n$

Table 4.4: STs from the generic state x with λ_{or} transition rate upon arrival of OEV_R

Conditions	**Destination State**
An idle CP exist	$\{j_p, j_e, j_{r1}, \cdots, j_{rk}+1, \cdots, j_{rn}, j_{eq}, j_{rq}\}$ $M - p(x) \geq k, 1 \leq k \leq n$
FCS is fully utilized. There are OEV_R with aggregated CPs	$\{j_p, j_e, j_{r1}+1, \cdots, j_{r(m-1)}+1,$ $j_{rm}-1, \cdots, j_{rn}, j_{eq}, j_{rq}\}$ $M - p(x) = 0;\ j_{rk} > 0, 1 < k \leq n;$ $m = \max\{k \vert j_{rk} > 0, 1 < k \leq n\}$
FCS is fully utilized. But QR is not full.	$\{j_p, j_e, j_{r1}, \cdots, \cdots, j_{rk}, \cdots, j_{rn}$ $j_{eq}, j_{rq}+1\}$ $M - p(x) = 0;\ j_{eq} < Q_R$
FCS is fully utilized. There are no OEV_R	$\{j_p, j_e, j_{r1}, \cdots, j_{rk}, \cdots, j_{rn},$ $j_{eq}, j_{rq}\}$ $M - p(x) = 0;\ j_{eq} = Q_R;$ $j_{rk} = 0, 1 \leq k \leq n$

Table 4.5: STs from the generic state x with $j_e\mu_{cp}$ transition rate on departure of OEV_E

Conditions	**Destination State**
There are OEV_E in QE	$\{j_p, j_e, j_{r1}, \cdots, j_{rk},$ $\cdots, j_{rn}, j_{eq}-1, j_{rq}\}$ $; j_{eq} > 0;$
QE is empty. There are OEV_R in QR.	$\{j_p, j_e-1, j_{r1}+1, \cdots, j_{rk},$ $\cdots, j_{rn}, j_{eq}, j_{rq}-1\}$ $; j_{eq} = 0;\ j_{rq} > 0$
Both QE and QR are empty.	$\{j_p, j_e-1, j_{r1}, \cdots, j_{rl}+1, j_{r(l+1)},$ $\cdots, j_{rn}, j_{eq}, j_{rq}\}$ $; j_{eq} = Q_E;\ j_{rq} = 0$ $l < n,\ l = \min\{k \vert j_{rk} > 0, 1 \leq k \leq n\}$
Both QE and QE are empty. There are no OEV_R.	$\{j_p, j_e-1, j_{r1}, \cdots, j_{rk}, \cdots, j_{rn}, j_{eq}, j_{rq}\}$ $; j_{eq} = 0;\ j_{rq} = 0$ $j_{rk} = 0, 1 \leq k \leq n$

4.4 Continuous Time Markov Chain Analytical Model

The proposed dynamic charging resource coordination strategy is modeled as a CTMC with a generic state $\mathbf{x}$ as described in Section 4.3. Letting $\mathbf{Q}$ be the transition rate matrix and π be the steady state probability vector of the system, the steady state probability of being in the state $\pi(x)$, is calculated using the global balance equation and the normalization equation expressed as ; $\pi\mathbf{Q} = 0, \sum_{x \in \mathbf{S}} \pi(x) = 1$.

Table 4.6: STs from the generic state x with $kj_k\mu_{cp}$ transition rate on departure of $\mathrm{OEV_R}$ with k aggregated CPs

Conditions	**Destination State**
There are $\mathrm{OEV_R}$ in QR	$\{j_p, j_e, j_{r1}, \cdots, j_{rk}, \cdots, j_{rn}, j_{eq}, j_{rq}-1\}$; $j_{rq} > 0$;
QR is empty. There are $\mathrm{OEV_E}$ in QR.	$\{j_p, j_e + k, j_{r1}, \cdots, j_{rk} - 1,$ $\cdots, j_{rn}, j_{eq} - k, j_{rq}\}$; $j_{rq} = 0$; $j_{eq} \geq k$
QR is empty. There are $\mathrm{OEV_E}$ in QE.	$\{j_p, j_e + j_{eq}, j_{r1}, \cdots, j_{rl} - (k - j_{eq}),$ $j_{r(l+1)} + (k - j_{eq}) \cdots j_{rk} - 1, \cdots,$ $j_{rn}, (j_{eq} - j_{eq}), j_{rq}\}$; $j_{rq} = 0$; $j_{eq} < k$; $l = \min\{k \vert j_{rk} > 0, 1 \leq k < n\}$ $j_{rl} \geq (k - j_{eq})$
QR is empty. There are $\mathrm{OEV_E}$ in QE.	$\{j_p, j_e + j_{eq}, j_{r1}, \cdots, j_{rl} - j_{rl},$ $j_{r(l+1)} + 2j_{rl} - (k - j_{eq}), j_{r(l+2)} + (k - j_{eq}) - j_{rl}$ $\cdots, j_{rk} - 1, \cdots, j_{rn}, 0, j_{rq}\}$; $j_{rq} = 0$; $j_{eq} < k$; $j_{rl} < (k - j_{eq})$ $j_{r(l+1)} > (k - j_{eq}) - 2j_{rl}$ $l = \min\{k \vert j_{rk} > 0, 1 \leq k < n\}$
QR is empty. There are $\mathrm{OEV_E}$ in QE.	$\{j_p, j_e + j_{eq}, j_{r1}, \cdots, j_{rl} - j_{rl},$ $j_{r(l+1)} - j_{r(l+1)}, j_{r(l+2)} + 2j_{rl} + 2j_{r(l+1)} - (k - j_{eq}),$ $j_{r(l+3)} + (k - j_{eq}) - j_{rl} - j_{r(l+1)}$ $\cdots, j_{rk} - 1, \cdots, j_{rn}, 0, j_{rq}\}$; $j_{rq} = 0$; $j_{eq} < k$; $j_{rl} < (k - j_{eq})$ $j_{r(l+1)} < (k - j_{eq}) - 2j_{rl}$ $j_{r(l+2)} > (k - j_{eq}) - 2j_{rl} - 2j_{r(l+1)}$ $l = \min\{k \vert j_{rk} > 0, 1 \leq k < n\}$
...	...
Both QE and QR are empty. There are $\mathrm{OEV_R}$	$\{j_p, j_e, j_{r1}, \cdots, j_{rl} - k, j_{r(l+1)} + k$ $\cdots j_{rk} - 1, \cdots, j_{rn}, j_{eq}, j_{rq}\}$; $j_{rq} = 0$; $j_{eq} = 0$; $j_{rl} > k$; $l = \min\{k \vert j_{rk} > 0, 1 \leq k < n\}$
Both QE and QR are empty. There are $\mathrm{OEV_R}$	$\{j_p, j_e, j_{r1}, \cdots, j_{rl} - j_{rl},$ $j_{r(l+1)} + 2j_{rl} - k, j_{r(l+2)} + k - j_{rl}$ $\cdots, j_{rk} - 1, \cdots, j_{rn}, j_{eq}, j_{rq}\}$; $j_{rq} = 0$; $j_{eq} = 0$; $j_{rl} < k$; $j_{r(l+1)} > (k - 2j_{rl})$ $l = \min\{k \vert j_{rk} > 0, 1 \leq k < n\}$
Both QE and QR are empty. There are $\mathrm{OEV_R}$	$\{j_p, j_e, j_{r1}, \cdots, j_{rl} - j_{rl},$ $j_{r(l+1)} - j_{r(l+1)}, j_{r(l+2)} + 2j_{rl} + 2j_{r(l+1)} - k,$ $j_{r(l+3)} + k - j_{rl} - j_{r(l+1)}$ $\cdots, j_{rk} - 1, \cdots, j_{rn}, j_{eq}, j_{rq}\}$; $j_{rq} = 0$; $j_{eq} = 0$; $j_{rl} < k$ $j_{r(l+1)} < k - 2j_{rl}$ $j_{r(l+2)} > k - 2j_{rl} - 2j_{r(l+1)}$ $l = \min\{k \vert j_{rk} > 0, 1 \leq k < n\}$
...	...
Both QE and QR are empty. There are no $\mathrm{OEV_R}$.	$\{j_p, j_e, j_{r1}, \cdots, j_{rk} - 1, \cdots, j_{rn}, j_{eq}, j_{rq}\}$; $j_{eq} = 0$; $j_{rq} = 0$ $j_{rk} = 0, 1 \leq k \leq n$

In $\mathbf{Q}$ matrix, the total transition rate from state i to state j denoted by q_{ij},$(i, j \in \mathbf{S})$ is calculated by getting the summation of transition rates which correspond to all possible STs from state i to state j, considering all possible corresponding events of EV arrival and departure. The diagonal elements of the $\mathbf{Q}$ matrix $(q_{ii}\ ; i \in \mathbf{S})$ are calculated using $q_{ii} = -\sum_{j \in \mathbf{S}, j \neq i} q_{ij}\ ; i, j \in \mathbf{S}$. Once $\pi(x)$ is determined the following performance evaluation parameters are derived in terms of $\pi(x)$ from the first principles.

4.4.1 Blocking Probability of OEVs

The blocking probability is the probability that a newly arrived EV charging request is blocked due to the unavailability of charging resources. In this proposed EV charging scheme, the EV blockage generally happens with OEVs. Therefore, separate expressions for blocking probabilities of $\mathrm{OEV_R}$ and $\mathrm{OEV_E}$ are derived as expressed in (4.1) and (4.2), respectively. A new OEV is blocked when these three conditions are met at the same time : (1) FCS is fully utilized. (2) There is no any ongoing $\mathrm{OEV_R}$ with aggregated CPs. (3) Relevant queue (QR or QE) is full.

$$P_{b,or} = \sum_{x \in \mathbf{S} | \alpha_R} \pi(x) \qquad (4.1) \qquad\qquad P_{b,oe} = \sum_{x \in \mathbf{S} | \alpha_E} \pi(x) \qquad (4.2)$$

Where $\alpha_R \equiv (p(x) = M,\ \sum_{i=2}^{n} j_{ri} = 0,\ j_{eq} = Q_R)$ and $\alpha_E \equiv (p(x) = M,\ \sum_{i=2}^{n} j_{ri} = 0\ j_{eq} = Q_E)$

4.4.2 Preempting Probability of OEVs

When the FCS is fully occupied, upon arrival of a PEV, one ongoing OEV charging process has to be preempted before it reaches the requested SoC depending on the charging resource availability. Consequently, the preempting probability is the probability that an active OEV charging process is forced to terminate before it regularly finishes. Preempting probability of OEV (P_p) is obtained by dividing the mean preempting rate of a OEV $(\bar{p})$ from the mean plugged-in rate of OEV $(\bar{g})$.
An ongoing $\mathrm{OEV_R}$ charging process subjects to be preempted when these three conditions are met at the same time : (1) FCS is full (2) There is at least one ongoing $\mathrm{OEV_R}$ charging process. (3) There is no any ongoing $\mathrm{OEV_R}$ charging with aggregated CPs. Therefore, $\bar{p}_{\mathrm{or}}$ and $\bar{g}_{\mathrm{or}}$ of $\mathrm{OEV_R}$ can be derived as (4.3) and (4.4), respectively.

$$\bar{p}_{or} = \sum_{x \in \mathbf{S} | \varepsilon_r} \lambda_p \pi(x) \qquad (4.3)$$

$$\bar{g}_{\mathrm{or}} = \lambda_{\mathrm{or}}(1 - P_{b,or}) \qquad (4.4)$$

Where $\varepsilon_r \equiv (p(x) = M,\ \sum_{i=1}^{n} j_{ri} > 0,\ \sum_{i=2}^{n} j_{ri} = 0)$ and hence, $P_{p,oe}$ can be expressed as (4.5) .

$$P_{p,or} = \sum_{x \in \mathbf{S} | \varepsilon_r} \frac{\lambda_p \pi(x)}{\lambda_{or} \left(1 - \sum_{x \in \mathbf{S} | \alpha_r} \pi(x)\right)} \qquad (4.5)$$

Upon a PEV arrival, if FCS is full, an ongoing $\mathrm{OEV_E}$ has to be forcibly terminated when these three conditions are met at the same time : (1) FCS is full (2) There is no any ongoing $\mathrm{OEV_R}$ charging process. (3) There is at least one ongoing $\mathrm{OEV_E}$ charging process. Similarly, $\bar{p}_{\mathrm{oe}}$ and $\bar{g}_{\mathrm{oe}}$ of $\mathrm{OEV_E}$ can be derived as as (4.6) and (4.7), respectively.

$$\bar{p}_{oe} = \sum_{x \in \mathbf{S}|\varepsilon_e} \lambda_p \pi(x) \qquad (4.6)$$

$$\bar{g}_{\mathrm{oe}} = \lambda_{\mathrm{oe}}(1 - P_{b,oe}) \qquad (4.7)$$

Where $\varepsilon_{oe} \equiv (p(x) = M,\ \sum_{i=1}^{n} j_{ri} = 0,\ j_e > 0)$ and hence, $P_{p,oe}$ can be expressed as (4.8) .

$$P_{p,oe} = \sum_{x \in \mathbf{S}|\varepsilon_r} \frac{\lambda_p \pi(x)}{\lambda_{oe}\left(1 - \sum_{x \in \mathbf{S}|\alpha_r} \pi(x)\right)} \qquad (4.8)$$

4.4.3 Mean Queue Length

The queue length at the FCS depends on the mean arrival rate of EVs and the service completion rate of the FCS. In the proposed CTMC based analysis, in a generic state x, j_{rq} and j_{eq} represent the length of physical queue for $\mathrm{OEV_R}$ and virtual queue for $\mathrm{OEV_E}$, respectively. Consequently, the mean queue length of the $\mathrm{OEV_R}$ and $\mathrm{OEV_E}$ $\left(\bar{l}_{QR} \text{ and } \bar{l}_{QE}\right)$ are given by (4.9) and (4.10), respectively.

$$\bar{l}_{QR} = \sum_{x \in \mathbf{S}} \pi(x) j_{rq} \qquad (4.9)$$

$$\bar{l}_{QE} = \sum_{x \in \mathbf{S}} \pi(x) j_{eq} \qquad (4.10)$$

4.4.4 Average Waiting Time in Queue

In this work, the average waiting time in the queue (T^q) is calculated by getting the mean queue length $(\bar{l})$ over the mean plugged-in rate $(\bar{g})$. As there are two queues in this proposed FCS operation scheme (QE and QR), corresponding two expressions are derived for each EV traffic type. The average waiting time in the QR and QE are expressed in (4.11) and (4.12), respectively.

$$T^q_{or} = \sum_{x \in \mathbf{S}} \frac{\pi(x) j_{rq}}{\lambda_{or}\left(1 - \sum_{x \in \mathbf{S}|\alpha_r} \pi(x)\right)} \qquad (4.11)$$

$$T^q_{oe} = \sum_{x \in \mathbf{S}} \frac{\pi(x) j_{eq}}{\lambda_{oe}\left(1 - \sum_{x \in \mathbf{S}|\alpha_e} \pi(x)\right)} \qquad (4.12)$$

4.4.5 Average Charging Time in FCS

The average charging time (T^c) for each EV traffic type is obtained from dividing the average number of ongoing charging services for a particular EV type in the system (N^c) by the mean plugged-in rate of the corresponding EV type $(\bar{g})$. Consequently, expressions for PEVs, N^c_p and T^c_p are expressed in (4.13) and (4.14), respectively.

$$N_p^c = \sum_{x \in \mathbf{S}} j_p \pi(x) \qquad (4.13) \qquad\qquad T_p^c = \sum_{x \in \mathbf{S}} \frac{j_p \pi(x)}{\lambda_p} \qquad (4.14)$$

(N^c) for OEV_E and OEV_R are expressed in (4.15) and (4.16), respectively.

$$N_{oe}^c = \sum_{x \in \mathbf{S}} j_e \pi(x) \qquad (4.15) \qquad\qquad N_{or}^c = \sum_{x \in \mathbf{S}} \sum_{k=1}^{n} k j_{rk} \pi(x) \qquad (4.16)$$

(T^c) of OEV_E and OEV_R are expressed in (4.17) and (4.18).

$$T_{oe}^c = \sum_{x \in \mathbf{S}} \frac{\pi(x) j_e}{\lambda_{oe} \left(1 - \sum_{x \in \mathbf{S} | \alpha_e} \pi(x)\right)} \qquad (4.17)$$

$$T_{or}^c = \sum_{x \in \mathbf{S}} \sum_{k=1}^{n} \frac{k j_{rk} \pi(x)}{\lambda_{or} \left(1 - \sum_{x \in \mathbf{S} | \alpha_r} \pi(x)\right)} \qquad (4.18)$$

4.4.6 Charging Completion Rate

The average number of charging completion per unit time is defined as charging completion rate ($\bar{c}$). This parameter highly affects the availability of the FCS. Separate expressions are derived for the charging completion rate of each EV type plugged-in the FCS. Charging completion rates for PEV, OEV_E and OEV_R are expressed in (4.19), (4.20) and (4.21), respectively.

$$\bar{c}_p = \sum_{x \in \mathbf{S}} j_p \mu_p \pi(x) \qquad (4.19) \qquad\qquad \bar{c}_{oe} = \sum_{x \in \mathbf{S}} j_e \mu_{oe} \pi(x) \qquad (4.20)$$

$$\bar{c}_{or} = \sum_{x \in \mathbf{S}} \sum_{k=1}^{n} k j_{rk} \mu_{or} \pi(x) \qquad (4.21)$$

In this work, $\mu_p = \mu_{oe} = \mu_{or} = \mu_{cp}$

4.4.7 Charging Resource Utilization

The charging resource utilization (U) inherently indicates how the available EVSE, grid supply, and the local energy supply are utilized at the FCS level. Therefore, U is an important parameter that indicates the overall performance of the FCS. In our analysis, we define U as the average number of utilized CPs over the total number of CPs. In a generic state x , $x \in \mathbf{S}$, a total number of $p(x)$ CPs out of M are utilized by EVs. (U) can be expressed as (4.22),

$$U = \sum_{x \in \mathbf{S}} \pi(x) \frac{p(x)}{M} \qquad (4.22)$$

Presented CTMC based analytical model assesses the performance of proposed dynamic charging resource coordination strategies.

4.5 Results and Discussion

The CTMC analytical model is developed in generic nature that can be used as a framework to evaluate the overall performance of any FCS with proposed strategies. In this section, the developed CTMC analytical model is validated and analyzed for selected cases to demonstrate its performance. In this work an EV FCS with 10 CPs (i.e, $M = 10$) capable of variable rate charging is considered. The adaptive power level variable (n) in the proposed dynamic EV charging resource coordination strategy is considered as 3 for this analysis. The maximum lengths of the virtual and physical queues are kept as $Q_E = 4$ and $Q_R = 2$, unless or otherwise stated explicitly.

4.5.1 CTMC Model Validation

We use the Monte-Carlo simulation (MCS) to validate the preciseness of the analytical model developed with CTMC using proposed strategies. Consequently, we have developed MCS considering PEV and OEV events to analyze the blocking probability and charging completion rates of OEVs associated with the proposed dynamic resource coordination strategies. The corresponding set of results obtained from the developed CTMC model is compared with that of the simulation. In the validation process, CTMC parameters are set as $\lambda_{oe} = 16\ h^{-1}$ and $\lambda_{or} = 24\ h^{-1}$ and $\mu_{\text{cp}} = 5\ h^{-1}$. Figure 4.3 (a) and (b) illustrate the blocking probability (P_b) of OEV_E and OEV_R against λ_p, respectively. And the average charging completion rate ($\bar{c}$) of OEV_E and OEV_R as a function of λ_p are depicted in Figure 4.4 (a) and (b), respectively. From these figures, we can clearly observe that the presented CTMC model results are in close proximity with MCS results.

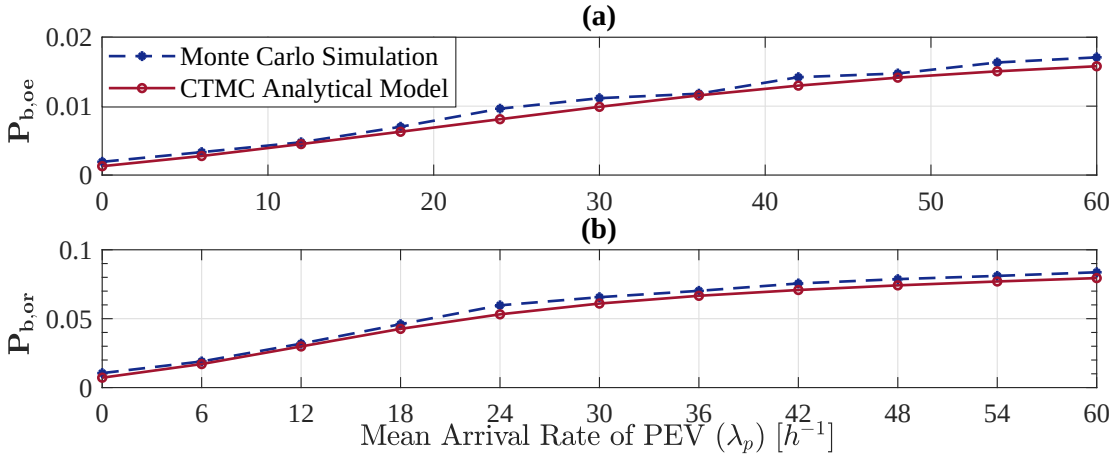

Figure 4.3: Blocking Probability (P_b) of OEVs with λ_p

4.5.2 Performance Evaluation

In this section, the performance of proposed strategies for EV charging with heterogeneous EV traffic is analyzed in terms of charging resource utilization, charging completion rates, blocking and preempting probabilities of OEVs.

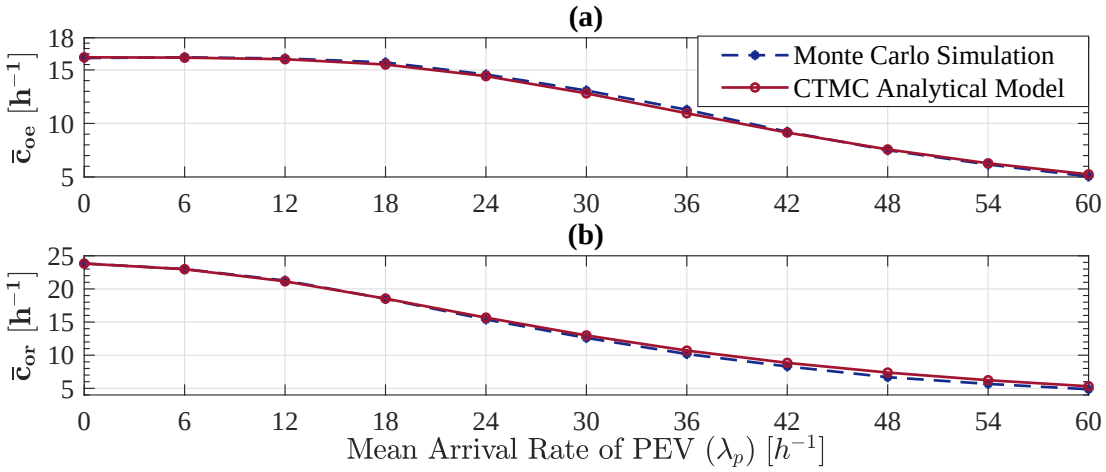

Figure 4.4: Average Charging Completion Rate ($\bar{c}$) of OEVs with λ_p

Charging Resource Utilization

Here we analyze how the charging resources utilization is improved with multiple EV charging options. In this analysis, λ_{oe} and λ_{or} are set as $18\,h^{-1}$ and $24\,h^{-1}$, respectively. λ_p varies from 0 to $60\,h^{-1}$.

Figure 4.5 depicts the variation of U against λ_p. It can be clearly observed from Figure 4.5, that our proposed strategy improves the U with OEVs. For lower values of λ_p, U is significantly improved by allowing OEVs to exploit the unused charging resources through charging resource aggregation. With the increment of λ_p, U shows continuous ascent but the percentage improvement is becoming lower due to high blockages and preempting of OEVs (Sub sections 4.5.2 and 4.5.2). The cases that are plotted in doted lines in Figure 4.5 shows that U can be further improved using queues for OEV_R and it is significant at higher values of λ_p.

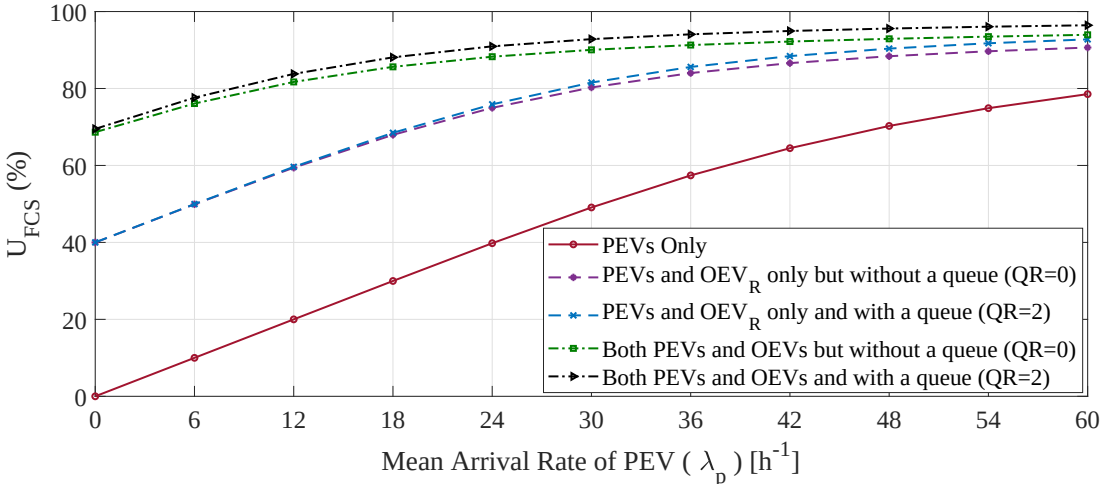

Figure 4.5: Charging Resource Utilization (U) with λ_p

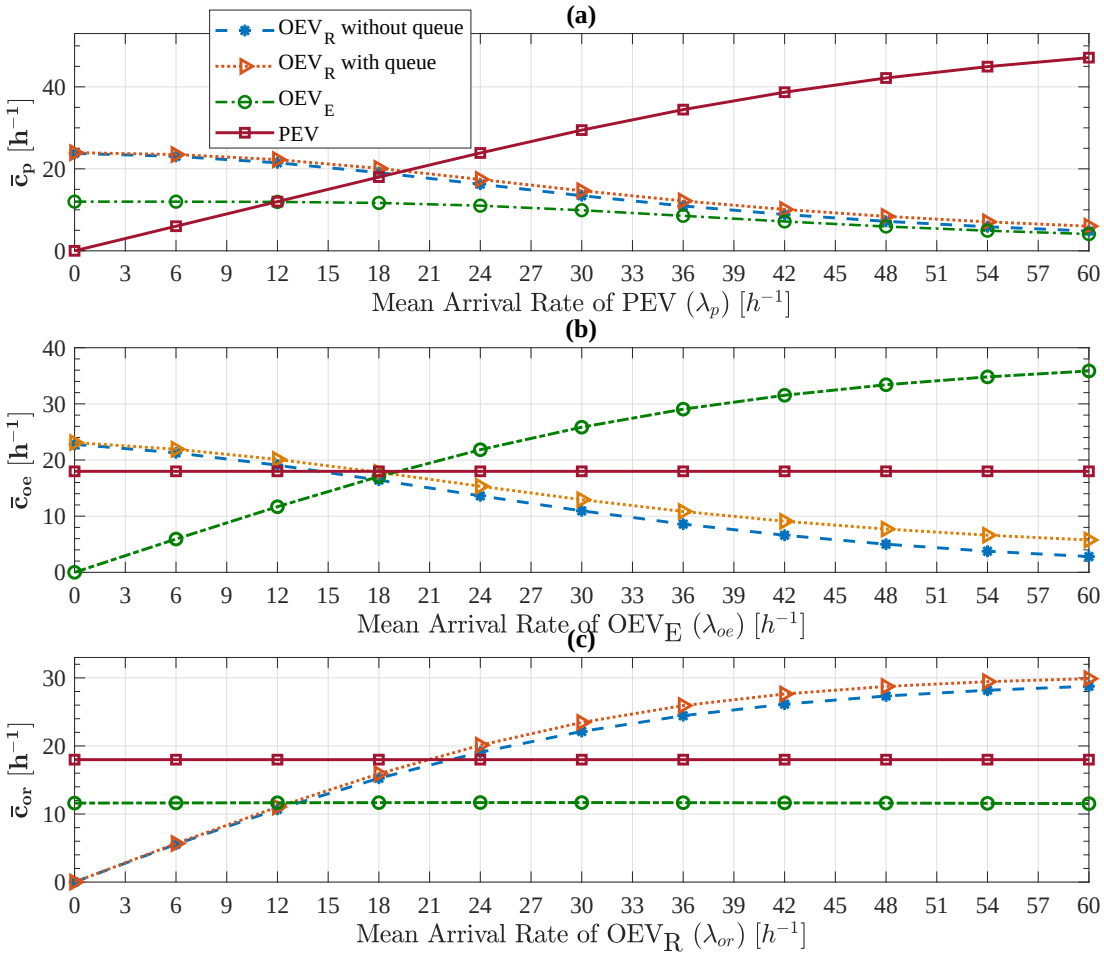

Figure 4.6: Average charging completion rate of EVs ($\bar{c}$)

Average Charging Completion Rate

The impact of proposed strategies on the average charging completion rate ($\bar{c}$) of each EV user type is analyzed here. Importantly, guaranteeing high quality of service to PEVs is vital in whole charging process. In the initial case, we set the CTMC parameters λ_{oe} and λ_{or} as $12\,h^{-1}$ and $24\,h^{-1}$, respectively and λ_p varies from 0 to $60\,h^{-1}$. Figure 4.6 (a) illustrates the variation of $\bar{c}$ of PEVs and OEVs as a function of λ_p. Figure 4.6 (a) clearly shows that the increment of λ_p reduces $\bar{c}_o$. $\bar{c}_p$) shows continuous ascent with the λ_p, more importantly, initially it increases linearly with λ_p but gradually the rate of increment reduces due to blockages of PEVs by PEVs. It is obvious that although the $\bar{c}_p$ is high at higher λ_p, it results PEV blockages due to non-availability of charging resources. When the FCS operates with a queue, $\bar{c}_{or}$ shows higher values in contrast with the FCS without a queue.

Next a range of λ_{oe} from 0 to $60\,h^{-1}$ is considered while keeping λ_p and λ_{or} at $18\,h^{-1}$ and $24\,h^{-1}$ to analyze the impact of OEV_E arrivals on charging completion of EVs. As Figure 4.6 (b) illustrates, obviously, increment of λ_{oe} doesn't make any impact on the $\bar{c}_p$ but $\bar{c}_{or}$ reduces with the λ_{oe}. The $\bar{c}_{oe}$ shows continuous ascent with λ_{oe} but the rate of change of increment is lower than that of PEV. This proves that even though OEV_E improve the U, they can not make any impact on PEV's

charging process but only for OEV_R. FCS with a queue shows better performance in terms of charging completion as compared to the FCS without queue.

Variation of $\bar{c}_{or}$ with λ_{or} is depicted in Figure 4.6 (c). Obviously the OEV_R have not shown any impact on the charging process of PEVs and OEV_E. Their $\bar{c}_{or}$ variation also follows the same shape as OEV_E shown in Figure 4.6 (b) due to charging resource aggregation. Similarly in previous two cases (Figure 4.6 (a) and (b), the FCS with a queue shows better performance in terms of charging completion in contrast to the FCS without queue.

Blocking Probability of OEVs

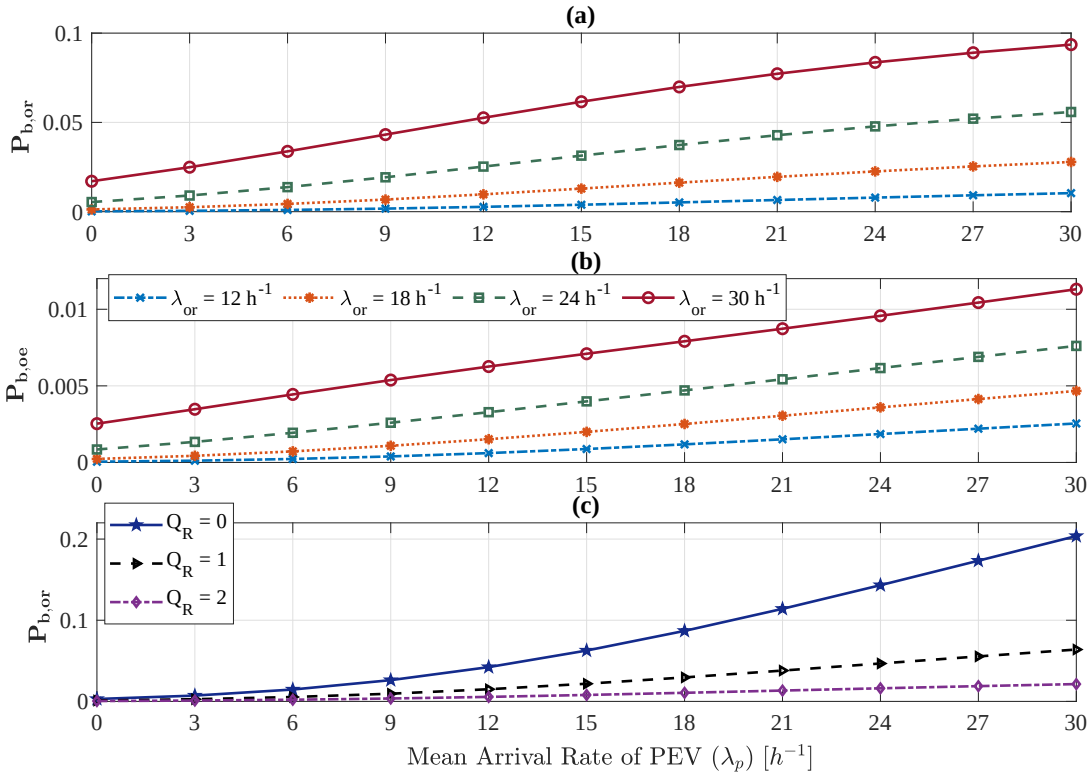

Figure 4.7: Blocking Probability (P_b) of OEVs with λ_p

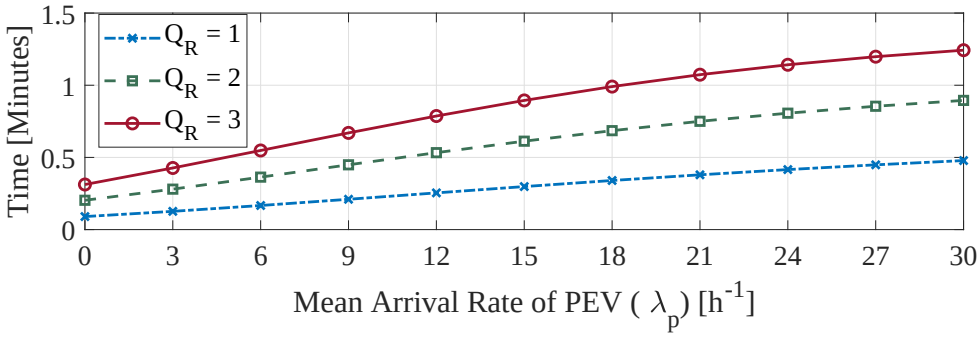

Figure 4.8: Average waiting time in QR as λ_p varies

When PEVs become more active in the FCS with higher arrival rates, OEVs are subject to be blocked. However, maintaining comparatively low blocking probabilities of OEVs is essential to attract OEVs to the FCS. Therefore, we have analyzed P_b of OEVs for different λ_{or} when λ_p varies from 0 to 30 h^{-1}. Figure 4.7 (a) depicts the variation of $P_{b,or}$ as a function of λ_p when $\lambda_{oe} = 18\ h^{-1}$. Figure 4.7 (a), shows continuous ascent in $P_{b,or}$ with λ_p as well as it increases when λ_{or} increases. In the considered scenario, for the available EV charging resources, proposed strategies with resource aggregation keep the blocking probability less than 0.1. The variation of $P_{b,or}$ with λ_p for different queue sizes (Q_R) is plotted in Figure 4.7 (c). It can be seen that $P_{b,or}$ is significantly reduced by allocating a queue space. From Figure 4.8, we can observe that the mean queue delay of QR increases with the queue size.

Consequently, to reduce $P_{b,or}$, the QR size can be increased at a cost of average waiting time in QR. Blockages of OEV_E is also possible in the proposed strategies when PEVs highly occupy the FCS. The $P_{b,oe}$ against λ_p is plotted in Figure 4.7 (c). It can be seen that blockages of OEV_E is not very significant like OEV_R due to the fact that OEV_E are privileged in allocating charging resources as compared to the OEV_R.

Preempting Probability of OEVs

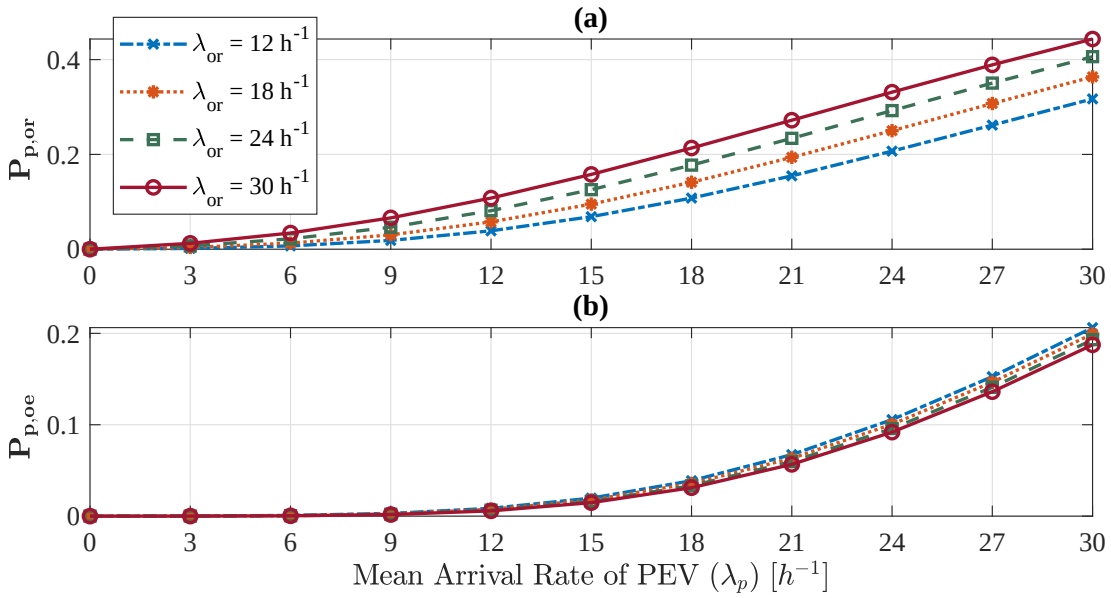

Figure 4.9: Preempting Probability of OEVs with λ_p

According to the proposed strategy, when the occupancy of PEVs are dominating at the FCS, the charging process of OEVs must be preempted to admit new coming PEVs depending on the available charging resources. Preempting probability of OEV_R and OEV_E are illustrated in Figure 4.9 as λ_p varies. It can be clearly seen that P_p increases when increasing more arrivals of PEVs. However, for the considered worst case with OEV_R (Figure 4.9 (a)), the maximum preempting probability is 0.45 when both the mean arrival rate of PEVs and OEV_R are at 30 h^{-1}.

It means that, with the proposed strategies, significant number of least privileged OEV_R get charged up to the requested SoC.

With the presented results for selected scenarios, the performance of proposed EV charging coordination strategies for an FCS are evaluated in terms of mainly charging resource utilization and charging completion rates of EV users. In addition to that, blocking probability and preempting probability of OEVs are analyzed.

4.6 Conclusion

In this chapter, we have developed a dynamic EV charging resource coordination strategy to maximally utilize the limited charging resources at an FCS with charging resource aggregation and demand elasticity. An analytical model is derived using CTMC to evaluate the performance of developed strategies. The CTMC model is validated with Montecarlo simulation. Proposed strategies enable opportunistic EV users (OEVs) to exploit unused charging resources by PEVs without disturbing ongoing PEV charging processes to enhance the charging resource utilization. Along with the proposed strategies, we have presented an analytical framework to evaluate the performance of an FCS in terms of charging resource utilization, charging completion rates of EV users, blocking probability, preempting probability, etc. We have proven with the presented results that the proposed charging resource coordination strategy significantly improves the charging resource utilization of the FCS at any arrival rate of PEVs.

For considered scenarios, it keeps the charging resource utilization always higher than 75% irrespective of the arrival rate of PEVs. The results show that the proposed strategies outperform the QoS parameters. The blocking probability of real-time OEVs can be further reduced by increasing the queue size at the cost of waiting time. The proposed analytical framework can be employed to evaluate the overall function of the FCS by taking traffic inflows and out flows into account either at initial planning stage or during the operation. The extended work of presented strategies for improving the charging reliability of OEVs is presented in Chapter 6.

Chapter 5

Priority-based Charging Resource Utilization with Heterogeneous EV Users

[5] *This chapter provides innovative dynamic resource allocation and charging coordination strategies for opportunistic fast charging users (FCUs) to exploit unused charging resources allocated for registered slow charging users (SCUs) at a charging station (CS). The charging coordination strategies are presented for both static and adaptive charging. Furthermore, a queue is employed in the dynamic resource allocation process to favor more fast charging requests through buffering non-critical slow-charging EVs (NCSCUs), as FCUs would otherwise be blocked or preempted. The performance of the proposed charging coordination strategies is analyzed in terms of the optimum utilization of charging resources, charging completion rate, and user satisfaction. For the considered scenario, it keeps the average charging resource utilization above 90% at higher arrival rates of EVs while the distribution transformer is being loaded only up to 50% of its rated capacity. Moreover, the charging completion rate and blocking probability of FCUs are used to evaluate the service quality of opportunistic users. Moreover, the presented results prove that charging coordination strategies with adaptive charging outperforms all the aforementioned performance parameters. The presented dynamic resource allocation and charging coordination strategies for heterogeneous EV traffic at a CS maximize the utilization of limited charging resources while assuring quality service to EV users without stressing the distributed network.*

[5]This chapter is based on the peer-reviewed journal paper, K. M. S. Y. Konara *et. al* , "Queue Based Dynamic Charging Resource Allocation and Coordination for Heterogeneous Traffic in an Electrical Vehicle Charging Station," *Energy Sources, Part A: Recovery, Utilization, and Environmental Effects (ISSN: 1556-7230)*, 1–18, 2021. doi: 10.1080/15567036.2021.1974983 and the peer reviewed international conference paper K. M. S. Y. Konara *et. al* "Charging Coordination of Opportunistic EV Users at Fast Charging Station with Adaptive Charging," In Proceedings of Transportation Electrification Conference (ITEC-India), IEEE, pp. 1–6, 2021. doi : 10.1109/ITEC-India53713.2021.9932507

5.1 Introduction

There is one category of EV users (eg. daytime workers) who plugged-in their EVs overnight preferably after arriving home from work and plugged out when departing for work. The same people might charge their EVs at the curbside or in a parking lot more especially during the day time. As they plugged their EVs for plenty of time they can charge with slow charging (Mode I or Mode II EV Charging [11, 13, 14]). EVs can also be charged in EV charging stations (CSs) at occasions where quick charging becomes inevitable. With the increasing population, in near future, a detached house for everyone or securing a charging point (CP) in a parking lot would not be possible at every time. Therefore, with the rapid adoption of EVs, charging autonomy would be a significant matter in EV charging. EV users may charge their EVs at lower prices at CSs as CS owners purchase bulk energy from the energy market and also due to the competition among CSs.

With the rapid integration of e-mobility, institutional and residential parking lots can be effectively converted into commercial CSs with fast-charging technology. This chapter intends to analyze the effectiveness of converting institutional and residential parking lots into fast charging stations (FCSs) where both slow-charging EV users (SCUs) and fast-charging EV users (FCUs) can charge their EVs. SCUs are the registered users with the FCS while FCUs access the FCS opportunistically. This chapter intends to analyze how limited charging resources of an FCS can be optimally distributed among SCUs and FCUs to enhance charging resource utilization.

FCUs access the FCS to exploit unused charging resources allocated for SCUs opportunistically. The FCS allocates and coordinates charging resources dynamically considering different user privileges based on the user category. FCUs can be considered as secondary users for the FCS. The privileges and constraints of SCUs and FCUs are tabulated in Table 5.1.

Table 5.1: Access Privileges and Constraints of EV users

SCU	**FCU**
• Pre-scheduled charging process	• Opportunistic charging
• Charged at specified charge rate $P_{scu};\ P_{scu} \in\ [P_{scu}^{min}, P_{scu}^{max}]$	• Charged at higher charge rate $P_{fcu};\ P_{fcu} \in [P_{fcu}^{min}, P_{fcu}^{max}]$
• CS availability is guaranteed on arrival.	• Charger is assigned if sufficient resources are available only.
• Very hardly subject to blockages	• Subject to blockages
• Requested SoC is assured at departure.	• Charging process is liable to be preempted before regularly finishes.
• Park EV for a significant time	• Expect to charge as quickly as possible

Basically, we intend to analyze the effectiveness of utilization of limited charging resources with FCUs. Moreover, we need to analyze the service satisfaction of oppor-

tunistic FCUs as they access the FCS with certain liabilities. The FCS is equipped with charging piles (CPs/ EV supply equipment (EVSE)) capable of variable rate charging and a buffer space for optimum resource allocation. To the authors best knowledge, all existing related works with queues mandate newly arrived EVs to be queued before plugging to a CP based on the first-come-first-served strategy; conversely, this work uses the queue to favor more real-time FCUs through buffering ongoing non-critical SCUs (NCSCUs). The criticality of SCUs' charging process is elaborated in Section 5.4.1.

In brief, the technical novelty and contributions of the charging coordination strategies proposed in this chapter can be summarized as follows,

1. Priority-based novel admission control and charging coordination strategy is proposed with a buffer space so that more opportunistic FCUs can exploit unused limited charging resources by registered slow charging users SCUs to enhance the utilization of limited charging resources at the CS.

2. In contrast to the conventional queue in a CS that keeps newly arrived unadmitted EVs until charging resources appear, the allocated buffer space in this work is employed to favor more FCUs by buffering NCSCUs to further enhance the utilization of limited charging resource while adhering the demand limit.

3. Priority-based heuristic charging management algorithm is proposed to properly coordinate the charging demand without stressing the distributed network while ensuring charging fairness among heterogeneous EV users.

4. An analytical framework is developed to evaluate the overall performance of the proposed dynamic charging resource coordination strategies using Motecarlo-simulation.

5.2 EV Charging Station Operation Mechanism

In this topology, CSs (sub-aggregators) are connected to a CS aggregator (central aggregator) for demand-side management through necessary communications with the electricity market and the utility. Central aggregator purchases power from the day-ahead energy market (spot-market) and allocates an appropriate demand limit (DL) for each CS. CS controllers are responsible to optimally utilizing the allocated demand with optimal charging resource allocation and charging coordination. The proposed charging station operation mechanism illustrated in Figure 5.1 effectively allocates the charging resources to maximize the CS profit by increasing the CS utilization.

Charging infrastructures are built so that the CS can provide variable rate charging. The EV fleet of a CS can be categorized into two types of users : (1) SCUs; the users who are considered as primary users as they have prior agreements (or

day-ahead scheduling) with the CS based on their user preferences. Depending on the EV capacity constraints they can choose either 3.3 kW ($slow\ charging$) or 7.3 kW ($medium\ charging$) charging rates. (2) FCUs; the users who can opportunistically utilize charging points that are not occupied for EV charging. Like in the SCUs, FCUs can choose either 50.0 kW ($fast\ charging$) or 120.0 kW ($super-fast\ charging$) charging rates. Based on the aforementioned different charging rates, users who are preferring slow, medium, fast and super-fast charging are designated as SCU_{slow}, SCU_{medium}, FCU_{fast}, and $FCU_{su.fast}$, respectively. Moreover, their corresponding mean arrival rates are denoted as $\lambda_{FCU,su.fast}$ and $\lambda_{FCU,fast}$, respectively.

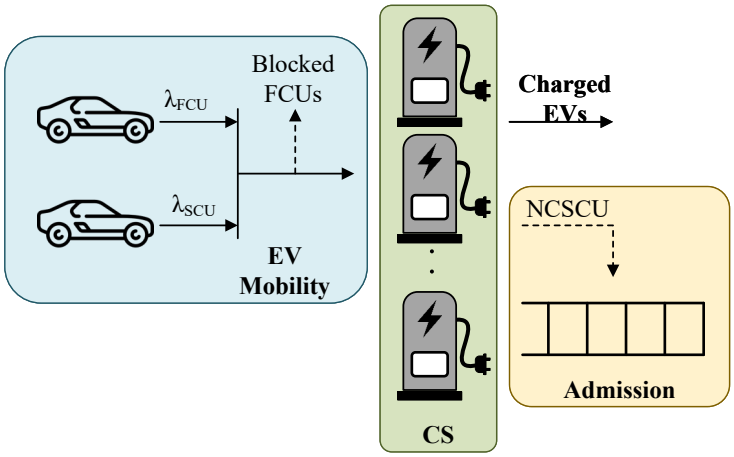

Figure 5.1: Illustration of the proposed EV charging scheme

5.3 Stochastic Electric Vehicle Arrival Process

In the proposed framework, the initial task is to develop a mathematical model for EV arrivals to analyze the performance of developed coordinated charging strategies for heterogeneous traffics. In this work, we have modeled the arrival of SCUs and FCUs separately. Among heterogeneous EV users in this framework, SCUs are considered daytime workers or users who do not have access to nighttime domestic charging. Therefore, SCUs arrive in the CS during either early morning or evening hours and park for a significantly long period in a day. Furthermore, SCUs have prior (day-ahead) agreements with the CS regarding arriving time, leaving time, charging rate, etc., and they pay for both charging and parking.

Consequently, we have modeled it as a normally distributed continuous time discrete space stochastic process. On the other hand, as compared to SCUs, arrivals of FCUs are very much uncertain, and therefore, it is modeled as a Poisson process (P) with the parameter λ [77].

- If the average arrival rate of FCUs be λ ($\lambda > 0$) over the $[t,\ t+\delta t]$, the probability of one arrival of EV during $[t,\ t+\delta t]$ is $\lambda t + O(\delta t)$; $O(\delta t)$: order of δt.

- The probability of more than one arrival of FCUs during $[t,\ t+\delta t]$ is $O(\delta t)$.
- The occurrence of arrivals in non-overlapping interval are mutually independent.

Then if $[N(t),\ t \geq 0]$ be the number of arrivals occur during $[0,\ t]$ can be modeled as a Poisson process (P) with parameters $\lambda_1,\ \lambda_2,\ ...,\ [N(t),\ t \geq 0] \sim P(\lambda_1 t, \lambda_2 t, ...)$.

5.4 Resource Allocation for Accepted EVs

In this work, a CS with M number of charging points (CPs) and a queue with Q number of queuing points (QPs) $(M, Q \in \mathbb{Z}^+)$ are considered for the dynamic resource allocation and charging coordination. The queue is reserved only for SCUs at arrival and during the charging process.

5.4.1 SCU Arrivals

Algorithm 5.1: Pseudo code for the resource allocation to SCUs

Input : $T_{CP}(t)$: Total number of occupied CPs at time t
Input : $T_{QP}(t)$: Total number of occupied QPs at time t
Input : $j_{fcu}(t)$: Total number of plugged-in FCUs at time t
Input : $j_q(t)$: Total number of occupied QPs at time t
Input : $j(t)$: Total number of plugged-in EVs at time t
Output: $\boldsymbol{A}^{ev}_{j(t)\times n}$: Plugged-in EVs matrix at time t
Output: $\boldsymbol{A}^{q}_{j_q(t)\times n}$: Queued EVs matrix at time t

```
if T_CP(t) < M then
    SCU is plugged into an idle CP
else if T_CP(t) == M AND j_q(t) < Q then
    SCU is queued
    Update A^q_{j_q(t)×n}
else if T_CP(t) == M AND T_QP(t) == Q AND j_fcu(t) > 0 then
    Rank FCUs in descending order based on SoC^k_FCU(t)
    Force terminate the FCU with SoC_{max,FCU}(t)
    SCU is plugged into the vacated CP by the FCU
else
    Block the SCU
end
Update A^ev_{j(t)×n}
```

From the resource allocation perspective, SCUs are considered as privileged users because they have prior agreements with the CS. Whereas they are no longer be prioritized users in the charging process. k^{th}; $(k \in K_{SCU})$ plugged-in SCU is treated as a critical SCU (CSCU) in the charging process, if its minimum required charging

Algorithm 5.2: Pseudo code for the resource allocation to queued SCUs

Input : $T_{CP}(t)$: Total number of occupied CPs at time t
Input : $j_{fcu}(t)$: Total number of plugged in FCUs at time t
Input : $j_{ncscu}(t)$: Total number of plugged-in NCSCUs at time t
Input : $j(t)$: Total number of plugged-in EVs at time t
Output: $\boldsymbol{A}^{ev}_{j(t)\times n}$: Plugged-in EVs matrix at time t
Output: $\boldsymbol{A}^{q}_{j_q(t)\times n}$: Queued EVs matrix at time t

if $(\tau^k_{SCU,min} + \tau_0) < H^k_{SCU}(t)$ **then**
  if $T_{CP}(t) < M$ **then**
    SCU is plugged into an idle CP
  else if $T_{CP}(t) == M \ AND \ j_{ncscu}(t) > 0$ **then**
    Rank plugged-in NCSCUs in descending order based on $SoC^k_{NCSCU}(t)$
    Queue the plugged-in NCSCU with $SoC_{max,NCSCU}(t)$
    SCU is plugged into the vacated CP by the NCSCU
    Update $\boldsymbol{A}^{q}_{j_q(t)\times n}$
  else if $T_{CP}(t) == M \ AND \ j_{fcu}(t) > 0$ **then**
    Rank FCUs in descending order based on $SoC^k_{FCU}(t)$
    Force terminate the FCU with $SoC_{max,FCU}(t)$
    SCU is plugged into the vacated CP by the force terminated FCU
else
  Keep in the queue
end
Update $\boldsymbol{A}^{ev}_{j(t)\times n}$

time ($\tau^k_{SCU,min}$) is lower than the parking horizon ($H^k_{SCU}(t)$) at time t. Otherwise, the k^{th} plugged-in SCU is regarded as a non-critical SCU (NCSCU) in charging coordination. Let C^k_{SCU} and $t^{dep,k}_{SCU}$ be the battery capacity and the departure time of the k^{th} plugged-in SCU and let P_{SCU} and η_{SCU} be the charging rate of slow charging (either SCU_{slow} or SCU_{medium}) and the charging efficiency, respectively, then $\tau^k_{SCU,min}$ and $H^k_{SCU}(t)$ are determined by (5.1) and (5.2), respectively.

$$\tau^k_{SCU,min} = \frac{\left[SoC^{dep,k}_{SCU} - SoC^k_{SCU}(t)\right] C^k_{SCU}}{\eta_{SCU} P_{SCU} \Delta t} \tag{5.1}$$

$$H^k_{SCU}(t) = t^{dep,k}_{SCU} - t \tag{5.2}$$

When an SCU arrives at the CS, it is definitely plugged into the CS. Thus, any ongoing charging process is not affected if there is at least one idle CP.

Algorithm 5.3: Pseudo code for the resource allocation to FCUs

Input : $T_{CP}(t)$: Total number of occupied CPs at time t
Input : $T_{QP}(t)$: Total number of occupied QPs at time t
Input : $j_{fcu}(t)$: Total number of plugged-in FCUs at time t
Input : $j_q(t)$: Total number of occupied QPs at time t
Input : $j(t)$: Total number of plugged-in EVs at time t
Input : $j_{ncscu}(t)$: Total number of plugged-in NCSCUs at time t
Output: $\boldsymbol{A}^{ev}_{j(t)\times n}$: Plugged-in EVs matrix at time t
Output: $\boldsymbol{A}^{q}_{j_q(t)\times n}$: Queued EVs matrix at time t

```
if T_CP(t) < M then
    FCU is plugged into an idle CP
else if T_CP(t) == M AND T_QP(t) < M AND j_ncscu(t) > 0 then
    Rank plugged-in NCSCUs in descending order based on SoC^k_NCSCU(t)
    Queue the NCSCU with SoC_max,NCSCU(t)
    FCU is plugged into the vacated CP by the NCSCU
    Update A^q_{j_q(t)×n}
else if T_CP(t) == M AND j_fcu(t) > 0 then
    Rank plugged-in FCUs in descending order based on SoC^k_FCU(t)
    if SoC_FCU,max(t) > SoC_FCU,T then
        Force terminate the plugged-in FCU with SoC_FCU,max(t)
        New FCU is plugged into the vacated CP by the ongoing FCU
    else
        Block the FCU
    end
else
    Block the FCU
end
Update A^ev_{j(t)×n}
```

Otherwise, the CS controller performs the resource allocation based on the Algorithm 5.1.

5.4.2 Queued SCUs

The resource allocation for queued SCUs is in accordance with the Algorithm 5.2. For each queued SCU, it is checked for its 'critical' status at each time slot over the complete time window as it depends on the minimum charging time ($\tau_{SCU,min}$) and the parking horizon ($H^k_{SCU}(t)$) at time t. A CP must be assigned for a CSCU by either sending an NCSCU to the queue or forcibly terminating an ongoing fast-charging process.

5.4.3 FCU Arrivals

The resource allocation for FCUs is described in Algorithm 5.3. Newly arrived FCU can access a CP without disturbing any ongoing charging process if at least one idle CP. On the other hand, if the CS is fully occupied, then the CS controller seeks a plugged-in NCSCU to send to the queue. Nevertheless, if it is not possible to find an NCSCU, a sufficiently charged plugged-in FCU has to forcibly terminate its ongoing charging process and donate the CP to the newly arrived FCU. It is regarded that the k^{th} plugged-in FCU is sufficiently charged if its SoC is higher than a pre-defined threshold ($SoC^k_{FCU}(t) > SoC_{FCU,T}$). Otherwise, the new FCU is blocked.

5.5 Dynamic EV Charging Coordination at FCS

For newly arrived EVs, charging resources are allocated based on Algorithm 5.1 to Algorithm 5.3. Thus, mentioned algorithms premise only a portion of arrived FCUs to be plugged in depending on the availability of the charging resources, while others are blocked. Furthermore, due to the DL enforced by the central aggregator, all the plugged-in EVs might not be charged during a time slot. Therefore, at each time slot, the charging priority of each plugged-in EV is determined based on the corresponding charging completeness measured in terms of SoC. As a result, CSCUs are the most prioritized EVs to be charged in the next time slot. Conversely, NPSCUs are the least prioritized users for charging. These requirements are handled with the help of a dynamic priority array $\boldsymbol{A}^p_{j_p(t)\times n}$ described in the Algorithm 5.4. Then, according to the order of the $\boldsymbol{A}^p_{j_p(t)\times n}$, the CS controller enables or disables plugged-in EVs for charging based on the Algorithm 5.5 and 5.6. How these Algorithms are interconnected to build the complete discrete simulation is illustrated in Figure. 5.2.

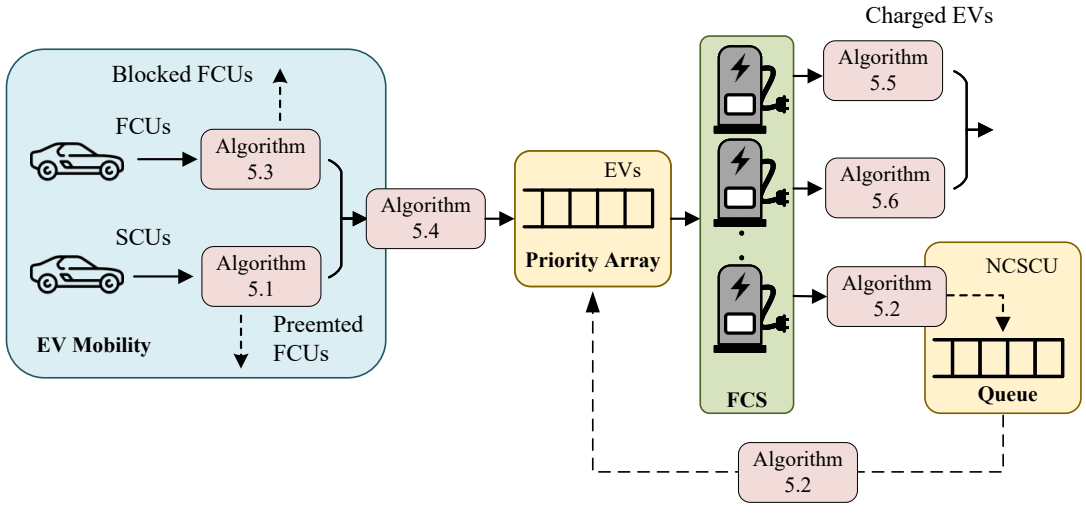

Figure 5.2: Dynamic EV charging coordination with developed Algorithms

The main objective of the CS controller is to maximize the CS profit by optimally utilizing the allocated DL, letting FCUs be charged when registered users are not very active within the CS.

Algorithm 5.4: Pseudo code for the Priority Array

Input : $j_{fcu}(t)$: Total number of plugged-in FCUs at time t
Input : $j_{scu}(t)$: Total number of plugged-in SCUs at time t
Input : $j_{cscu}(t)$: Total number of plugged-in CSCUs at time t
Input : $j_{ncsu}(t)$: Total number of plugged-in NCSCUs at time t
Input : $\boldsymbol{A}^{ev}_{j(t)\times n}$: Plugged-in EVs matrix at time t
Input : $\boldsymbol{A}^{scu}_{j_{scu}(t)\times n}$: Plugged-in SCUs matrix at time t
Input : $\boldsymbol{A}^{fcu}_{j_{fcu}(t)\times n}$: Plugged-in FCUs matrix at time t
Input : $\boldsymbol{A}^{cscu}_{j_{cscu}(t)\times n}$: Plugged-in CSCUs matrix at time t
Input : $\boldsymbol{A}^{ncscu}_{j_{ncscu}(t)\times n}$: Plugged-in NCSCUs matrix at time t
Output: $\boldsymbol{A}^{p}_{j_p(t)\times n}$: Priority array of plugged in EVs at time t

if $j_{scu}(t) > 0$ **then**
  Compute $\boldsymbol{A}^{scu}_{j_{scu}(t)\times n}$ from $\boldsymbol{A}^{ev}_{j(t)\times n}$
if $j_{fcu}(t) > 0$ **then**
  Compute $\boldsymbol{A}^{fcu}_{j_{fcu}(t)\times n}$ from $\boldsymbol{A}^{ev}_{j(t)\times n}$
  Rank $\boldsymbol{A}^{fcu}_{j_{fcu}(t)\times n}$ according to the $SoC^{k}_{FCU}(t)$
for *i=1 to* $j_{scu}(t)$ $\left(\forall \boldsymbol{A}^{scu}_{j_{scu}(t)\times n}\right)$ **do**
  if $\tau^{i}_{SCU,min} < H^{i}_{SCU}(t)$ **then**
    Put i^{th} SCU in $\boldsymbol{A}^{cscu}_{j_{cscu}(t)\times n}$
    Rank $\boldsymbol{A}^{cscu}_{j_{cscu}(t)\times n}$ according to the $SoC^{i}_{SCU}(t)$
  else
    Put i^{th} SCU in $\boldsymbol{A}^{ncscu}_{j_{ncscu}(t)\times n}$
    Rank $\boldsymbol{A}^{ncscu}_{j_{ncscu}(t)\times n}$ according to the $SoC^{i}_{SCU}(t)$
  end
end
Compute $\boldsymbol{A}^{p}_{j_p(t)\times n}$ from $\boldsymbol{A}^{cscu}_{j_{cscu}(t)\times n}$, $\boldsymbol{A}^{fcu}_{j_{fcu}(t)\times n}$ and $\boldsymbol{A}^{ncscu}_{j_{ncscu}(t)\times n}$

According to the order of the $\boldsymbol{A}^{p}_{j_p(t)}$, at each charging time slot (Δt), the FCS controller enable plugged-in EVs for charging according to the heuristic Algorithm 5.5 and 5.6. Therefore, the CS controller should optimally dispatch the power while adhering to the constraints enforced by the distribution grid and the central aggregator by maintaining high CS utilization, high CS capacity, low blocking probability, low force termination probability, and user satisfaction.

In the proposed coordinated EV charging strategy, connected SCUs will be fully charged at the departure ($SoC^{dep,k}_{SCU} = 1$). Nevertheless, there is no guarantee for connected FCUs to be fully charged at the departure as they may be subject to force termination upon arrival of an SCU when both the CS and queue are fully occupied. However, proposed charging strategies make sure connected FCUs to be charged sufficiently at the departure.

Charging completeness in terms of SoC is the main parameter that has to be addressed in EV charging. Consequently, SCUs expect their EVs to be fully charged at the departure ($SoC_{scu}^{dep,k} = 100\%$) as they park their EVs for long period and pay for both parking and charging. Conversely, FCUs are not assured for fully charged at the departure and hence, they pay only for the electricity consumption for charging. In this work, two coordinated charging schemes are proposed using fixed rate charging and variable rate charging. The proposed fixed rate power dispatching strategy is illustrated in algorithm 5.5.

Algorithm 5.5: Heuristic Charging Coordination with Static Charging

Input : $j_p(t)$: Total number of plugged in EVs at time t
Input : $P_{total}(t)$: Total EV charging power at time t
Input : $P_{EV}^{k}(t)$: Charging power of k^{th} EV at time t
Input : $\boldsymbol{A}^{p}_{j_p(t)\times n}$: Priority Array at time t
Input : $DL(t)$: Demand limit

for *k=1 to* $j_p(t)$ $\left(\forall \boldsymbol{A}^{p}_{j_p(t)\times n}\right)$ **do**
  if *the* k^{th} *EV is a SCU* **then**
    $P_{EV}^{k} = \eta_{SCU} P_{SCU}$
  else
    $P_{EV}^{k} = \eta_{FCU} P_{FCU}$
  end
  $P_{total}(t) = P_{total}(t) + P_{EV}^{k}$
  if $P_{total}(t) < DL(t)$ **then**
    k^{th} EV is charging
  else
    k^{th} EV is not charging
  end
end

Fixed rate charging may not be able to optimally utilize the allocated power when the CS utilization is low due to the energy gaps. But with the variable rate charging, this issue can be avoided enhancing the completion rate. Algorithm 5.6 describes the proposed variable rate charging coordination scheme in which charging rates ($P_{SCU,new}(t)$ and $P_{FCU,new}(t)$) will be varied dynamically.

Vacated CP by a charged EV will be allocated to a queued SCU. These proposed strategies let FCUs to be accessed the CS opportunistically to charge their EVs to enhance their driving range and to avoid range anxiety in long trips. Therefore, when admitting a FCU to the CS, they know that the CS does not guarantees FCUs to be fully charged at the departure and hence, they pay only for the electricity consumption for charging. Power dispatching controller charges FSUs in the order of current SOC ($SOC_{FCU}^{k}(t)$) from the lowest to highest within each charging period (Δt) while adhering all the constraints.

Algorithm 5.6: Heuristic Charging Coordination with Adaptive Charging

Input : $P_{total}(t)$: Total EV charging power at time t
Input : $\Delta P_{max}(t)$: Total extra power required to charge FCUs at P_{fcu}^{max} at time t
Input : $DL(t)$: Demand limit
Output: $P_{EV}^{k}(t)$: Charging power of k^{th} EV at time t

for *k=1 to* $j_p(t)$ $\left(\forall \boldsymbol{A}_{j_p(t)}^{p}\right)$ **do**
  if *the* k^{th} *EV is a SCU* **then**
    $P_{EV}^{k} = \eta_{scu} P_{scu}^{k}$
  else
    $P_{EV}^{k} = \eta_{fcu} P_{fcu}^{k}$
  end
  $P_{total}(t) = P_{total}(t) + P_{EV}^{k}$
  if $P_{total}(t) < DL(t)$ **then**
    k^{th} EV is enabled for charging
  else
    k^{th} EV is not enabled for charging
  end
end
$\Delta P(t) = DL(t) - P_{total}(t)$
if $\Delta P(t) > 0$ **then**
  for *k=1 to* $j_P(t)$ $\left(\forall \boldsymbol{A}_{j_{fcu}(t)}\right)$ **do**
    if $\Delta P(t) < \Delta P_{max}(t)$ **then**
      $P_{fcu,new}^{k}(t) = P_{fcu}^{k}(t) + \Delta P(t)(P_{fcu}^{max} - P_{fcu}^{k})/\Delta P_{max}(t)$
    else
      $P_{fcu,new}^{k}(t) = P_{fcu}^{max}$
    end
  end
Charge all EVs

Dynamic admission control and charging coordination strategies do not guarantee FCUs to be fully charged but make every possible effort to complete FCU charging process as fast as possible so that more FCUs can be plugged-in.

5.6 Results and Discussion

This section analyzes the results obtained from the presented models in previous sections to validate the performance of developed dynamic resource allocation and charging coordination strategies. It is considered that the central aggregator uses the day-ahead DL to minimize the load variance at the distribution transformer.

This DL constraint affects the charging process from various user comfort perspectives such as charging time, waiting/queuing time, blockage, forced termination, etc. To determine the overall performance of the proposed coordinated charging scheme, charging demand is taken into comprehensive consideration along with the EV user comfort aspects.

The CS controller (sub-aggregator) optimally utilizes the allocated power by the central-aggregator to plugged-in EVs in real-time, adhering to the constraints enforced by the utility and satisfying the users' preferences. A case study with a CS with 50 CPs and 10 QPs is considered to demonstrate the power flow management of the developed strategies. When any EV arrives to the CS, it is considered that the capacity and SoC of the EV battery are uniformly distributed. The variation of the power required for both coordinated and uncoordinated EV charging are illustrated in Figure 5.3.

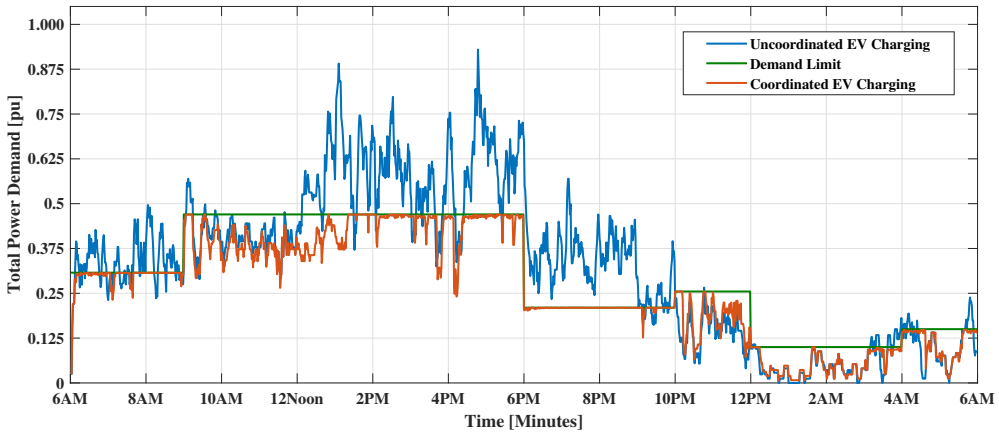

Figure 5.3: Charging demand profiles for both coordinated and uncoordinated EV charging

In this study, it can be seen that the CS highly stresses the electric network during morning hours (6 AM to 9.30 AM) and 12 Noon to 6 PM due to the high arrival rate of fast charging EVs, resulting in a peak demand of 0.925 pu, if the EV charging is left uncoordinated. During this period, the power demand of the CS has to be kept at 0.47 pu to maintain a sort of minimum load variance at the distribution transformer. Figure 5.3 depicts that the proposed strategies optimally utilize the allocated power for EV charging without stressing the electric network. SCUs do not charge in their whole parking horizon even though they are connected to a charger.

By putting SCUs in a queue when they are not being charged, the resource could be allocated to an opportunistic FCU if it does not violate the constraints. It can be seen that the proposed strategies use the limited charging resources optimally with the benefits of having four different fixed charging rates for heterogeneous EV user.

Figure 5.4 illustrates EV charging demand profiles for uncoordinated charging, proposed coordinated charging scheme without a queue, and coordinated charging scheme with a queue in the same plot.

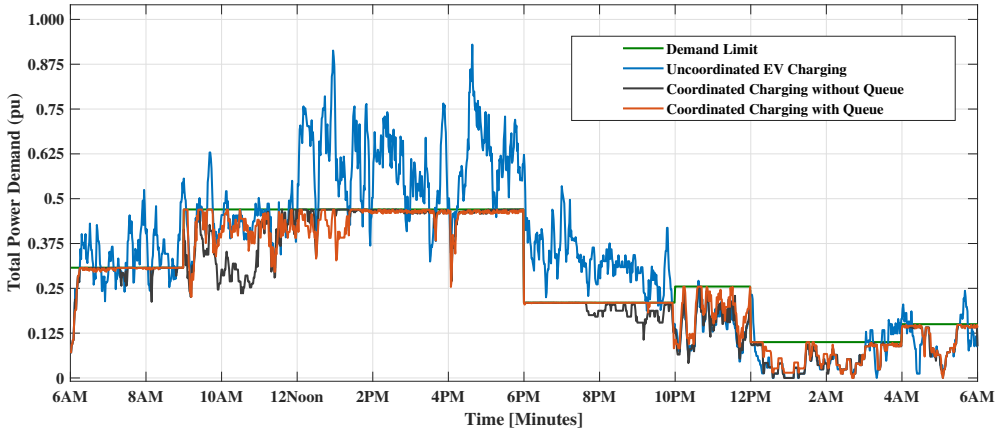

Figure 5.4: Charging demand profiles for uncoordinated and coordinated EV charging with and without queue

By analyzing the power profiles in Figure 5.4, it can be clearly observed that both the cases of developed charging scheme well maintain the allocated power demand without exerting stresses to the electric network. As depicted in Figure 5.5, the optimal demand attainment capability of the scheme with a queue is higher than that of the scheme without a queue due to the fact that more FCU requests can be accepted with the buffer. From 9.30 AM to 12 Noon and 7 PM to 10 PM, charging strategies with a queue maximally utilize the allocated demand compared to the charging scheme without a queue.

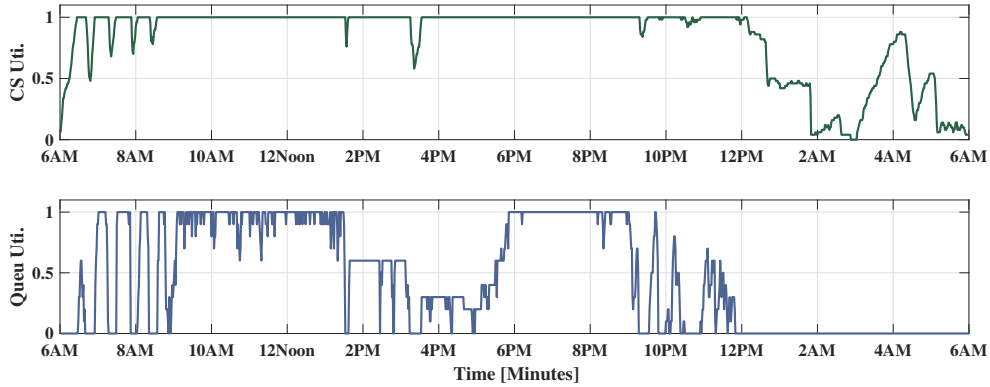

Figure 5.5: Charging resource and queue utilization

We analyze the performance of developed charging resource allocation and charging coordination strategies with adaptive charging. We consider that the day-ahead DL given by the CS aggregator intends to flatten the load curve of the distribution transformer. Here, we are going to analyze the effectiveness of exploiting unused charging resources by SCUs for opportunistic FCUs with adaptive EV charging.

An FCS with 30 CPs and 10 QPs is considered to demonstrate the performance of the proposed strategies. We have considered 82 SCUs in the EV mobility model whose plug-in times are uniformly distributed. Figure 5.6 depicts the variation of charging power for both coordinated and uncoordinated EV charging. From Figure 5.6, we can clearly observe that the proposed strategies well maintain the allocated power demand without exerting stresses to the electric network. The optimal demand attainment capability with adaptive charging is higher than that of with fixed-rate charging due to high charging resource utilization and charging completion.

The expected profit from the SCUs can be enhanced with opportunistic FCUs on top of the primary SCUs. Therefore, profit maximization performance is also analyzed in terms of charging resource utilization and average charging completion rate ($minute^{-1}$) for different arrival rates of FCUs.

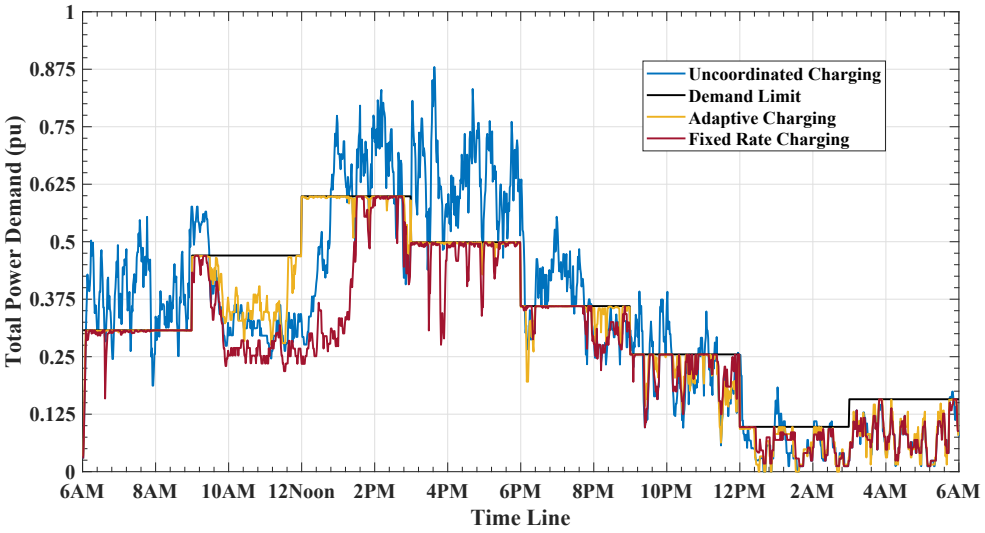

Figure 5.6: Charging power variation with adaptive charging

Figure 5.7 and Figure 5.8 illustrate the charging resource utilization and the average charging completion rate of EVs as the mean arrival rate (daily average rate) of FCUs (λ_{FCU}) varies from 0 to 2 $minute^{-1}$, respectively. From these figures, we can observe that both charging resource utilization and average charging completion show continuous ascent with the mean arrival rate of FCUs resulting in high yield at the end of the day. Moreover, both parameters give better performance with adaptive charging of FCUs as compared that of with fixed rate charging.

It can be noted that the average charging completion rate of EVs starts becoming saturated after the mean arrival rate of 1.2 $minute^{-1}$ of FCUs. Above this mean arrival rate of FCUs, more arrived EVs would be blocked as all CPs are likely to be fully utilized at the event of arrivals.

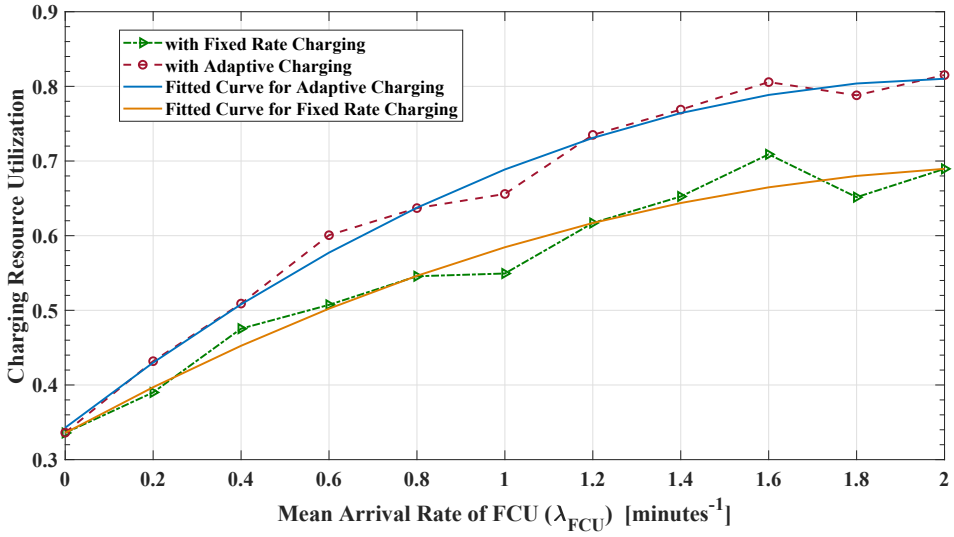

Figure 5.7: Charging Resource Utilization as a function of λ_{FCU}

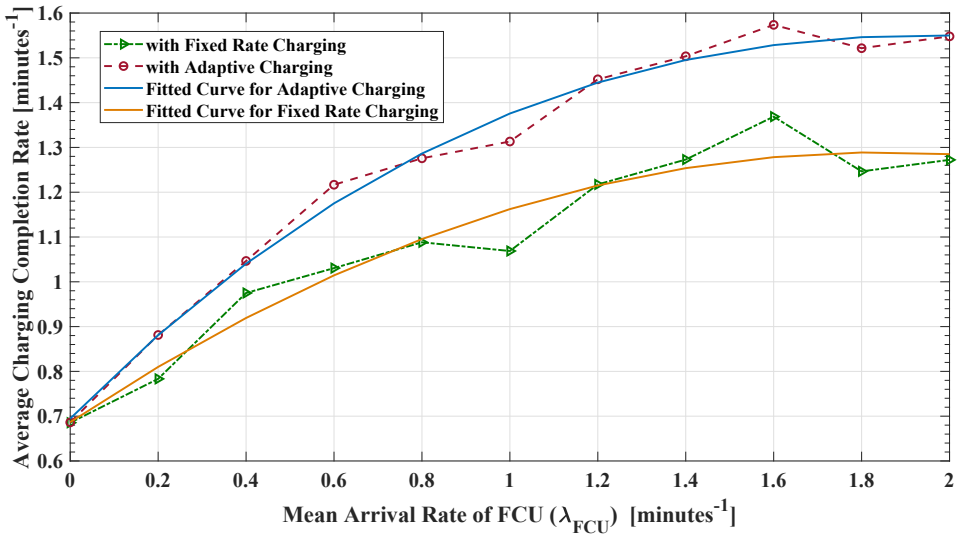

Figure 5.8: Average Charging Completion Rate of EVs

High service quality for SCUs is guaranteed with 100% completion of the requested SoC at the departure. Conversely, to assess the long-term willingness of EV users to select this CS, blocking probability is essential. As a performance parameter associated with the quality of service assured for FCUs by the FCS where both registered and opportunistic users are served, blocking probability of FCUs is plotted in Figure 5.9 against λ_{FCU}.

This would be essential in considering the capacity expansion. Blocking probability shows a continuous ascent when λ_{FCU} increases. Nevertheless, the blocking probability has been effectively reduced with adaptive charging for FCUs in place of fixed-rate charging.

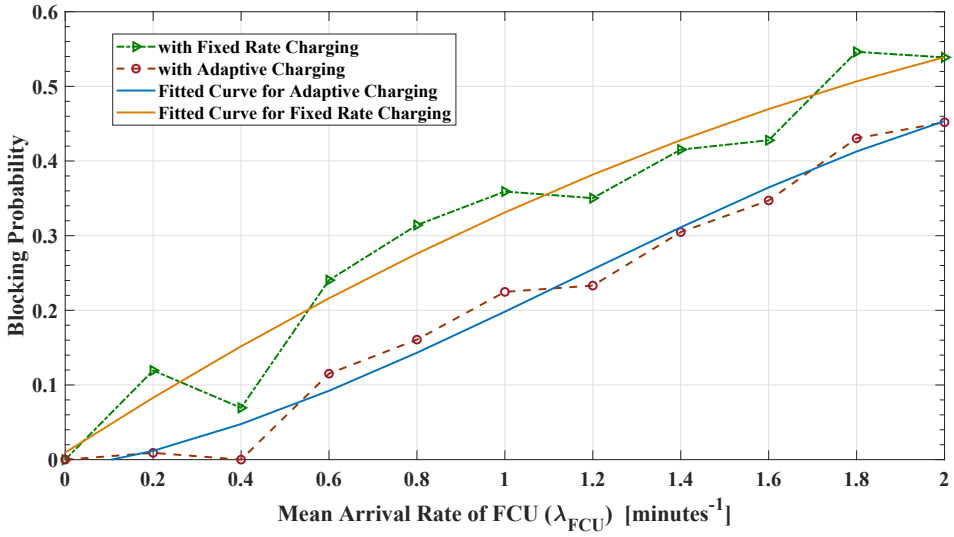

Figure 5.9: Blocking Probability of FCUs with λ_{FCU}

5.7 Conclusion

This chapter effectively analyzes the performance of developed dynamic resource allocation and charging coordination strategies to maximize charging resource utilization without jeopardizing the electric network stability. The day-ahead demand limit is allocated by the CS aggregator level to minimize the load variance in the distributed network. The proposed queue-based dynamic resource allocation and coordinated EV charging strategies enable FCUs to charge their EVs opportunistically when registered users are not active to utilize the allocated demand optimally; hence it keeps the average charging station utilization above 90% at higher arrival rates of EVs

With the proposed strategies, opportunistic FCUs can attain an SoC of more than 95% at the departure as EVs are prioritized in the order of the charging completeness measured in terms of the SoC of EV battery at each charging time slot. Moreover, the distribution transformer is loaded only up to 50% of its rated capacity at the peak demand, and this is a 40% reduction compared to uncoordinated EV charging. Therefore, the priority-based heuristic algorithm properly coordinates the charging demand without stressing the distributed network for heterogeneous EV traffic. Therefore, it can be concluded that the queue-based CS operation mechanism outperforms the one without a queue in terms of power utilization, CS utilization, and charging completion rates. Furthermore, this chapter presents a framework to evaluate QoS of heterogeneous EV users. It proves that the adaptive charging approach enhances the charging resource utilization further. The adaptive charging approach reduces the blocking probability of FCUs. Moreover, as the proposed charging management algorithm is a priority-based heuristic, the computational complexity is not very sophisticated, and the computational time is comparatively lesser than others; hence, this is very suitable for real-time operation.

Chapter 6

Reliability of Fast Charging Station under Electric Vehicle Supply Equipment Failures and Repairs

[6] *Rapid deployment of fast-charging stations (FCSs) promotes the proliferation of electric vehicles (EVs) alleviating long charging time and range anxiety of long-trip drivers. This chapter focuses on the enhancement of the charging reliability of both registered primary (scheduled) (PEVs) and opportunistic (OEVs) EV users in an EV fast charging station (FCS). Proposed charging coordination strategies allow OEVs to exploit unused charging resources to optimally utilize the limited charging resources of FCS. However, the optimum utilization of limited charging resources of an FCS while assuring a reliable charging process for plugged-in EVs under random failures of electric vehicle supply equipment (EVSE) is a real challenge for the FCS controller. When the FCS admits OEVs in addition to PEVs, assuring a satisfactory quality of service to both EV user categories is also dispensable. Therefore, we analyze the performance of reservation of off-board mobile chargers (MOBCs) to enhance the charging reliability of EV users while achieving high charging resource utilization. This work proposes resource allocation and charging coordination strategies for an FCS where MOBCs are used to enhance the charging reliability of both PEVs and OEVs. Moreover, the proposed dynamic charging resource coordination strategies are analyzed with a continuous time Markov-Chain (CTMC). Presented results from the CTMC model demonstrate that the proposed strategies outperform the EV charging process of the FCS in terms of high resource utilization and reliability while guaranteeing a satisfactory quality of service to EV users.*

[6]This chapter is based on the peer-reviewed journal paper, K. M. S. Y. Konara *et. al* "Reliability Enhancement of Fast Charging Station under Electric Vehicle Supply Equipment Failures and Repairs," *Energies (ISSN: 1996-1073)*, vol 16, 2933, 2023. doi : 10.3390/en16062933

6.1 Introduction

EV charging process at a fast charging station (FCS) is affected by various uncertainties such as energy supply uncertainties, energy price uncertainties, spatiotemporal uncertainties, EV supply equipment failures, etc. as illustrated in Figure 6.1. In EV charging coordination, a number of EV supply equipment (EVSE) or chargers plays a major role in relation to the quality of EV charging in terms of EV blockage, preemptage, reliability, availability, etc. In a more realistic charging coordination scheme, the number of chargers/ EVSE and their individual capacity put another constraint to the charging coordination.

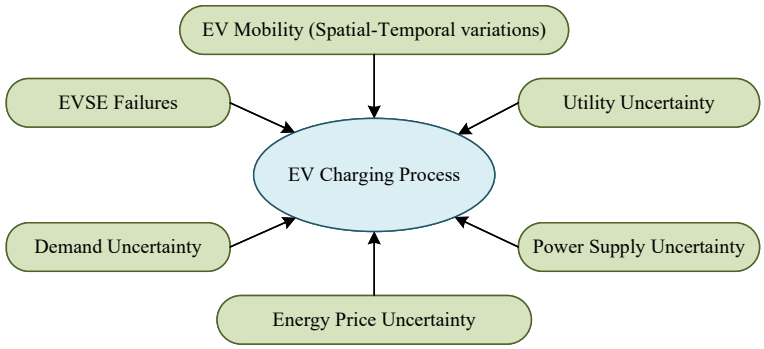

Figure 6.1: Uncertain aspects for EV Charging Process

Nevertheless, due to various uncertainties shown in Figure 6.1, limited charging resources including both energy resources and chargers/EVSE might not be optimally utilized by the registered/scheduled EV users (PEVs) in real-time operation. Moreover, treating the charging processes with a few minutes duration (long-trip drivers or ultra-fast charging users) as opportunistic charging processes instead of scheduled ones would be more realistic. Although substantial research efforts have been devoted on the optimal scheduling of EVs at a CS, how to effectively exploit unused limited charging resources under uncertain conditions to further enhance resource utilization is not adequately analyzed. Furthermore, due to random failures and repairs of EVSE, the capacity of the FCS would be uncertain to maintain high availability for EV arrivals and high reliability for plugged-in EV users. If we ignore random failures of EVSE, we overestimate the average capacity of the FCS to analyze charging resource coordination. Therefore, we propose an event-based dynamic charging resource coordination strategy with a focus on the impact of random EVSE failure and repair so that opportunistic ultra-fast charging opportunistic users (OEVs) can exploit limited charging resources allocated for PEVs. Consequently, the novel technical contribution is to propose a dynamic charging resource allocation strategy for both registered PEVs and opportunistic OEVs together with mobile off-board chargers (MOBCs) and to analyze the reliability enhancement of FCS under EVSE failure and repair. In this work, we employ a continuous time Markov Chain (CTMC) approach to model the proposed strategies.

6.2 Dynamic Charging Resource Allocation under EVSE Failure

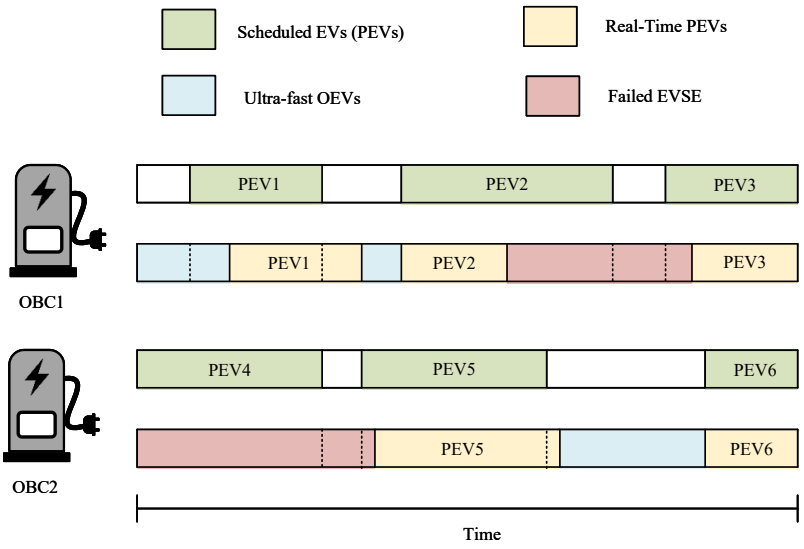

Figure 6.2: Utilization of charging resources by OEVs

Figure 6.2 illustrates the under-utilization and capacity reduction of an FCS due to various uncertainties associated with EV charging including EVSE failures. When we consider the charging resource utilization of scheduled EVs (PEVs) at an FCS, limited charging resources might not be optimally utilized due to various uncertainties illustrated in Figure 6.1. This wasted energy can be compensated by allowing opportunistic ultra-fast charging EV users (OEVs) along with PEVs. At the same time, we should note that EVSE are susceptible to fail due to hardware failures or protection issues. Owing to those failures of EVSE, the capacity of FCS or the effective number of plugged-in and charged EVs (throughput) decreases and the average charging time may rise.

If we evaluate the FCS's performance without considering this downtime of EVSE, it overestimates the FCS capacity and performance. To overcome the adverse impact of downtime of EVSE, we employ MOBCs at the FCS. In this work, we focus on dynamic charging resource allocation and coordination of the FCS under EVSE failure and repair as depicted in Figure 6.3. Dynamic charging coordination strategies are proposed for mainly OEVs so that OEVs do not interfere with PEV charging process. As OEVs can aggregate charging resources to achieve higher charging rates, they can quickly increase the state of charge of their EV batteries with economical pricing schemes as compensation.

Basically, two types of EV users are considered : (1) PEVs and (2) OEVs. The distinct privileges and constraints of both EV user types in accessing the FCS is tabulated in Table 6.1.

Table 6.1: Access Privileges and Constraints of EV users

PEVs	**OEVs**
• Pre-scheduled charging process	• Opportunistic charging
• Charged at specified charge rate $P_p;\ P_p \in [P_p^{min}, P_p^{max}]$	• Charged at specified higher charge rate $P_o = nP_p; (n \in \mathbb{Z}^+)\ ,\ P_o \in [P_o^{min}, P_o^{max}]$
• Charger is guaranteed on arrival.	• Charger is assigned if sufficient resources are available only.
• Very hardly subject to blockages	• Subject to blockages
• Charging process regularly finishes.	• Charging process is liable to be preempted before regularly finishes.
• Prioritized users at the MOBCs	• Charging process is liable to be preempted at the MOBCs.
• Expect uninterruptible EV charging	• Expect to charge as quickly as possible

The operation mechanism of FCS under EVSE failure and repair is illustrated in Figure 6.3.

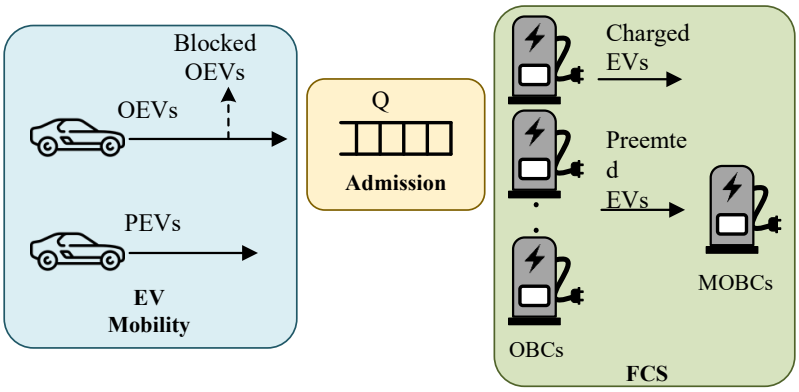

Figure 6.3: Proposed operation mechanism of the FCS

In this work, we have considered an already deployed FCS with $M\ ;\ (M \in \mathbb{Z}^+)$ number of off-board chargers (OBCs) and $N\ ;\ (N \in \mathbb{Z}^+)$ number of MOBCs that are used to enhance the reliability of ongoing charging processes. It is assumed that the charging power of each charger both in OBCs and MOBCs can be adjustable. The FCS schedule and execute the charging processes of PEVs in line with EV user preferences. In the meantime, FCS admits opportunistic OEVs to exploit non-utilized limited charging resources. In this work, we consider that PEVs are charged at a specified charge rate of $P_p;\ P_p \in [P_p^{min}, P_p^{max}]$ while OEVs are charged at nP_p depending on charging resource availability at arrival.

The value n is chosen such that nP_p is less than the rated power output an OBC/MOBC $(P_c^{max})\ ;\ nP_p^{max} \leq P_c^{max}$. Consequently, the capacity of FCS becomes MP_p^{max}. The energy supply of FCS should meet this capacity throughout the operating horizon. PEVs demand an uninterruptible charging process where as OEVs are liable to be interrupted upon arrival of PEVs if charging resources are not adequate. MOBCs identical to OBCs are deployed to retain ongoing charging processes without affecting from EVSE failures and forced terminations of OEVs.

In this work, we develop a performance assessment framework using continuous-time Markov-Chain to evaluate the performance of an FCS in terms of reliability under EVSE failure and repair.

The charging coordination of FCS is taken place with main three stages : (1) Optimal scheduling of PEVs to maximize the profit. They utilize charging resources as primary users. (2) Admitting OEVs as secondary users to exploit non-utilized limited charging resources. (3) Shifting interrupted charging processes due to EVSE failures and preemption of OEVs to MOBCs. In this work, we analyze the impact of opportunistic secondary users over PEVs and themselves under effective FCSs' capacity changes due to EVSE failures.

6.2.1 Stochastic EV Mobility Model

The performance of the FCS with proposed charging coordination strategies is analyzed using a continuous-time Markov chain (CTMC) model. Therefore, the following assumptions are made to develop the CTMC analytical model.

- Both PEV and OEV arrivals are Poisson processes with mean arrival rates of λ_p and λ_o, respectively. Where (λ denotes the average number of charging requests made by the respective category of EVs per unit time)
- All OBCs and MOBCs are homogeneous and the service time of an EVSE is exponentially distributed with the service rate of μ_c. (μ_c rate denotes the average number of charged EVs per EVSE per unit time)
- All failures are homogeneous. The inter-failure time (during which an OBC functions well) of an OBC is exponentially distributed with a failure rate of λ_f per EVSE.
- The repair time of an OBC is exponentially distributed, with a repair rate per EVSE of μ_r.

In order to develop the CTMC analytical model to assess the reliability of FCS under EVSE failures, the following events are considered for state transitions; (1) PEV Arrivals at FCS (2) PEV Departures from FCS (3) OEV Arrivals at FCS (4) OEV Departures from FCS. (5) Failure of EVSE to which a PEV is connected. (6) Failure of EVSE to which a OEV is connected. (7) Idle OBC failure. (8) Repair of a failed EVSE. In CTMC model, we have defined a generic state $\mathbf{x}$; $\mathbf{x} = \{x_s, x_u, x_{sm}, x_{um}, x_f\}$ to model system dynamics at each event aforementioned. In a generic state $\mathbf{x}$, x_s and x_{sm} denote the number of PEVs plugged into normal OBCs and MOBCs, respectively. The number of OEVs plugged into normal OBCs and MOBCs is denoted by x_u and x_{um}, respectively. Furthermore, x_f indicates the number of failed OBCs at FCS.

6.2.2 Dynamic Charging Coordination Model

Initially, the set of feasible states of the system ($\mathbf{S}$) is obtained from the whole state space. $\mathbf{S} = \{\mathbf{x}|x_s, x_u, x_{sm}, x_{um}, x_f \geq 0;\ x_s \leq M,\ x_u \leq \lfloor (M/n) \rfloor,\ x_{sm} \leq N,\ x_{um} \leq \lfloor (N/n) \rfloor\ x_f \leq M,\ \sum(x_s, nx_u) \leq M,\ \sum(x_s, x_u, x_f) \leq M,\ \sum(x_{sm}, nx_{um}) \leq N\}$. The level of charging resource aggregation by OEVs is up to n steps as per the charging resource availability. The state transitions (STs) triggered by the aforementioned events at the FCS are described in the subsequent subsections. Power utilization of EVs and EVSE utilization of normal and mobile OBCs are expressed in (6.1), (6.2) and (6.3) respectively.

$$a(\mathbf{x}) = x_s + nx_u + x_f \quad (6.1) \qquad b(\mathbf{x}) = x_s + x_u + x_f \quad (6.2) \qquad c(\mathbf{x}) = x_{sm} + x_{um} \quad (6.3)$$

Arrivals of EVs at FCS

Arrivals of PEVs (APEVs) and OEVs (AOEVs) at FCS are considered in this Section. The STs triggered due to the APEVs and AOEVs are tabulated in ST Table 6.2. It is considered that the FCS is obliged to allocate charging resources immediately after arrival of an PEV as they have prior-agreements. Consequently, upon an arrival of an PEV, if at least one idle OBC, the PEV is plugged-in without disrupting others. Otherwise, any ongoing OEV charging process must be interrupted. However, this interrupted OEV can be shifted to MOBCs if at least one idle EVSE. Otherwise, the concerned OEV charging process has to be preempted.

Table 6.2: STs from $\mathbf{x}$ triggered by EV Arrivals

Conditions		Destination State	ST Rate
APEVs, At least an idle OBC	$M - a(\mathbf{x}) > 0$;	$\{x_s + 1, x_u, x_{sm}, x_{um}, x_f\}$	λ_p
APEVs, FCS is full. OEVs exist. idle MOBC exist	$M - a(\mathbf{x}) = 0$; $c(\mathbf{x}) < N$; $x_u > 0$;	$\{x_s + 1, x_u - 1, x_{sm}, x_{um} + 1, x_f\}$	λ_p
APEVs, FCS is full. OEVs exist No idle MOBCs	$M - a(\mathbf{x}) = 0$; $c(\mathbf{x}) = N$;$x_u > 0$;	$\{x_s + 1, x_u - 1, x_{sm}$ $, x_{um}, x_f\}$	λ_p
APEVs, FCS is full. OEVs exist No idle MOBCs	$M - a(\mathbf{x}) = 0$; $c(\mathbf{x}) = N$;$x_u > 0$;	$\{x_s + 1, x_u - 1, x_{sm}, x_{um}, x_f\}$	λ_p
APEVs, FCS is full. No OEVs	$M - a(\mathbf{x}) = 0$; $x_u = 0$;	$\{x_s, x_u, x_{sm}, x_{um}, x_f\}$	λ_p
AOEVs, At least an idle OBC Enough CRs available	$M - a(\mathbf{x}) \geq n$	$\{x_s, x_u + 1, x_{sm}, x_{um}, x_f\}$	λ_o
AOEVs, FCS is full.	$M - a(\mathbf{x}) < n$;	$\{x_s, x_u, x_{sm}, x_{um}, x_f\}$	λ_o

Moreover, in an occasion where all OBCs are occupied by PEVs, newly arrived PEV must be blocked. The destination states related to STs triggered by PEV arrivals with respect to the generic state $\mathbf{x}$ at λ_p transition rate (TR) are tabulated in Table 6.2.

The FCS accepts OEVs if PEVs do not occupy all the OBCs. Upon a new OEV arrival at the FCS, it is plugged-in, if at least an OBC and enough energy resources are available to provide charging power of P_o^{max}. Otherwise, the OEV has to be blocked as the charging processes of plugged-in OEVs are not preempted upon the arrival of the new OEV. Similarly, the STs triggered due to the arrivals of OEVs are tabulated in ST Table 6.2. The corresponding STs are taken place at λ_o TR.

Departures of EVs from FCS

Departures of PEVs (DPEVs) and OEVs (DOEVs) from FCS are considered in this Section. Upon completion of charging, both PEVs and OEVs depart from the FCS leaving an idle OBC or MOBC. As one OEV aggregate charging resources of n OBCs, it releases such amount of charging resources at the departure. A similar situation happens for MOBCs as well. The corresponding STs from $\mathbf{x}$ upon departure of PEV under the conditions aforementioned are tabulated in Table 6.3.

Table 6.3: STs from $\mathbf{x}$ triggered by EV Departures

Conditions		Destination State	ST Rate
DPEVs from an OBC	$x_s > 0;$	$\{x_s - 1, x_u, x_{sm}, x_{um}, x_f\}$	$x_s\mu_{cp}$
DOEVs from an OBC	$x_u > 0;$	$\{x_s, x_u - 1, x_{sm}, x_{um}, x_f\}$	$x_u\mu_{cp}$
DPEVs from an MOBC	$x_{sm} > 0;$	$\{x_s, x_u, x_{sm} - 1, x_{um}, x_f\}$	$x_{sm}\mu_{cp}$
DOEVs from an MOBC	$x_{um} > 0;$	$\{x_s, x_u, x_{sm}, x_{um} - 1, x_f\}$	$x_{um}\mu_{cp}$

EVSE Failures and Repairs

In order to retain ongoing charging processes during the failures of EVSE, a limited number of MOBCs are placed at the FCS. When comes to failures of EVSE, STs are considered depending on the user category of the EV connected with the failed EVSE. At a failure of EVSE, initially, the FCS seeks for an idle OBC regardless of the EV user category and if it fails only the EV is shifted to MOBCs. At a failure of PEV-connected EVSE (FPEV), it gets the high priority to continue the charging process at MOBCs. If it can find an idle MOBC, the PEV is shifted to MOBCs without interrupting any ongoing OEV charging process. Otherwise, an OEV (if any) has to terminate its charging process at MOBCs and donate the MOBC to the PEV. Still if it fails, the PEV charging process has to be terminated. However, at a failure of OEV-connected EVSE (FOEV), the OEV is shifted to MOBCs if an idle MOBC is available only. The STs triggered because of the failures and repairs of EVSE are tabulated in ST Table 6.4.

Table 6.4: STs from $\mathbf{x}$ triggered by EVSE Failures and Repairs

Conditions		Destination State	ST Rate
Idle EVSE Failure	$M - b(\mathbf{x}) > 0$;	$\{x_s, x_u, x_{sm}, x_{um}, x_f + 1\}$	$\lambda_f(M - b(\mathbf{x}))$
FPEVs, idle OBC exists	$M - b(\mathbf{x}) > 0$; $x_s > 0$;	$\{x_s, x_u, x_{sm}, x_{um}, x_f + 1\}$	$\lambda_f x_s$
FPEVs, No idle OBC idle MOBC exists	$M - b(\mathbf{x}) = 0$; $x_s > 0$; $c(\mathbf{x}) < N$;	$\{x_s - 1, x_u, x_{sm} + 1, x_{um}, x_f + 1\}$	$\lambda_f x_s$
FPEVs, No idle MOBC OEVs are at MOBCs	$M - b(\mathbf{x}) = 0$; $x_s > 0$; $c(\mathbf{x}) = N$; $x_{um} > 0$;	$\{x_s - 1, x_u, x_{sm} + 1, x_{um} - 1, x_f + 1\}$	$\lambda_f x_s$
FPEVs, No idle MOBC No OEVs are at MOBCs	$M - b(\mathbf{x}) = 0$; $x_s > 0$; $c(\mathbf{x}) = N$; $x_{um} = 0$;	$\{x_s - 1, x_u, x_{sm}, x_{um}, x_f + 1\}$	$\lambda_f x_s$
FOEVs, idle OBC exists	$M - b(\mathbf{x}) > 0$; $x_u > 0$;	$\{x_s, x_u, x_{sm}, x_{um}, x_f + 1\}$	$\lambda_f x_u$
FOEVs, No idle OBC idle MOBC exists	$M - b(\mathbf{x}) = 0$; $x_u > 0$; $c(\mathbf{x}) < N$;	$\{x_s, x_u - 1, x_{sm}, x_{um} + 1, x_f + 1\}$	$\lambda_f x_u$
FOEVs, No idle MOBC	$M - b(\mathbf{x}) = 0$; $x_u > 0$; $c(\mathbf{x}) = N$;	$\{x_s, x_u - 1, x_{sm}, x_{um}, x_f + 1\}$	$\lambda_f x_u$

6.2.3 FCS Centric Performance Evaluation Parameters

In this work, we analyze the charging reliability of FCS under EVSE failure and repair as an event-driven model. We model the FCS operation and proposed a charging resource coordination scheme using CTMC with continuous time and discrete states.

The performance of the proposed charging coordination strategies is analyzed in terms of reliability. System dynamics are studied with the steady state probability vector ($\pi(\mathbf{x})$) that gives the steady state probability of being in the corresponding state $\mathbf{x}$. To derive the ($\pi(\mathbf{x})$), we use the global balance equation and the normalization equation expressed in (6.5). In (6.5), Φ is the TR matrix where non-diagonal elements ($\varphi_{x_i x_j}$; $x_i, x_j \in \Phi$) are calculated by getting the summation of TRs that are corresponding to all possible STs from x_i to x_j. Diagonal elements ($\varphi_{x_i x_i}$) of Φ are found using (6.4).

$$\varphi_{x_i x_i} = - \sum_{x_j \in \Omega, j \neq i} \varphi_{x_i x_j \ ; \ x_i, x_j \in \Omega} \quad (6.4) \qquad \pi\Phi = 0, \sum_{\mathbf{x} \in \Omega} \pi(\mathbf{x}) = 1 \quad (6.5)$$

For the long-term sustainable operation of the FCS, the availability of FCS and reliability of charging processes under random EVSE failures and repairs are very indispensable. Reliability and availability aspects are very essential for the FCS to provide high-quality service to EV users. In this Section, performance parameters for the reliability and availability are derived in terms of $\pi(\mathbf{x})$.

Availability of FCS for EVs (A)

FCS accepts OEVs opportunistically to enhance the utilization of limited charging resources, but, there may be occasions where a charging request from an OEV is blocked due to limited or unavailability of charging resources. Under such situations, the FCS is said to be unavailable for new OEVs. Even FCS might not be

available for PEVs if they arrive in time periods other than scheduled ones. Therefore, availability-related performance assessments are very important for both PEVs and OEVs. In this paper, we define the availability of FCS for OEVs as the probability that the FCS allocates charging resources for newly arrived OEV without any failure.

Let (A_{oev}) denote the availability of FCS for OEVs, then A_{oev} can be expressed as in (6.6).

$$A_{oev} = 1 - \sum_{\substack{\mathbf{x}\in\Omega, \\ M-a(\mathbf{x})\geq n,\ M-b(\mathbf{x})>0}} \pi(\mathbf{x}) \tag{6.6}$$

However, as PEVs are registered users, they have a high priority in accessing the FCS. Generally, it is considered that the FCS is available for PEVs when they arrive in the scheduled time. However, If all OBCs are occupied by PEVs, the FCS is not available for newly arrived PEV. Therefore, the EVSE availability for PEVs is obtained by

$$A_{pev} = 1 - \sum_{\substack{\mathbf{x}\in\Omega,\ x_s=b(\mathbf{x}), \\ a(\mathbf{x})=M,\ M-b(\mathbf{x})=0}} \pi(\mathbf{x}) \tag{6.7}$$

Reliability of Charging Process (R)

The ability of a charging process to retain its operational state without being interrupted by any means until it regularly finishes is defined as the reliability of a charging process. Upon a failure of an EVSE, the corresponding charging process has to be preempted if idle OBCs are not available irrespective of EV user type. Nevertheless, charging processes of OEVs are liable to be preempted if charging resources are not adequate to admit PEVs. Therefore, the probability that an ongoing charging process, once commenced, continues to operate without interruptions until regularly finish can be used to quantitatively express the reliability of the charging process.

Due to random failures of EVSE, the charging processes of both PEVs and OEVs can be affected. When considering the charging reliability of OEVs, the charging process of an OEV has to be preempted in the following three cases: (1) PEV-connected OBC is failed and either an idle OBC or MOBC is not available. (2) OEV-connected OBC is failed and either an idle OBC or MOBC is not available. (3) Upon the arrival of new PEV, all OBCs are occupied and an idle MOBC is not available. Therefore, in order to find the charging reliability of each user category, firstly we need to find the mean preempting rate of OEVs ($\dot{\alpha}_{oev}$) for the aforementioned three cases. Therefore, the mean preempting rates of OEVs in those three cases ($\dot{\alpha}_{uev1}$), ($\dot{\alpha}_{uev2}$) and ($\dot{\alpha}_{uev3}$) are derived as expressed in (6.8), (6.9) and (6.10), respectively.

$$\dot{\alpha}_{oev,1} = \sum_{\substack{\mathbf{x}\in\Omega,\\ b(\mathbf{x})=M,\ c(\mathbf{x})=N,\\ x_s>0\ x_{um}>0}} x_s\lambda_f\pi(\mathbf{x}) \quad (6.8) \qquad \dot{\alpha}_{oev,2} = \sum_{\substack{\mathbf{x}\in\Omega,\\ b(\mathbf{x})=M,\ c(\mathbf{x})=N,\\ x_u>0}} x_u\lambda_f\pi(\mathbf{x}) \quad (6.9)$$

$$\dot{\alpha}_{oev,3} = \sum_{\substack{\mathbf{x}\in\Omega,\\ a(\mathbf{x})=M,\ c(\mathbf{x})=N,\\ x_u>0}} \lambda_p\pi(\mathbf{x}) \quad (6.10)$$

We can derive the preempting probability of an EV user type by getting the ratio between the mean preempting rate ($\dot{\alpha}$) and the corresponding plugging rate ($\dot{\beta}$). The mean plugging rate of OEV ($\dot{\beta}_{oev}$) can be obtained as $\lambda_o A_{oev}$. Therefore, the charging reliability of OEV charging process (R_{oev}) can be expressed as (6.11).

$$R_{oev} = \frac{\sum_{i=1}^{3} \dot{\alpha}_{oev,i}}{\lambda_o A_{oev}} \quad (6.11)$$

Even charging processes of PEVs might be preempted due to EVSE failures. Therefore, it is very important to analyze the charging reliability of PEVs R_{pev}. The mean preempting rate of PEVs ($\dot{\alpha}_{pev}$) can be obtained as in (6.12) under EVSE failures.

$$\dot{\alpha}_{pev} = \sum_{\substack{\mathbf{x}\in\Omega,\\ b(\mathbf{x})=M,\ c(\mathbf{x})=N,\\ x_s>0\ x_{um}=0}} x_s\lambda_f\pi(\mathbf{x}) \quad (6.12)$$

The plugging rate of PEVs ($\dot{\beta}_{pev}$) can be obtained as $\lambda_p A_{pev}$. Therefore, the charging reliability of PEV charging process (R_{pev}) is expressed as (6.13).

$$R_{pev} = \frac{\dot{\alpha}_{pev}}{\lambda_p A_{pev}} \quad (6.13)$$

Presented CTMC analytical model assesses the availability of FCS for EVs and the reliability of the charging process with proposed dynamic charging resource coordination strategies.

6.3 Results and Discussion

The reliability of the ongoing EV charging process and availability of FCS for new EV arrivals under EVSE failures and repairs are analyzed in this work. This Section elaborates on the behavior of FCS with MOBCs under EVSE failures. In this Section, we have in-cooperated derived expressions for A and R in Section 6.2.3. To analyze the performance of developed charging coordination strategies, we have considered a scenario where the FCS is equipped with 10 CPs (i.e, $M = 10$) whose charging power can be adjusted within a specified range in steps. The CTMC parameter n is set to 2.

6.3.1 Reliability of OEVs

In this scenario, an ongoing charging process of OEV can be preempted due to the unavailability of resources upon arrival of new PEV or EVSE failure. In this Section, we analyze the charging reliability of both PEVs and OEVs. We plot the charging reliability of PEVs and OEVs under EVSE failure by considering the derived equation in Section 6.2.3. Figure 6.4 shows the charging reliability of OEVS as λ_p varies. In Figure 6.4, we have analyzed charging reliability of OEVs for different λ_o when λ_p varies from 0 to 60 h^{-1}. The charging reliability of OEVs decreases with the increment of λ_o. At lower λ_p, a charging process of an OEV is unlikely to be preempted due to the under-utilization of charging resources. Figure 6.4 very clearly illustrates that the charging reliability of OEVs can significantly be improved with reserved MOBCs. For instance, when $\lambda_p = 60\,h^{-1}$ and $\lambda_o = 42\,h^{-1}$, proposed charging coordination scheme with MOBCs has improved charging reliability of OEVs by 56% compared that of with FCS without MOBCs. Figure 6.4 also depicts that higher charging reliability of OEVs can be achieved with more MOBCs at a cost of under-utilization.

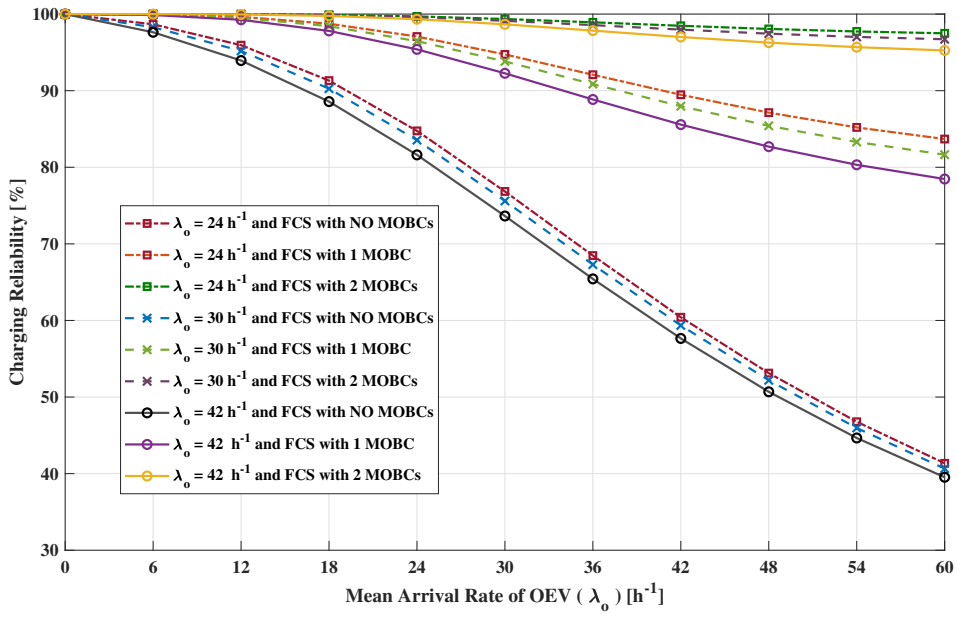

Figure 6.4: Reliability of charging completion of OEVs as a function of λ_p

6.3.2 Reliability of PEVs

Unlike in OEVs, the charging reliability of PEVs is significantly high due to their prior agreements with FCS. However, an ongoing charging process of a PEV has to be preempted upon an EVSE failure if there is no any idle OBC or ongoing OEV charging process. Figure 6.5 depicts the charging reliability of PEVs as λ_F varies. According to defined charging coordination strategies, the charging reliability of PEVs does not depend on the increment of λ_o.

Figure 6.5 very clearly illustrates that the charging reliability of PEVs can significantly be improved with reserved MOBCs. For instance, when $\lambda_F = 0.6\ h^{-1}$, the proposed charging coordination scheme with MOBCs has improved the charging reliability of PEVs by 91% compared that of with FCS without MOBCs.

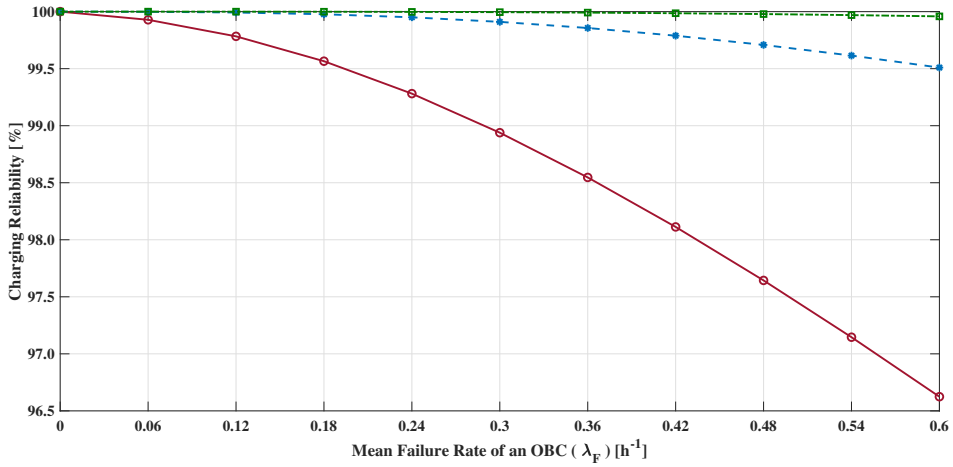

Figure 6.5: Reliability of charging completion of PEVs as a function of λ_F

6.3.3 Availability of FCS PEVs

Figure 6.6 evaluates the availability of FCS for OEVs under EVSE failures. Due to the prior agreement with FCS, it is considered that FCS is available for PEVs upon arrival.

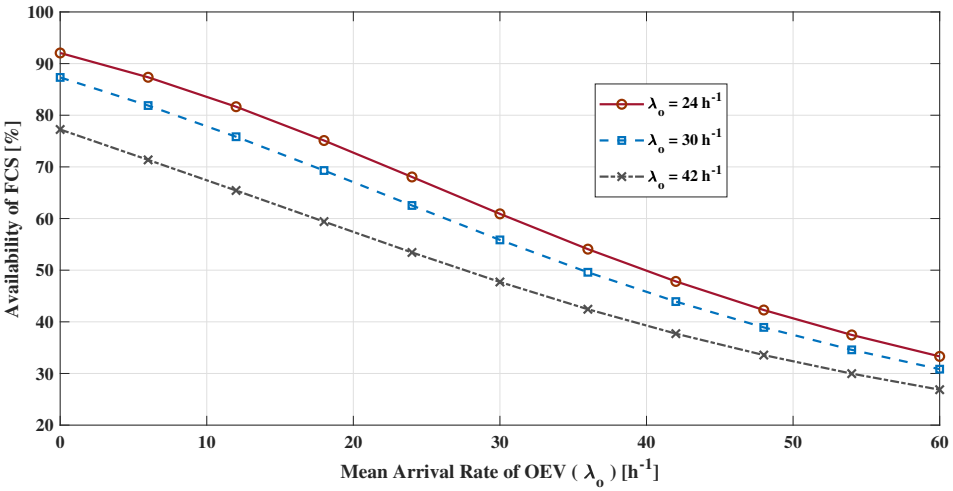

Figure 6.6: Availability of FCS for OEVs as a function of λ_p

At lower λ_p, the FCS is available for PEVs even they arrived in out of the schedule. However, when λ_p increases, the availability of FCS for OEVs is decreasing. According to the proposed charging resource coordination strategies, a newly arrived EV (PEV or OEV) will not be plugged into a MOBC.

Figure 6.6 very clearly shows that the availability of FCS for both PEV and OEV solely depends on the arrival rate of EVs. With the presented results for selected scenarios, we have analyzed the charging reliability improvement of both PEVs and OEVs with proposed EV charging resource coordination strategies under EVSE failures and repairs. Presented results showed that reserving MOBCs at FCS outperforms the charging reliability of both PEVs and OEVs under EVSE failures.

6.4 Conclusion

In this chapter, we have analyzed how MOBCs can be in-cooperated to enhance the charging reliability of OEVs and PEVs. The proposed strategy enables OEVs to exploit unused charging resources allocated for scheduled EV users at FCS to enhance charging resource utilization. However, increasing more arrival of PEVs and EVSE failures, the charging reliability of OEVs is severely affected. The presented results prove that reserving the limited charging resources as mobile chargers at FCS can enhance the charging reliability of opportunistic EV users significantly. The proposed charging resource coordination strategies have improved the charging reliability of OEVs by 56% and PEVs by 91% in considered worst-case scenarios, compared that of with FCS without MOBCs.

Along with the proposed strategies, we have derived a framework in generic nature using CTMC to assess the FCS-centric performance in terms of charging reliability and availability of FCS. This FCS-centric performance assessment framework can be in-cooperated to ensure an undisturbed charging process for EV users. How the rapidly varying power-intensive EV load demand is properly managed with innovative dynamic control strategies is presented in Chapter 7.

Chapter 7

Power Management of Photovoltaic based Active Generator integrated at Fast Charging Station

[7] *This chapter presents the architecture and control strategies for a photovoltaic (PV) based active generator (AG) that can be embedded as the local distributed generator (DG) at an electric vehicle (EV) fast charging station (FCS). FCS that accepts opportunistic EV users with dynamic charging resource aggregation is a rapidly varying power-intensive load to the power grid. The proposed PV-AG with a hybrid energy storage including a battery array and a super-capacitor (SC) bank is going to work as an AG with innovative load management and power flow control strategies for managing the active power demand locally considering the grid constraints. This chapter proposes an architecture for a PV-based active generator, which can provide active power in a controlled manner while maintaining frequency stability within the power grid. With the proposed architecture and innovative control strategies, the rapidly changing power-intensive load demand of the FCS can be effectively coordinated. The PV-generated power can be maximally utilized locally and the power fluctuations can be compensated using the embedded energy storage using the proposed architecture and innovative control strategies. The power flow is managed using the hierarchical approach with the state flow and droop characteristics as a finite state machine.*

[7]This chapter is based on the peer-reviewed journal papers, K. M. S. Y. Konara *et. al*, "Power Flow Management Controller within a Grid Connected Photovoltaic Based Active Generator as a Finite State Machine using Hierarchical Approach with Droop Characteristics," *Renewable Energy (ISSN 1879-0682)*, Vol 155, 1021–1031, 2020. doi : 10.1016/j.renene.2020.03.138 and K. M. S. Y. Konara *et. al*, "Power Dispatching Techniques as a Finite State Machine for a Standalone Photovoltaic System with a Hybrid Energy Storage," *AIMS Energy (ISSN 2333-8334)*, vol 8, 214–230, 2020. doi : 10.3934/energy.2020.2.214

7.1 Introduction

Although the sparse deployment of fast-charging stations (FCSs) promote rapid adoption of EVs providing effective solutions for issues related with charging time, range anxiety and charging autonomy, high penetration of FCSs poses substantial impacts on the power grid in terms of network capacity, power system stability, and power quality[23, 24]. Due to rapid changes of charging demand frequency fluctuations within and outside the FCS can be taken place [22]. Therefore, increasing penetration of FCSs into the power grid requires costly grid reinforcements or reconstructions to avoid issues related to power quality, network capacity, and energy market operation [25–28].

However, these costly grid reinforcements and reconstructions can be mitigated by embedding a renewable energy system (RES) or energy storage (ES) into the FCS as a local distributed generator. [29–31]. Photovoltaic (PV)-based FCS is illustrated in Figure 7.1. FCS is a rapidly changing power-intensive load that may cause issues in the power grid in terms of power system stability. To avoid grid stresses, the power supply of the FCS should strictly adhere to grid constraints while maximally utilizing the local energy supply.

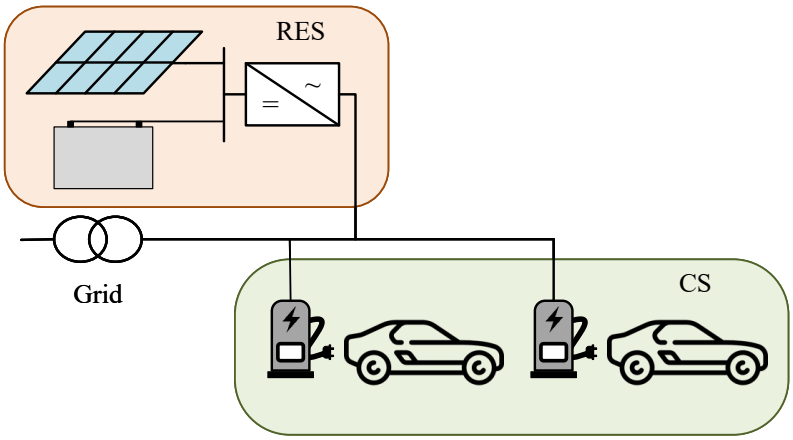

Figure 7.1: RE based EV FCS

Even though a PV system is one of the prominent sources of DGs, some problems can arise due to the stochastic and intermittent nature of PV systems while integrating the system into the grid [80, 81]. When the penetration of PV energy is getting increased, large fluctuations in frequency, voltage and power in the grid will take place. As a consequence of this, the centralized control system of the power system has to take part in controlling the fluctuations of grid parameters [82–84]. The stored kinetic energy of a power system can maintain power delivery even with small disturbances for several seconds due to its system inertia [85, 86]. Further, the governor system and the automatic generation control system at the synchronous generators in a conventional power system control the grid frequency and the voltage magnitude by varying the active and reactive power delivery, respectively [86].

In the conventional grid, most of the PV arrays are connected via passive power conditioning devices which do not involve in controlling grid parameters. But with the exponential increase of PV penetration in distributed networks, the centralized control system of the power system may lose the capability of controlling the grid parameters [87, 88].

Therefore, in order to overcome the intermittency of PV systems, hybrid energy storage could be in-cooperated. PV arrays and the energy storage as a unit need to be controlled to inject the required amount of active and reactive power to the grid. In order to address the discussed issues related to the PV integration, a PV-based active generator (PV-AG) with embedded hybrid energy storage could be used as an alternative solution. The AG system should be designed with innovative load management and power flow control strategies to achieve a high penetration of PV energy. In a PV-AG, the local loads can be supplied in coordination with the grid during both grid-connected and islanding conditions.

A PV system integrated with an array of lead-acid batteries and supercapacitors (SCs) in a DC-coupled structure as a PV-based hybrid generator is proposed in [81]. The system is designed to supply the required active and reactive power to the grid by ensuring a high state of charge (SOC) and overcharge security of the battery with a dedicated local control system. In this design, the control system consists of three levels : (1). Power control unit (PCU) (2). An automatic control unit (ACU) (3). Switching control unit (SCU). The PCU decides the required power reference values for the PV array, battery and SC based on the required active and reactive power. Current mode control of the voltage source inverter (VSI) is used to control the active and reactive power flow through the VSI at the SCU but the application of droop characteristics has not been considered. In this design, although significant research has been devoted to managing the power flow among the available multi-sources, less attention has been paid to the coordinated power extraction from the grid and to mitigating the frequency variations caused by the high penetration of PV power.

The research work presented in [89] evaluates the effectiveness of the active and reactive power flow control of a distributed PV inverter system, to manage network voltage rise problems. Most of the previous research works have focused on active and reactive power flow control to manage over-voltage problems, but it has not been adequately addressed the methods of controlled and coordinated power extraction from the grid while mitigating frequency variations due to high penetration of PV power.

The adaptive event-based control system is presented in [90] for a non-linear system. It is proposed the observer-based fuzzy adaptive controller and can be used for micro-grid controller and operation, where the system is going to be non-linear and dynamic.

But, such type of control system may require relatively more computing and can have complex operations. The observer-based fuzzy adaptive controller can be further modified for some typical applications of load management (e.g. electric vehicle charging management) within the micro-grid. Ref. [91] presents energy management of a PV-AG in DC-coupled architecture which includes storage units with batteries for long-term energy supply and SCs for fast dynamic power regulation. Research into power dispatching according to the availability of primary sources and the level of stored energy can be useful, but to counterbalance the healthy operation of the PV-AG, it is important to consider the grid constraints and the stability within the system as well as in the grid.

Therefore, this work proposes innovative demand management strategies implemented in a hierarchical manner as a finite state machine (FSM) for a PV-AG in the AC-coupled architecture. Proposed power flow control strategies can help not only in maximally utilizing the PV-generated power within the system to supply the local demand with controllable active and reactive power injection but also going to help in improving the power system dynamics and control in addition to the demand side management. The proposed architecture consists of a PV array and hybrid energy storage including an array of lead acid batteries and SCs as multi-power sources which can meet the local load demand while compensating the intermittent nature of the PV power generation. In order to interface these multi-sources with the DC and AC buses of the PV-AG, power conditioning devices are embedded. Since all of the multi-sources generate DC power, the power conversion should be comprised of two stages : DC-DC and DC-AC. The grid integration of the AG system is achieved through an isolation transformer and the control strategies are proposed so that the grid supply is coordinated with grid constraints enforced by the utility.

The major contributions of this paper are,

- Proposed PV-AG architecture with the control strategies dispatch power from the grid adhering to demand side management. As the grid is connected to the AG system with a demand limit, sudden power system stresses could be avoided, and grid stability can be accomplished.

- The proposed hierarchical control strategies of the PV-AG as an FSM effectively share the power-intensive load demand among multi-power sources (PV array, battery and SC) in coordination with the grid maintaining system stability.

- The developed primary control strategies of power converters connected with power sources effectively maintain the frequency stability within the PV-AG system and the grid.

7.2 System Architecture of the Proposed PV-AG

The proposed AC-coupled architecture of the PV-based AG (Figure 7.2) is discussed in this section.

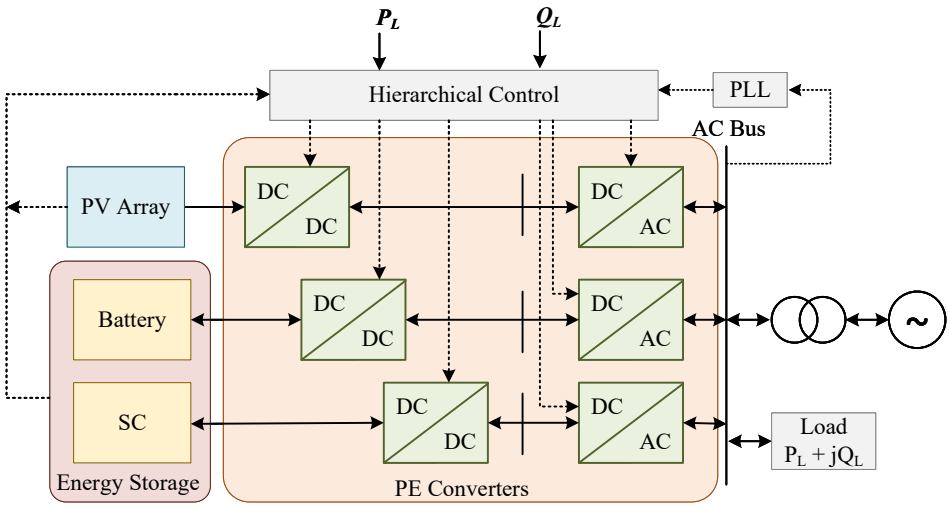

Figure 7.2: System architecture of the proposed AC coupled PV based AG.

The proposed system consists of multi-power sources such as a PV array, lead-acid battery and SC to supply the local load demand in coordination with the grid according to a demand limit enforced by the utility. With this system, the power flow from the grid when the load is directly connected to the grid can be effectively reduced. In the proposed PV-AG system, PV-produced power is maximally utilized to meet the local load demand and the hybrid energy storage compensates for the power fluctuations caused by the PV generation in coordination with the utility grid. The system is proposed for an application where the average load demand is always higher than the PV generation.

In the proposed architecture, the following basic functions are done by the different components.

- PV array is integrated into the AC bus in a low penetration fashion. It injects the maximum available power with a unity power factor. It does not involve in controlling the active and reactive power demand of the load.
- Hybrid energy storage (Battery and SC) is responsible for controlling the active and reactive power demand while maintaining the frequency stability within the system.
- The AC bus is connected to the grid through an isolation transformer so that the power can be dispatched from the grid according to a demand limit as shown in Figure 7.2.

In this work, a 215 kW (peak) solar PV array is selected. The array consists of 54 strings in parallel and each string is having 20 panels in series.

To model the solar panel, the parameters of a mono-crystalline 200 W Solar Panel manufactured by Merkasol® are employed to model the PV array output at the Maximum power point (MPP). A lead-acid battery array is used as the long term power buffer which dispatch power at low rates. The battery capacity with reference to the load and the PV capacity has been selected based on the study presented in [88, 92, 93]. Therefore, a 250 Ah lead-acid battery array with the nominal voltage of 400 V is used. The DC bus to which the battery is connected through a bi-directional DC-DC converter is kept at 800 V. To handle short-term power fluctuations and rapid transients, SCs are used in this architecture which in consequence leads to maintaining the high life cycle of the battery array. Any element of the hybrid energy storage is only available for power dispatching if its state of charge (SoC) is within the prescribed range, otherwise, it stops discharging instead of getting charged.

As depicted in Figure 7.2, the proposed PV-AG system consists of three DC-DC converters connected with the PV array, lead-acid battery and the SC. The power flow is uni-directional from the PV array to the AC bus of the AG and the hybrid energy storage is capable of handling bi-directional power flow to achieve both charging and discharging. Therefore, a conventional DC-DC boost converter with a maximum power point tracker (MPPT) is used with the PV array to inject the power to the AC bus. Two bi-directional DC-DC converters connected with the lead-acid battery and the SC are employed with feedback controllers. In this work, three VSIs are used with each power source of the AG. The independent control of active and reactive power flow with frequency stability implemented in the VSI controllers of the hybrid energy storage enables any energy storage element to be charged or discharged whenever necessary.

The power flow control is designed in a hierarchical approach as an FSM with PID control and state-flow control by taking all the power ratings and the availability of the system components as well as the constraints enforced by the utility into account. Basically, PV-AG optimally manages the power flow among the multi-sources while adhering to system stability. Based on the availability, accessibility, power ratings and allowable capacities, there are several finite states at which PV-AG can dispatch power to meet the local power-intensive load demand. Therefore, control strategies of the PV-AG are proposed in a hierarchical manner. Upper layers work as an FSM performing the secondary control of the PV-AG while primary switching control is managed by the lower layers.

7.3 Load management and Control of the Proposed PV-AG

The hierarchical control approach which includes several hierarchical stages with specific control tasks is used to properly manage the load demand while maintain-

ing frequency stability. In this design, the load management and power flow control system includes four stages each with its own control task acting as an FSM depending on the hierarchical position as illustrated in Figure 7.3.

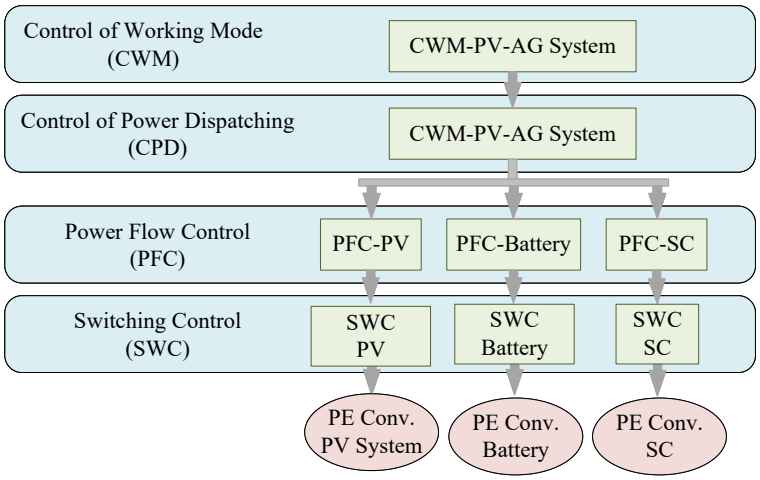

Figure 7.3: Hierarchical control in load management and control.

As illustrated in Figure 7.3, four levels of the control system are listed below.

- Control of working modes **(CWM)**
- Control of power dispatching **(CPD)**
- Power flow control **(PFC)**
- PWM Switching control of converters **(SWC)**

The CWM decides the working mode of the PV-based AG considering the limits imposed by the utility, power ratings of each storage unit, current load demand and the available PV-generated power. Then the CPD level checks the state of each power source and enables the suitable power sources for dispatching the power according to the load demand, providing the required reference values for the active power to the PFC level. Based on the reference values received from the CPD level, PFC calculates the required direct and quadrature axis current references $(i_{d,ref}, i_{q,ref})$ for the SWC level where PWM signals are generated in the VSI control system to switch the converters. The upper two layers (CWM, CPD) can be identified as event-driven systems since each layer contains several mutually exclusive modes or states. The transitions among these states take place according to a logic associated with the system parameters as described in Section 7.3.1.

7.3.1 Control of Working Modes (CWM) of PV-AG System

This stage decides the working mode of the whole AG system. With the help of CWM, it is possible to keep the power flow from the grid to the AG in a controllable manner while adhering to the constraints enforced by the utility.

This approach helps to control the peak demand which in consequence leads to maintaining the system stability. In order to accomplish optimal load management and control with demand side management from the available power sources in the AG, limits imposed by the utility are employed in an event-driven fashion to reduce grid stresses. In this design, three major working modes are selected : (1). 'Grid Connected' mode, (2). 'Standalone' mode, (3). 'Disconnected' mode. But in this paper, the control strategies are proposed only for the 'Grid Connected' mode.

Grid connected mode

In this mode, the AG system supplies the load in coordination with the grid following a demand limit enforced by the utility. Therefore, in this mode, all the multi-power sources are possibly available and accessible for power dispatching to meet the load demand depending on the current demand limit and the power ratings of each storage unit. Based on the grid power share of the load demand and the demand limit at a particular time, there are two subsequent states : (I). 'Normal' state (II). 'Stress Reduced' state.

Standalone mode

If it is detected any planned or unplanned utility failure/islanding condition, the grid should be disconnected from the PV-AG to avoid damage to utility operations, equipment, and maintenance workers resulting in the grid power share is to be zero but the remaining power sources continuing to supply the demand as long as the PV source and the hybrid energy storage can meet the load demand. This working mode is known as the 'Standalone' mode. In this mode, all the power sources are possibly available and accessible depending on their state except the grid to maintain an uninterruptible power supply to the local load.

Disconnected mode

In this mode, if the algebraic summation of the maximum allowable power share of each power source is less than the load demand, the load is disconnected from the system. In order to maintain stable operation, all the sources are disconnected from the AG system which in consequence leads to disconnecting the load from the supply.

The state transition diagram of the CWM is shown in Figure 7.4 and the transition logic is tabulated in Table 7.1.

g : Grid connected mode.
d : Disconnected mode
s : Standalone mode

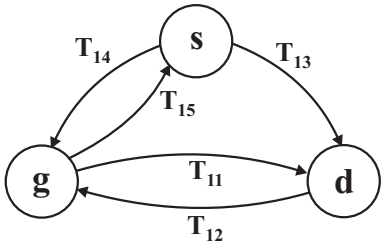

Figure 7.4: State transition diagram of the CWM.

Table 7.1: State transition logic of CWM

Transition	**Logic**
T_{11}	$(P_{DL}(t) + P_{max,sc}C_{sc}(t) + P_{max,bat}C_{bat}(t) + P_{pv,mpp}(t)) < P_L(t)$
T_{12}	$(P_{DL}(t) + P_{max,sc}C_{sc}(t) + P_{max,bat}C_{bat}(t) + P_{pv,min}(t)) > P_L(t)$
T_{13}	$(P_{max,sc}C_{sc}(t) + P_{max,bat}C_{bat}(t) + P_{pv,mpp}(t)) < P_L(t)$
T_{14}	$isd(t) == 1$
T_{15}	$isd(t) == 0$

$P_{DL}(t)$	: current demand limit of the grid
$P_{x,max}$	: power rating of the ES element x
x	: battery-bat, SC-sc
$Ppv, mpp(t)$	: current maximum power generation of the PV array
Ppv, min	: minimum power generation of the PV array
$P_{grid}(t)$	: current power delivery from the grid
$isd(t)$	: islanding detection
$P_L(t)$	: current load demand
$C_x(t)$	: connection (when connected, 1 or wise-versa)

To keep the grid power share below the prescribed demand limit, the grid power is dispatched in two different states **s** (i.e.**n** or **r**), when the system is running in 'Grid connected' mode. The state transition diagram of the subsequent states of the 'Grid Connected' mode is shown in Figure 7.5 and the state transition logic is tabulated in Table 7.2.

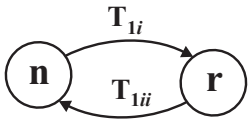

Figure 7.5: State transition diagram of the 'Grid Connected' mode

n	: normal state.
r	: stress reduced state

Table 7.2: State transition logic of 'Grid Connected' mode

Transition	Logic
T_{1i}	$P_{DL}(t) < P_{grid}(t)$
T_{1ii}	$P_{DL}(t) > P_L(t)$

For the grid-connected operation, the required power reference value of the hybrid energy storage ($P_{ref,hes}(t)$) is determined at the relevant operating state of the 'Grid Connected' mode using (7.1). This reference value will be transferred to the CPD layer to calculate the individual power reference value of each storage element.

$$P_{ref,hes}(t) = \begin{cases} P_0 & ;\text{if } s = n \\ P_L(t) - P_{pv,mpp}(t) - (P_{DL}(t) - \hat{P}) & ;\text{if } s = r \\ 0 & ;\text{otherwise} \end{cases} \tag{7.1}$$

7.3.2 Control of Power Dispatching (CPD Control)

At this stage, according to the working mode selected by the CWM, suitable power sources get enabled for power dispatching. If sufficient power sources are not available for dispatching power to meet the load demand, the load will be disconnected from the system. In order to get the decision, the SOC of the storage units, demand limits given by the utility and the generation capacity of the PV array are considered.

Power Dispatching Control of the PV Array (CPD-PV)

In the PV based AG system, the PV array injects available maximum power to the AC bus at unity power factor. The power flow should be kept in uni-directional. The PV array should be disconnected from the bus bars, when the generation capacity of the PV array becomes very low to avoid the reverse power flow into the PV array. Therefore, two states are used for CPD of PV array as illustrated in Figure 7.6. The corresponding state transition logic of CPD of PV array is tabulated in Table 7.3.

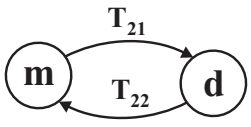

Figure 7.6: State transition diagram of the CPD in PV array.

m : MPPT state.
d : PV array disconnected state

Table 7.3: State transition logic of CPD-PV

Transition	Logic
T_{21}	$GTI(t) < GTI_{min}$
T_{22}	$GTI(t) > GTI_{min}$

In the MPPT state, the PV panel is available and accessible for load sharing while in the disconnected state, PV array is disconnected from the AC bus to avoid reverse power flow into the PV array. CPD-PV decides the suitable state based on the global tilted irradiance (GTI) on the PV array. Then $P_{pv,mpp}$ is selected using (7.2).

$$P_{pv,mpp}(t) = \begin{cases} P_{pv,mppt}(t) & ;\text{if } s = m \\ 0 & ;\text{if } s = d \end{cases} \tag{7.2}$$

Power Dispatching Control of the Hybrid Energy Storage (CPD-HES)

CPD-HES keeps the SOC of each unit of the hybrid energy storage within the allowable range by switching into charging and discharging modes while maintaining the availability and accessibility of each unit. CPD-battery and CPD-SC are built separately for the independent control of each storage unit. CPD-x (x denotes battery or SC) consists of three states: 'Dispatchable' state, 'Max' state and 'Min' state.

In the 'Dispatchable' state, the respective energy storage (either battery or SC) is available and accessible for power dispatching as the corresponding SOCx is within the allowable range. In this state, the storage unit is available for either charging or discharging at a time. When the SOCx is out of the allowable range, CPD-x transits to either 'Min' state or 'Max' state depending on the corresponding state transition logic. Once the CPD-x comes to a state, it gives the required reference values for active and reactive power based on the activated state in the CWM mode and the reference values for the frequency and voltage control in PFC stage. 'Max' state is defined to prevent any storage element from being overcharged when they are charging. The state transition diagram is shown in Figure 7.7 and the state transition logic are tabulated in Table 7.4.

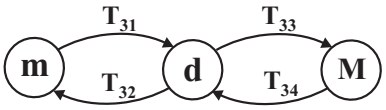

Figure 7.7: State transition diagram of the CPD-HES.

m : min mode.
d : dispatchable mode
M : max mode

Table 7.4: State transition logic of CPD-HES

Transition	Logic
T_{31}	$SOC_x(t) > SOC_{min}$
T_{32}	$SOC_x(t) < SOC_{min}$
T_{33}	$SOC_x(t) > SOC_{max}$
T_{34}	$SOC_x(t) < SOC_{max}$

$SOC_x(t)$: current state of charge of the source x
SOC_{max}, SOC_{min} : Maximum and minimum state of charge of the source x

At the CPD-HES stage, the required power reference values for the battery array and the SC array are calculated from the overall power reference of the hybrid energy storage determined at the CWM mode for 'Normal' and 'Stress Reduced' states separately using (7.3), (7.4) and (7.5), (7.6), respectively. If the active CWM state is 'Normal', predefined individual power shares of storage elements are used for power dispatching as the grid coordinates the system. But in the 'Stress Reduced' state, the power shares of each storage element will be determined by using the power transient filtering technique with the transfer function of $h_{LP}(t)$ considering the load increment rate and the power transient frequency.

$$P_{ref,bat,n}(t) = \begin{cases} P_{1,bat}(t) & ;\text{if } s = d \\ P_{1,bat} & ;\text{if } s = M \\ -P_{2,bat} & ;\text{otherwise} \end{cases} \tag{7.3}$$

$$P_{ref,sc,n}(t) = \begin{cases} P_{es}(t) - P_{ref,bat,n}(t) & ;\text{if } s = d \\ P_{es}(t) - P_{ref,bat,n}(t) & ;\text{if } s = M \\ -P_{1,sc} & ;\text{otherwise} \end{cases} \tag{7.4}$$

$$P_{ref,bat,r}(t) = \begin{cases} h_{LP}(t) * P_{es}(t) & ;\text{if } s = d \\ h_{LP}(t) * P_{es}(t) & ;\text{if } s = M \\ 0 & ;\text{otherwise} \end{cases} \tag{7.5}$$

$$P_{ref,sc,r}(t) = \begin{cases} P_{es}(t) - P_{ref,bat,r}(t) & ;\text{if } s = d \\ P_{es}(t) - P_{ref,bat,r}(t) & ;\text{if } s = M \\ 0 & ;\text{otherwise} \end{cases} \tag{7.6}$$

Power Dispatching Control of the Grid Connection (CPD-Grid)

In the PV-AG system, the CPD-Grid control layer helps to draw the power from the grid according to a demand limit enforced by the grid. Therefore, the CPD-Grid decides the operating state based on the time. In this work, two different demand limits are considered for power dispatching from the grid. Two states are used for the CPD-Grid: 'Peak' and 'Offpeak'.

The state transition diagram and the state transition logic of the CPD-Grid is illustrated in Figure7.8 and are tabulated in Table 7.5, respectively.

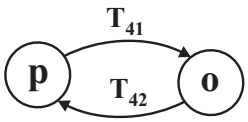

Figure 7.8: State transition diagram of the CPD-Grid

p : Peak mode.
o : Off Peak mode

Table 7.5: State transition logic of CPD-Grid

Transition	Logic
T_{41}	$t > t_{peak}$
T_{42}	$t < t_{peak}$

t : current time
t_{peak} : duration of peak hours

7.3.3 Active and Reactive Power Flow Control (PFC) and PWM Switching Control (SWC)

The main function of this hierarchical stage is to calculate the required reference values for PWM switching controls of VSIs connected with the PV array and the hybrid energy storage based on the control parameters received from the CPD level as illustrated in Figure 7.9.

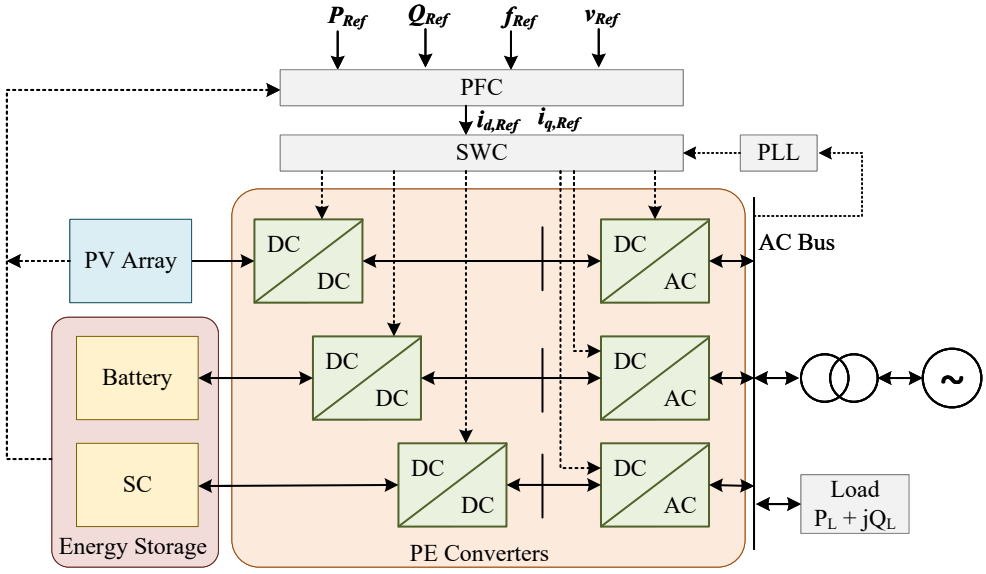

Figure 7.9: PFC and SWC of the PV-AG

The PV-AG system is intended to properly dispatch the power from available multi-power sources to meet the power-intensive local load demand. The PV array injects power to the AC bus of the AG system with a unity power factor in MPPT mode, and so, hybrid energy storage compensates the active and reactive power demand of the AC load in coordination with the grid. The overall control block diagram of the PFC and SWC layers of the PV-AG is illustrated in Figure 7.10.

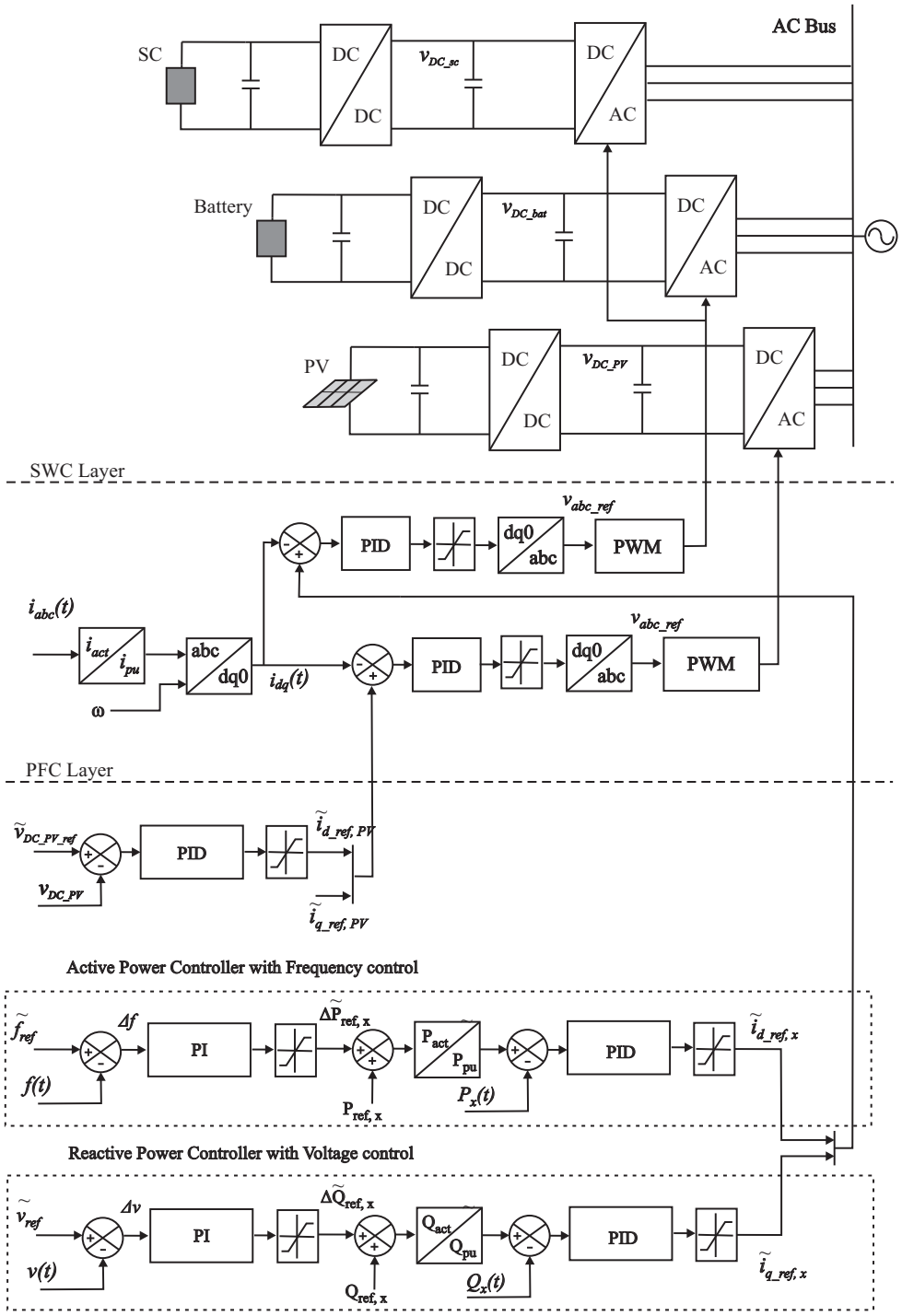

Figure 7.10: Control block diagram for PFC and SWC of the PV-AG

The PFC layer comprises two control blocks each with two cascaded control loops to maintain the frequency stability and the voltage stability within the system as illustrated in Figure 7.10. The active and reactive power flow control are implemented using VSI controllers using current mode control at the SWC layer.

$v_{DC,x}$	: VSI input DC link voltage of the storage element x
$v_{DC,pv}$	: VSI input DC link voltage of the PV array
$i_{abc}(t)$	: current measured at the PCC of the AC bus
$i_{dq}(t)$	: corresponding dq component of the $i_{abc,measured}$
$\tilde{v}_{DC,pv,ref}$	: DC link reference voltage for the voltage controller in the PV system
$\tilde{i}_{d,ref,x}$	: reference direct axis current component of the x element
$\tilde{i}_{q,ref}$	: reference quadrature axis current component of the x element
$\tilde{f}_{ref}$	: reference system frequency
$f(t)$	: measured frequency at the PCC of the AC bus
$P_{ref,x}$	: active power reference value of the x element calculated at the CPD layer
$\Delta\tilde{P}_{ref,x}$	: required power change of the x element to mitigate frequency fluctuations
$P_x(t)$	: delivered power share of the x element
$\tilde{v}_{ref}$	: reference system voltage
$v(t)$	: measured voltage at the PCC of the AC bus
$Q_{ref,x}$	: reactive power reference of the x element value calculated at the CPD layer
$\Delta\tilde{Q}_{ref}$	: required reactive power change of the x element to mitigate voltage fluctuations
$Q_x(t)$	: delivered reactive power share of the x element
$v_{abc,ref}$	: 3ϕ reference voltage for PWM generator

Active Power Controller with Frequency Stability

Two cascade control loops (the frequency control loop and the active power control loop) construct the active power controller for each energy storage unit as illustrated in Figure 7.10. In the frequency control loop shown in Figure 7.10, the concept of frequency droop is used to calculate the required change in power delivery, to keep the system frequency at its reference value. The equations (7.7) and (7.8) give the required change in active power to maintain the frequency stability.

$$\Delta P_{ref}(t) = P_0 + k_f \left[f(t) - f_0 \right] \tag{7.7}$$

$$\Delta P_{ref} = P_0 + k_f \Delta f \tag{7.8}$$

According to the equation (7.7), when the system undergoes dynamic frequency changes with demand changes, steady state error of the frequency may not become zero as the droop control of frequency is only proportional control [86].

$$(\Delta f|_{steady\ \ state} \neq 0)$$

Therefore, in order to address the dynamic frequency changes and to have the zero steady-state error of frequency, proportional plus integral (PI) control can be used with droop control [86]. Then the equation (7.8) can be modified with PI control and expressed in (7.9). This active power controller with frequency stability is illustrated in Figure 7.10.

$$\Delta P_{ref}(S) = P_0 + k_f \Delta F(s) + \Delta F(s)(k_p + \frac{1}{T_i s}) \tag{7.9}$$

P_0 : active power set value
f_0 : nominal frequency
k_f : frequency droop
k_p : proportional gain
T_i : integral time constant

Reactive Power Controller with Voltage Stability

Two cascade control loops (the voltage control loop and the reactive power control loop) construct the reactive power controller as shown in Figure 7.10 . In the voltage control loop shown in Figure 7.10, the concept of voltage droop is used to calculate the required change in reactive power delivery, to keep the system voltage at its nominal value. The equations (7.10) and (7.11) give the required change in reactive power to maintain the voltage stability.

$$\Delta Q_{ref}(t) = Q_0 + k_v \left[v(t) - v_0\right] \tag{7.10}$$

$$\Delta Q_{ref} = Q_0 + k_v \Delta v \tag{7.11}$$

As in the case of frequency stability discussed in section 5.1, in order to address the dynamic voltage changes and to have the zero steady-state error of voltage, proportional plus integral (PI) control is used with the voltage droop and it is expressed in (7.12). This reactive power controller with voltage stability is illustrated in Figure 7.10.

$$\Delta Q_{ref}(S) = Q_0 + k_v \Delta V(s) + \Delta V(s)(k_p + \frac{1}{T_i s}) \tag{7.12}$$

Q_0 : reactive power set value
v_0 : nominal voltage
k_v : voltage droop
k_p : proportional gain
T_i : integral time constant

7.4 Results and Discussion

The performance of the proposed load management and power flow control strategies of the PV-AG are analyzed for selected scenarios as described in Section 7.4.1. To represent the intermittent nature of PV energy, variable solar radiation with the GTI shown in Figure 7.11 is used.

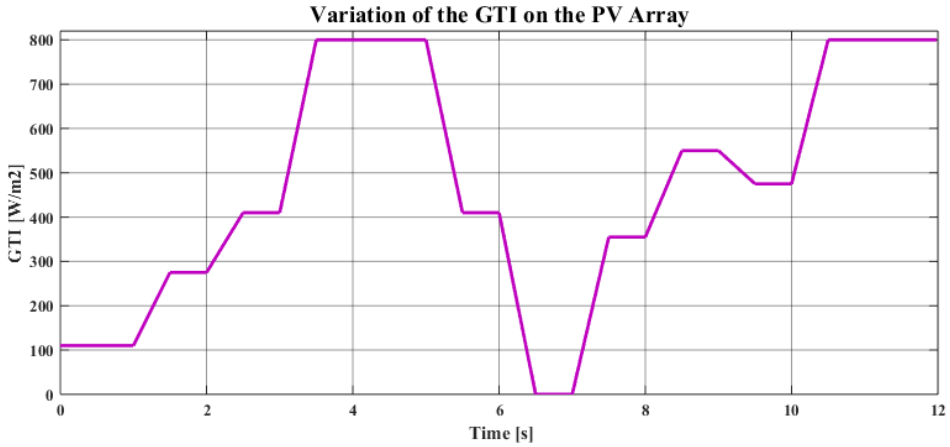

Figure 7.11: Variation of the GTI on the PV array

In the AG system, PV array is considered as the main source of power and it is operated at the MPP. In the analysis, 215 kW (Peak) PV array is employed.

7.4.1 Load Demand Sharing among the Multi-Sources in the AG

The active load demand is shared among the available power sources (PV array, grid and hybrid energy storage) in the PV-AG system. The PV array injects the available maximum power to meet the local load demand. The remaining load demand should be shared among the other sources while maintaining frequency stability within the system.

Active Load Demand Sharing : Scenario-I

A variable load profile that varies from 300 kW to 600 kW with rising and falling edges is considered to represent dynamic changes of a typical load model (Figure 7.12). For dispatching power from the grid, two demand limits (i.e. 200 kW from 0 s to 5 s and 300 kW from 5 s to 12 s) are considered as illustrated in Figure 7.12. The active power sharing among the multi-sources of the PV-AG is illustrated in Figure 7.12. The power shares of the storage units maintain the frequency stability.

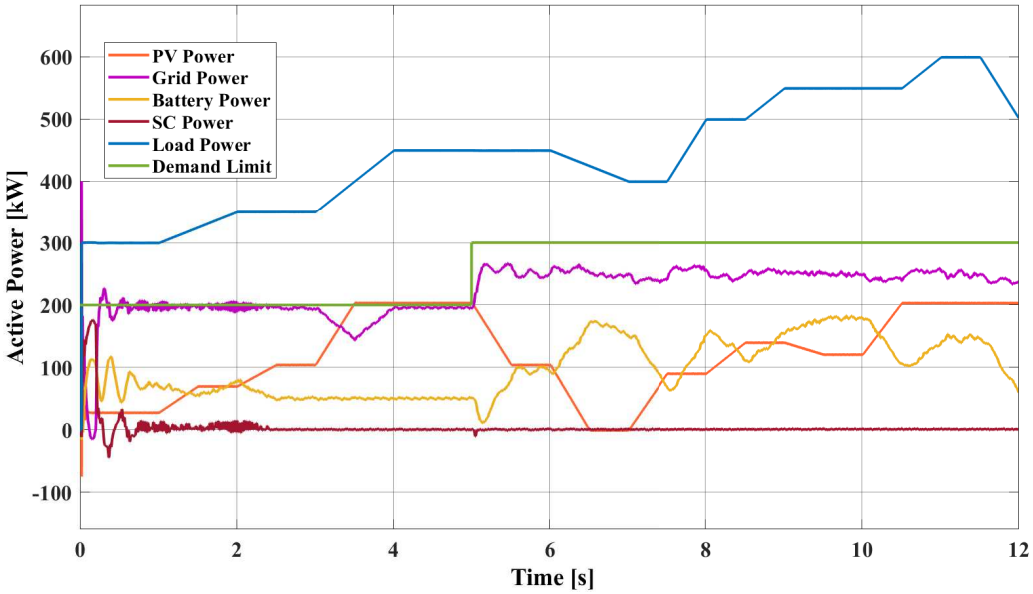

Figure 7.12: Active load demand sharing among the multi-sources in PV based AG in Scenario-I

It is observed that approximately after 0.35 s from the system start, PV array injects the maximum available power to the AG system (Figure 7.12). Due to the very low GTI incident, the PV generated power is around 30 kW. Since the PV-generated energy is not sufficient to meet the load demand, other sources come into the picture for power sharing in 'Grid connected' (g) mode and 'stress reduced' (r) state within the first 3 s. It can be seen that the sudden power fluctuations of the grid power are compensated by the SC during this short period. With the gradual increment of PV power, the other sources try to reduce their power shares by shifting to 'normal' (n) state, while keeping the power shares of the hybrid energy storage at a constant level until the 5^{th} s.

In first 5 s, the system runs in the 'Peak' (p) mode hence the active power share of the grid remains lower than the utility imposed demand limit of 200 kW. But after 5^{th} s, the demand limit is increased to 300 kW and the active power share of the grid is also increased following the demand limit increment. After 5^{th} s, the system runs in the r states resulting in the battery power being changed according to the load increment in coordination with the grid. During this period SC does not appear as there are no any sudden power fluctuations. During 6.5 s to 7 s, the PV produced energy becomes zero and hence, PV generation system switches to the 'PV array disconnected' (d) state for preventing the reverse power from entering to the PV array. Figure 7.12 shows that during this period, the active power share of the battery increases to meet the load demand.

Active Load Demand Sharing : Scenario-II

In this scenario, a constant demand limit (i.e. $220\,kW$) is used throughout the period with the same variable load profile which varies from $300\,kW$ to $600\,kW$ used in Scenario-I. The active power sharing among the multi-sources of the PV-based AG for the second scenario is illustrated in Figure 7.13. The grid power fluctuations are compensated by the SC after the $5^{th}\ s$.

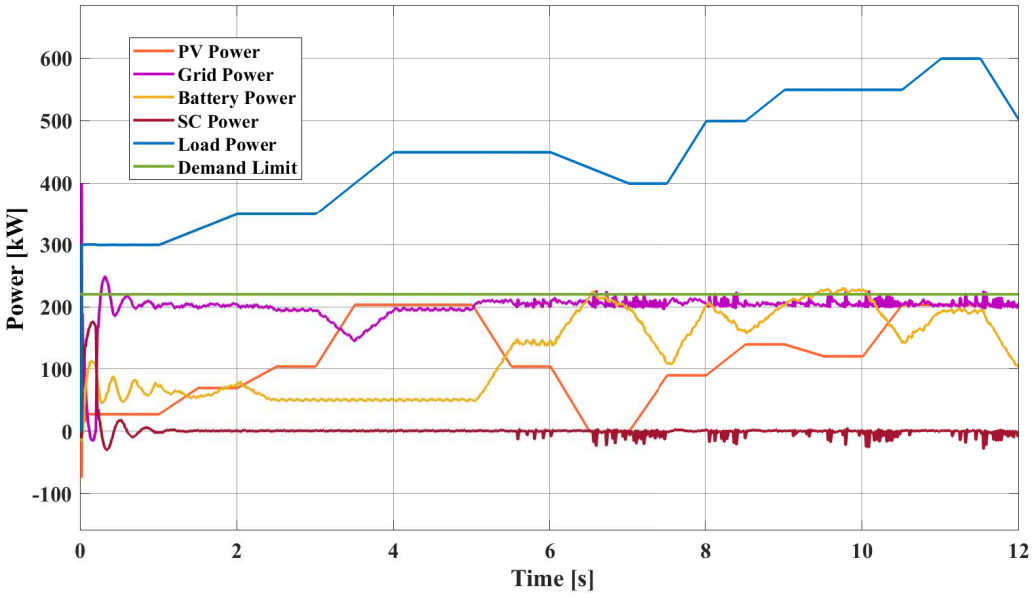

Figure 7.13: Active load demand sharing among the multi-sources in PV based AG in Scenario-II

Active Load Demand Sharing : Scenario-III

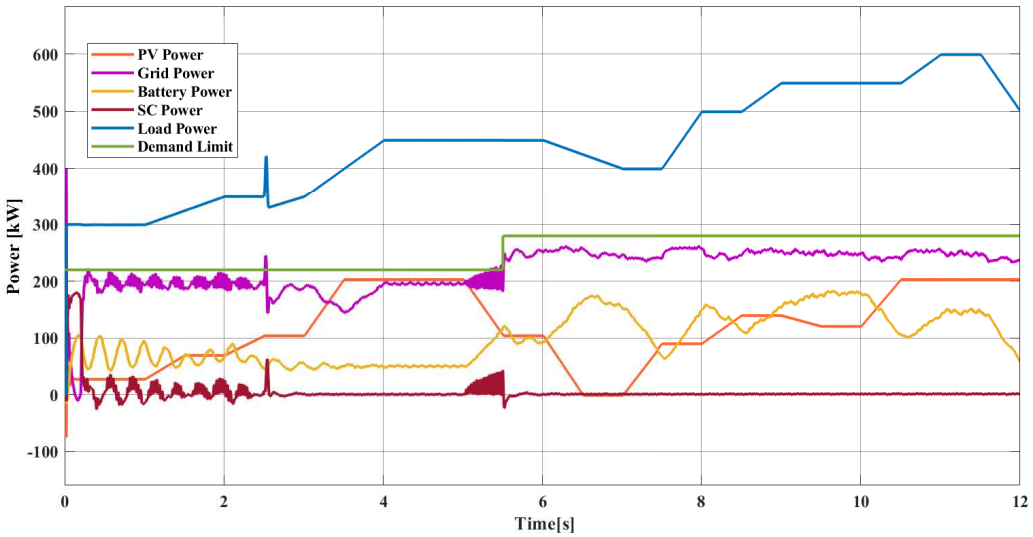

Figure 7.14: Active load demand sharing among the multi-sources in PV-based AG in Scenario-III

An impulse load change at 2.5 s is considered with the same variable load profile which varies from 300 kW to 600 kW used in Scenario-I. The Active power sharing among the multi-sources of the PV-based AG for the second scenario is illustrated in Figure 7.14. As in Scenario I and II, the load demand is properly shared among the power sources according to the developed control strategies. The grid power fluctuations are compensated by the SC. Especially, the impulse demand change is addressed by the SC in coordination with the grid power but the battery does not take part in compensating for sudden fluctuations in the grid supply or the demand.

7.4.2 Frequency and Voltage Stability of the AG System

The load management and control strategies of the proposed PV-AG architecture ensure frequency stability within the system. The variation of frequency of the AC bus of the AG system for the considered demand management scenarios are shown in Figure 7.15, 7.16, 7.17.

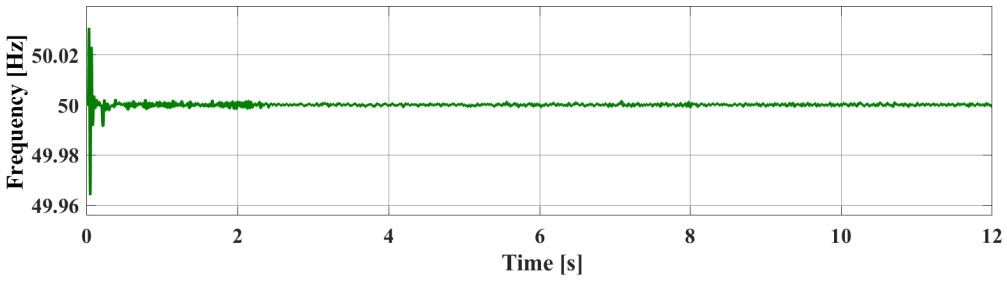

Figure 7.15: Variation of the frequency of the PV-AG system in Scenario-I

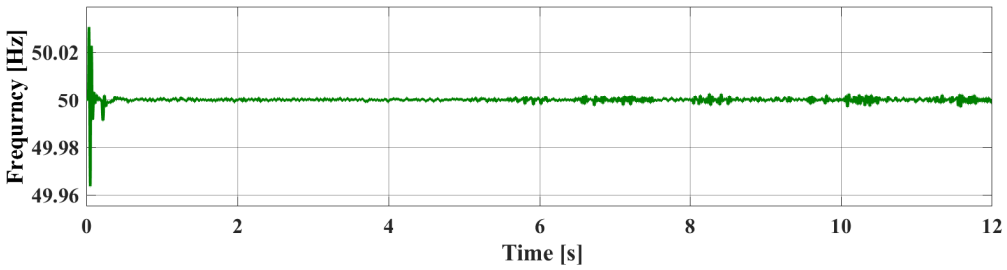

Figure 7.16: Variation of the frequency of the PV-AG system in Scenario-II

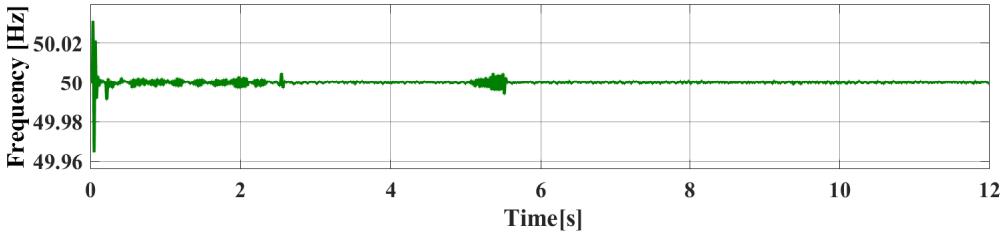

Figure 7.17: Variation of the frequency of the PV-AG system in Scenario-III

It can be seen that the frequency is well maintained at its nominal value (i.e 50 Hz) in all three scenarios while injecting the required active power to the AC bus. When we compare and contrast the results obtained for considered three scenarios with a typical power-intensive load profile, it is evident that the proposed control strategy ensures the PV power is maximally utilized and the battery array to be taken the large portion of the load demand while the SC to be taken care of rapid dynamics in coordination with the grid. In all three scenarios, it can be seen that the reference values for individual power shares will be determined according to the corresponding algorithm specified at the enabled mode and state for each source.

7.5 Conclusion

The proposed PV-AG in this chapter is an effective solution for increasing the penetration of PV-produced energy into an FCS as an embedded local energy source. An AC-coupled architecture in which all the power sources (PV array, lead-acid battery and the SC) are connected to a common AC bus through the separate DC-DC and DC-AC conversion stages enables independent power flow control of each power source.

The overall control system of the PV-AG is developed in a hierarchical approach as an FSM with state-flow control and droop characteristics. The hierarchical control approach is very much suitable for such type of real-time power management systems as it helps not only in managing and controlling the power flow but also helps in maintaining the frequency stability. For the proposed PV-AG, the topmost level selects the appropriate working mode based on the rated power values and the grid constraints while the second layer enables the appropriate power sources to be dispatched power to meet the EV load demand. Power flow control and frequency control are constructed at the subsequent layers with the switching controllers of the VSIs in the PV-AG. The presented PV-AG model can be integrated within the distributed network to operate as a microgrid.

Chapter 8

Conclusions

This chapter concludes the completed research work by providing contributions, key research findings and future works.

8.1 Introduction

Rapid deployment of electric vehicle (EV) fast charging stations (FCSs) can mitigate issues related to long charging time, range anxiety and charging autonomy. FCSs give an opportunity to penetrate more renewable energy (RE) sources within the distributed networks as micro-grids/ active generators (AGs). The contract demand with the utility, distributed local energy source integrated with the FCS and a number of EV chargers/ EV supply equipment (EVSE) can be considered as limited charging resources of the FCS. It is considered that the EV chargers/ EVSE are capable of supplying variable rate charging (VRC) that facilitates heterogeneous EV users. This thesis presents innovative charging resource allocation and coordination strategies to maximize the utilization of limited charging resources while assuring quality service to heterogeneous EV users. The proposed strategies found that allowing opportunistic EV users to exploit unused limited charging resources can enhance charging resource utilization.

Moreover, this thesis evaluates the performance of developed strategies in terms of charging resource utilization, charging completion and EV user satisfaction. To evaluate EV user satisfaction, various quality of service parameters such as EV blockage, charging process preemptage, mean waiting time, mean charging time, availability of FCS, charging reliability, etc are used. The primary/ registered EV users (PEVs) of the FCS access the FCS with specific privileges according to prior agreements. However, these limited charging resources would not be fully utilized due to various uncertainties associated with the primary charging process such as EV mobility-related uncertainties, EVSE failures, energy resource uncertainties, energy price uncertainties, etc. In an FCS, the generated energy is wasted if the FCS does not fully utilize it. Moreover, due to the charging schedule and uncertainties associated with the EV charging process, there can be idle chargers and vacant spaces

for EVs at the FCS even for short durations. However, such idle chargers and vacant space for EVs at the FCS leave a space for further utilizing them with innovative charging resource coordination strategies. Therefore, how to effectively exploit such unused limited charging resources with opportunistic secondary EV users (OEVs) with defined liabilities is analyzed in this thesis. We propose innovative and dynamic charging resource allocation, admission control and charging coordination strategies for both EV user types.

8.2 Conclusions

We can conclude that the first research objective is achieved as the limited charging resources of an EV FCS can be maximally utilized by OEVs to exploit available charging resources with dynamic event-driven charging resource allocation and coordination strategies apart from PEVs. The second research objective is achieved using the developed innovative charging resource allocation and coordination strategies with resource aggregation and demand elasticity. We can conclude that aggregation and demand elasticity-based charging coordination strategies further enhance charging resource utilization while providing a high quality of service (QoS) in EV charging for both PEVs and OEVs. The third research objective is achieved so that the charging reliability of FCS is enhanced with developed charging resource allocation and coordination strategies along with a set of mobile off-board chargers at FCS. Pertaining to the fourth or final research objective, the frequency stability affected by the rapid change of power-intensive EV demand of FCS is assured within the FCS with the PV-based active generator(AG) along with an innovative finite state machine-based hierarchical control approach. The PV-AG is developed in a hierarchical approach as a finite state machine (FSM) with state-flow control and droop characteristics. The following specific conclusions are made based on the achievement of considered research objectives.

- The developed dynamic event-based charging resource allocation and coordination strategies provide effective solutions to mitigate the underutilization of limited charging resources due to uncertainties associated with EV charging process.

- The presented charging coordination strategy at FCS can facilitate the distinct demand of heterogeneous EV users. Those EV users who need an uninterruptible or scheduled charging process can get the service as PEVs while those EV users who need an opportunistic charging process can charge their EVs as OEVs with optimum utilization of available charging resources. Therefore, OEVs can work as a flexible load to the FCS.

- The presented results prove that the developed charging resource coordination strategy significantly improves the charging resource utilization of the FCS at any arrival rate of PEVs. At higher arrival rates of EVs, FCS can accomplish

more than 90% of resource utilization which is bounded to 78% only in the case of PEVs.

- The proposed charging resource allocation and coordination strategies allow OEVs to exploit available charging resources without impacting the charging process of PEVs.
- It assures high QoS for both EV user types even though they access the FCS with distinct privileges. Although FCS employs OEVs as a flexible load to maximally utilize limited charging resources, adequate QoS is assured to OEVs.
- A performance assessment framework is derived in generic nature using different stochastic modeling techniques such as Monte-Carlo simulation (MCS), continuous-time Markov chain (CTMC) to assess the FCS-centric performance in terms of charging resource utilization, charging completion rates of EV users, blocking probability, preempting probability, waiting time, charging time, etc.
- At the operating stage of an FCS, the developed FCS-centric performance assessment framework provides a quantitative overview of the whole charging process within and outside the FCS.
- Results of the considered cases show that the dynamic charging resource aggregation and demand elasticity with heterogeneous EV users significantly improves the charging resource utilization of the FCS at any arrival rate of PEVs. Even though more than 80% of resource utilization can not be achieved only with PEVs, FCS accomplishes all most all 100% of resource utilization with charging resource aggregation and demand elasticity with heterogeneous EV users. Even for the considered cases, the resource utilization is always higher than 50% irrespective of the arrival rate of PEVs.
- Presented results show that the developed aggregation-based strategies outperform QoS parameters such as charging completion rate, blocking probability, preempting probability, etc. contrast to the constant rate strategy.
- The blocking probability of real-time OEVs can be further reduced by increasing the queue size at the cost of waiting time.
- The presented priority queue-based charging resource allocation and coordination strategies allow opportunistic fast-charging users (FCUs) with VRC to enhance the resource utilization of an institutional parking lot initially allocated only for slow-charging users (SCUs). More FCUs can be accommodated by holding/buffering the charging process of SCUs based on the parking time and required minimum charging time. Adaptive charging for FCUs can further enhance charging resource utilization.
- The presented results show that increasing more arrival of PEVs and EVSE failures severely affect the charging reliability of OEVs. It concludes that reserving mobile chargers (MOBCs) at FCS can enhance the charging reliability

of OEVs significantly. The developed charging resource coordination strategies have improved the charging reliability of OEVs by 56% and PEVs by 91% in the scenario where the considered PEV arrival rate is maximum, compared to that of FCS without MOBCs.

- The developed hierarchical power management strategies for grid-connected FCS integrated with PVAG help not only in managing and controlling the power flow but also helps in maintaining frequency stability. In the PVAG, the topmost level selects the appropriate working mode based on the rated power values and the grid constraints while the second layer enables the appropriate power sources to be dispatched power to meet the EV charging demand.

8.3 Future Works

The presented research work can be further extended considering the following tasks.

- The presented FCS-centric performance assessment framework can be used for the planning and deployment stage to find the optimum siting and sizing of FCS.
- The presented work can be further enhanced by allowing PEVs to charge at higher rates with charging resource aggregation.
- This work can be extended considering techno-economic aspects integrated with charging coordination strategies to evaluate the performance of developed charging resource allocation and coordination strategies.
- Innovative prizing mechanisms in line with the privileges of heterogeneous EV users can be developed to evaluate the performance of presented charging resource allocation and coordination strategies.
- Developed charging resource allocation and coordination strategies can be extended to EV parking lots with round-trip drivers to evaluate the performance in terms of the charging resource utilization and QoS aspects of commercial EV customers.
- Charging reliability aspects need further investigation by reserving some existing EVSE for improving the reliability of the FCS. The same work can be further extended for both static reservation and dynamic reservation of the limited charging resources of the FCS
- Charging reliability enhancement of heterogeneous EV users considering charging preemptage and EVSE failures can be extended to improve the availability of the FCS in both time and space domains.
- Developed hierarchical control strategies for grid-integrated FCS with PV-AG can be extended to analyze the power quality aspects considering different micro-grid architectures.

Nomenclature

AC	: Alternating Current
AG	: Active Generator
ASEV	: Arrival of a SEV
AUEV	: Arrival of a UEV
CCS	: Combined Charging System
CP	: Charging Point
CPD	: Control of Power Dispatching
CRC	: Constant Rate Charging
CSCU	: Critical SCU
CS	: Charging Station
CTMC	: Continuous Time Markov Chain
CWM	: Control of Working Mode
DC	: Direct Current
DG	: Distributed Generator
DSEV	: Departure of a SEV
DUEV	: Departure of a UEV
ES	: Energy Storage
ESS	: Energy Storage System
EV	: Electric Vehicle
EVSE	: EV Supply Equipment
FCS	: Fast Charging Station
FCU	: Fast Charging User
FCU_{fast}	: Fast Rate Charging User
$FCU_{su.fast}$	: Super Fast Rate Charging User
FSEV	: A failure of SEV connected EVSE
FSM	: Finite State Machine
FUEV	: A failure of UEV connected EVSE
GTI	: Global Tilted Irradiance
HES	: Hybrid ES
IEA	: International Energy Agency
IEC	: International Electrotechnical Commission
LF	: Line Frequency
MPPT	: Maximum Power Point Tracking
MOBC	: Mobile Off-Board Chargers
MCS	: Monte-Carlo Simulation

NCSCU : Non-Critical SCU
OBC : Off-Board Chargers
OEV_E : Elastic OEV
OEV_R : Real-Time OEV
PCS : Portable Charging Station
PFC : Power Flow Control
PV : Photovoltaic
OBC : Off-Board Chargers
Q_E : Queue for OEV_E
Q_R : Queue for OEV_R
QoS : Quality of Service
QP : Queue Points
RES : Renewable Energy System
SAE : Society of Automobile Engineers
SC : Super Capacitor
SCU : Slow Charging User
SCU_{slow} : Slow Rate Charging User
SCU_{medium} : Medium Rate Charging User
SDG : Sustainable Development Goals
SoC : State of Charge
ST : State Transition
SWC : Switching Control
TR : Transition Rate
VSI : Voltage Source Inverter

P_x^{min} : Minimum charging power of x ; x ≡ p for PEVs, s for OEVs
P_c^{min} : Minimum charging power of OBC/CP
P_x^{max} : Maximum charging power of x ; x ≡ p for PEVs, s for OEVs
P_c^{max} : Maximum charging power of OBC/CP
P_x : Charging power of x ; x ≡ p for PEVs or s for OEVs c for Charger
M : Number of OBCs/CPs
λ_x : Mean arrival rate of x ; x ≡ p for PEVs, o for OEVs
λ_{oe} : Mean arrival rate of elastic OEVs
λ_{or} : Mean arrival rate of real-time OEVs
$\lambda_{SCU,slow}$: Mean arrival rate of SCU_{slow}
$\lambda_{SCU,medium}$: Mean arrival rate of SCU_{medium}
$\lambda_{FCU,fast}$: Mean arrival rate of FCU_{fast}
$\lambda_{FCU,su.fast}$: Mean arrival rate of $FCU_{su.fast}$
λ_f : Mean failure rate of an OBC
μ_c : Mean service rate of an OBC/CP
μ_r : Mean repair rate of an OBC
t_k^a : The arrival time of the kth $(k \in \mathbb{Z}^+)$ plugged-in EV
t_k^a : The plugged-in time of the kth plugged-in EV
t_k^c : The required charging time of the kth plugged-in EV
t_k^r : The remaining charging time of the kth plugged-in EV

α_k : EV user type of the kth plugged-in EV
β_k : EV index of the kth plugged-in EV
$j_s(t_k)$: Number of plugged-in PEVs at time t_k
$j_u(t_k)$: Number of plugged-in OEVs at time t_k
$j_{sa}(t_k)$: Total number of arrived PEVs at time t_k
$j_{ua}(t_k)$: Total number of arrived PEVs at time t_k
$j_q(t_k)$: Total number of queued OEVs at time t_k
$j_{ev}(t_k)$: Total number of plugged-in EVs by time t_k
$\boldsymbol{A}^{ev}_{j_{ev}(t_k)}$: Plugged-in EVs matrix at time t_k
$\boldsymbol{A}^{q}_{j_q(t_k)}$: Queued EVs matrix at time t_k
$\mathbf{x}$: Generic state of the CTMC
x_r : The number of PEVs plugged-in at FCS
x_{sk} : The number of OEVs with k aggregated CPs plugged-in at FCS
x_q : The number of queued OEVs
x_u : The number of ultra-fast OEVs plugged-in at FCS
x_{um} : The number of ultra-fast OEVs plugged-in at MOBCs
x_f : The number of PEVs plugged-in at FCS
j_e : The number of failed OBCs at FCS
j_{rk} : The number of real-time OEVs with k aggregated CPs
j_{eq} : The number of queued OEVs in Q_E
j_{rq} : The number of queued OEVs in Q_R
$a(\mathbf{x})$: The total number of CPs utilized by plugged-in EVs
$b(\mathbf{x})$: The available CPs for OEVs
$c(\mathbf{x})$: The number of CPs utilized by plugged-in OEVs
$\pi(\mathbf{x})$: The steady-state probability vector
$\mathbf{\Phi}$: The transition rate matrix
$\dot{\alpha}_{oev}$: The mean preempting rate of OEVs
$\dot{\beta}_{oev}$: The mean plugging rate of OEVs at FCS
$DL_j(t)$: Demand limit of the j^{th} CS at time t
$D(t)$: Non-EV demand profile of the distribution transformer at time t
$D_j(t)$: Non-EV demand profile of the j^{th} CS at time t
P_j^{min} : Minimum power level of the j^{th} CS
P_j^{max} : Maximum power level the j^{th} CS
$p_j(t)$: Optimum power allocation for the j^{th} CS at time t
K_{SCU} : Set of plugged-in SCUs
$\tau^k_{SCU,min}$: Minimum required charging time of k^{th} plugged-in SCU
$P_{b,oev}$: Blocking Probability of OEVs
$P_{p,oev}$: Preempting Probability of OEVs
$P_{b,oe}$: Blocking Probability of elastic OEVs
$P_{p,or}$: Preempting Probability of real-time OEVs
$\bar{t}_c$: Mean Charging Time at the FCS
$\bar{t}_{q,oev}$: Mean waiting time of OEVs
$\dot{c}$: Mean Charging Completion Rate
U : Charging Resource Utilization of the FCS

A_{pev} : Availability of PEVs
A_{oev} : Availability of OEVs
R_{pev} : Reliability of PEVs
R_{oev} : Reliability of OEVs
$H^k_{SCU}(t)$: Parking horizon of k^{th} plugged-in SCU at time t
C^k_{SCU} : Battery capacity of the k^{th} plugged-in SCU
$t^{dep,k}_{SCU}$: Departure time of the k^{th} plugged-in SCU
P_{SCU} : Charging rate of slow charging
η_{SCU} : Charging efficiency
$SoC^k_x(t)$: State of charge of k^{th} x at time t; x $\equiv$ SCU,FCU,CSCU or NCSCU
$SoC_{x,max}(t)$: Maximum SoC of x at time t; x $\equiv$ SCU,FCU,CSCU or NCSCU
$T_{CP}(t)$: Total number of occupied CPs at time t
$T_{QP}(t)$: Total number of occupied QPs at time t
$j_{scu}(t)$: Total number of plugged-in SCUs at time t
$j_{fcu}(t)$: Total number of plugged-in FCUs at time t
$j_{cscu}(t)$: Total number of plugged-in CSCUs at time t
$j_{ncscu}(t)$: Total number of plugged-in NCSCUs at time t
$j(t)$: Total number of plugged-in EVs at time t
$j_q(t)$: Total number of queued EVs at time t
$\boldsymbol{A}^{ev}_{j(t)\times n}$: Plugged-in EVs matrix at time t
$\boldsymbol{A}^{q}_{j_q(t)\times n}$: Queued EVs matrix at time t
$\boldsymbol{A}^{scu}_{j_{scu}(t)\times n}$: Plugged-in SCUs matrix at time t
$\boldsymbol{A}^{fcu}_{j_{fcu}(t)\times n}$: Plugged-in FCUs matrix at time t
$\boldsymbol{A}^{cscu}_{j_{cscu}(t)\times n}$: Plugged-in CSCUs matrix at time t
$\boldsymbol{A}^{ncscu}_{j_{ncscu}(t)\times n}$: Plugged-in NCSCUs matrix at time t
$\boldsymbol{A}^{p}_{j_p(t)\times n}$: Priority array of plugged in EVs at time t
$P_{DL}(t)$: current demand limit of the grid
$P_{x,max}$: power rating of the ES element x
x : battery-bat, SC-sc
$Ppv, mpp(t)$: current maximum power generation of the PV array
Ppv, min : minimum power generation of the PV array
$P_{grid}(t)$: current power delivery from the grid
$isd(t)$: islanding detection
$P_L(t)$: current load demand
$C_x(t)$: connection (when connected, 1 or wise-versa)
$SoC_x(t)$: current state of charge of the source x
SoC_{min} : Minimum state of charge of the source x
SoC_{max} : Maximum state of charge of the source x
$v_{DC,x}$: VSI input DC link voltage of the storage element x
$v_{DC,pv}$: VSI input DC link voltage of the PV array
$i_{abc}(t)$: current measured at the PCC of the AC bus
$i_{dq}(t)$: corresponding dq component of the $i_{abc,measured}$
$\tilde{v}_{DC,pv,ref}$: DC link reference voltage for the PV system

$\tilde{i}_{d,ref,x}$: reference direct axis current component of the x element
$\tilde{i}_{q,ref}$: reference quadrature axis current component of the x element
$\tilde{f}_{ref}$: reference system frequency
$f(t)$: measured frequency at the PCC of the AC bus
$P_{ref,x}$: active power reference value of the x element calculated at the CPD layer
$\Delta\tilde{P}_{ref,x}$: required power change of the x element to mitigate frequency fluctuations
$P_x(t)$: delivered power share of the x element
$\tilde{v}_{ref}$: reference system voltage
$v(t)$: measured voltage at the PCC of the AC bus
$Q_{ref,x}$: reactive power reference of the x element value calculated at the CPD layer
$\Delta\tilde{Q}_{ref}$: required reactive power change of the x element to mitigate voltage fluctuations
$Q_x(t)$: delivered reactive power share of the x element
$v_{abc,ref}$: 3ϕ reference voltage for PWM generator
P_0 : active power set value
f_0 : nominal frequency
k_f : frequency droop
k_p : proportional gain
T_i : integral time constant
Q_0 : reactive power set value
v_0 : nominal voltage
k_v : voltage droop
k_p : proportional gain
T_i : integral time constant

Bibliography

[1] S. Habib, M. Kamran, and U. Rashid, "Impact analysis of vehicle-to-grid technology and charging strategies of electric vehicles on distribution networks–a review," *J. Power Sources*, vol. 277, pp. 205-214, 2015

[2] Transforming Our World: The 2030 Agenda for Sustainable Development. 2021. Available online: https://sdgs.un.org/2030agenda (accessed on 18 July 2022).

[3] Z. Darabi and M. Ferdowsi, "Aggregated Impact of Plug-in Hybrid Electric Vehicles on Electricity Demand Profile," *IEEE Trans. Sustain. Energy*, vol. 2, no. 4, pp. 501-508, Oct. 2011.

[4] Global EV Outlook 2021, IEA, Paris, 2021, Accessed : Nov. 10, 2021. [online] Available://www.iea.org/reports/global-ev-outlook-2021.

[5] Z. P. Cano et al., "Batteries and fuel cells for emerging electric vehicle markets, " *Nature Energy*, vol. 3, no. 4, pp. 279, 2018

[6] T. Muneer, M. Kolhe and A. Doyle, Electric Vehicles: Prospects and Challenges, Elsevier, 2017.

[7] M. Keyser et al., "Enabling fast charging–battery thermal considerations," *J. Power Sources*, vol. 367, pp. 228-236, Nov. 2017.

[8] S. Ahmed et al., "Enabling fast charging—A battery technology gap assessment," *J. Power Sources*, vol. 367, pp. 250-262, Nov. 2017.

[9] I. Aretxabaleta, I. M. De Alegría, J. Andreu, I. Kortabarria and E. Robles, "High-Voltage Stations for Electric Vehicle Fast-Charging: Trends, Standards, Charging Modes and Comparison of Unity Power-Factor Rectifiers,"*IEEE Access*, vol. 9, pp. 102177-102194, 2021.

[10] P. Fan, B. Sainbayar and S. Ren, "Operation Analysis of Fast Charging Stations With Energy Demand Control of Electric Vehicles," *IEEE Trans. Smart Grid*, vol. 6, no. 4, pp. 1819-1826, Jul. 2015.

[11] "*Electric vehicle conductive charging system - Part 1: General requirements*",IEC 61851-1:2017 , pp. 1, Feb. 2017.

[12] L. Liu, F. Kong, X. Liu, Y. Peng, and Q. Wang, "A review on electric vehicles interacting with renewable energy in smart grid," *Renew. Sust. Energ. Rev.*, vol. 51, pp. 648–661, Nov. 2015.

[13] "*SAE Electric Vehicle and Plug in Hybrid Electric Vehicle Conductive Charge Coupler*", SAE, J1772, pp. 1, Oct. 2017.

[14] Y. Zheng, S. Niu, Y. Shang, Z. Shao, and L. Jian, "Integrating plugin electric vehicles into power grids: A comprehensive review on power interaction mode, scheduling methodology and mathematical foundation," *Renew. Sust. Energ. Rev.*, vol. 112, pp. 424–439, Sep. 2019.

[15] Protocol Development: Constantly Evolving with the market, Accessed : Nov. 10, 2021. [online] Available:https://www.chademo.com/activities/protocol-development

[16] "*Plugs, Socket-Outlets, Vehicle Connectors and Vehicle Inlets—Conductive Charging of Electric Vehicles—Part 3: Dimensional Compatibility and Interchangeability Requirements for D.C. and A.C./D.C. Pin and Contact-Tube Vehicle Couplers*",IEC, 62196-3:2014, pp. 1, Jun. 2014.

[17] H. Tu, H. Feng, S. Srdic and S. Lukic, "Extreme Fast Charging of Electric Vehicles: A Technology Overview," *IEEE Trans. Transp. Electrif.*, vol. 5, no. 4, pp. 861-878, Dec. 2019

[18] N. I. Nimalsiri, C. P. Mediwaththe, E. L. Ratnam, M. Shaw, D. B. Smith and S. K. Halgamuge, "A Survey of Algorithms for Distributed Charging Control of Electric Vehicles in Smart Grid," *IEEE Trans. Intell. Transp. Syst.*, vol. 21, no. 11, pp. 4497-4515, Nov. 2020.

[19] M.A. Hannan, M.M. Hoque, A. Hussain, Y. Yusof, P.J. Ker, "State-of-the-art and energy management system of lithium-ion batteries in electric vehicle applications: Issues and recommendations," *IEEE Access*, vol. 6, no. 4, pp. 19362-19378, 2018.

[20] U.K. Das, P. Shrivastava, K.S. Tey, M.Y.I.B. Idris, S. Mekhilef, E. Jamei, M. Seyedmahmoudian, A. Stojcevski, "Advancement of lithium-ion battery cells voltage equalization techniques: A review," *Renew. Sustain. Energy Rev.*, vol. 134, pp. 110227, 2020.

[21] Z.P. Cano, D. Banham, S. Ye, A. Hintennach, J. Lu, M. Fowler, Z. Chen, "Batteries and fuel cells for emerging electric vehicle markets," *Nat. Energy*, vol. 3, pp. 279-289, Nov. 2018.

[22] L. Wang, Z. Qin, T. Slangen, P. Bauer and T. van Wijk, "Grid Impact of Electric Vehicle Fast Charging Stations: Trends, Standards, Issues and Mitigation Measures - An Overview," *IEEE Open Journal of Power Electronics*, vol. 2, pp. 56-74, 2021.

[23] K. J. Dyke, N. Schofield, and M. Barnes, "The Impact of Transport Electrification on Electrical Networks," *IEEE Trans. Ind. Electron.*, vol. 57, no. 12, pp. 3917-3926, Dec. 2010.

[24] S. Deilami, A. S. Masoum, P. S. Moses and M. A. S. Masoum, "Real-Time Coordination of Plug-In Electric Vehicle Charging in Smart Grids to Minimize Power Losses and Improve Voltage Profile," *IEEE Trans. Smart Grid*, vol. 2, no. 3, pp. 456-467, Sept. 2011.

[25] Shang, Y.; Liu, M.; Shao, Z.; Jian, L. Internet of smart charging points with photovoltaic Integration: A high-efficiency scheme enabling optimal dispatching between electric vehicles and power grids. *Appl. Energy*, vol. 278, pp. 115-140, 2020.

[26] S. Deilami, A. S. Masoum, P. S. Moses and M. A. S. Masoum, "Real-Time Coordination of Plug-In Electric Vehicle Charging in Smart Grids to Minimize Power Losses and Improve Voltage Profile," *IEEE Trans. Smart Grid*, vol. 2, no. 3, pp. 456-467, Sep. 2011.

[27] I. Aretxabaleta, I. M. De Alegría, J. Andreu, I. Kortabarria and E. Robles, "High-Voltage Stations for Electric Vehicle Fast-Charging: Trends, Standards, Charging Modes and Comparison of Unity Power-Factor Rectifiers," *IEEE Access*, vol. 9, pp. 102177-102194, Jun. 2021.

[28] N. Rotering and M. Ilic, "Optimal Charge Control of Plug-In Hybrid Electric Vehicles in Deregulated Electricity Markets," *IEEE Trans. Power Syst.*, vol. 26, no. 3, pp. 1021-1029, Aug. 2011.

[29] M. A. H. Rafi and J. Bauman, "A Comprehensive Review of DC Fast-Charging Stations With Energy Storage: Architectures, Power Converters, and Analysis," *IEEE Trans. Transp. Electrif.*, vol. 7, no. 2, pp. 345-368, Jun. 2021.

[30] K. M. S. Y. Konara, M. L. Kolhe and A. Sharma,"Power Dispatching Techniques as a Finite State Machine for a Standalone Photovoltaic System with a Hybrid Energy Storage," *AIMS Energy*, vol. 8, no. 2, pp. 214-230, Feb. 2020.

[31] K. M. S. Y. Konara, M.L. Kolhe and A. Sharma, "Power Flow Management Controller within a Grid Connected Photovoltaic Based Active Generator as a Finite State Machine using Hierarchical Approach with Droop Characteristics," *Renew. Energ.*, vol. 155, pp. 1021-1031, Aug. 2020.

[32] C. Luo, Y. Huang and V. Gupta, "Placement of EV Charging Stations—Balancing Benefits Among Multiple Entities," *IEEE Trans. Smart Grid*, vol. 8, no. 2, pp. 759-768, March 2017.

[33] S. R. Etesami, W. Saad, N. B. Mandayam and H. V. Poor, "Smart routing in smart grids," in *Proc. IEEE Conference on Decision and Control (CDC)*, Dec. 2017.

[34] Z. Sun, X. Zhou, J. Du and X. Liu, "When traffic flow meets power flow: On charging station deployment with budget constraints," *IEEE Trans. Veh. Technol.*, vol. 66, no. 4, pp. 2915-2926, Apr. 2017.

[35] H. Zhang, S. J. Moura, Z. Hu and Y. Song, "PEV fast-charging station siting and sizing on coupled transportation and power networks," *IEEE Trans. Smart Grid*, vol. 9, no. 4, pp. 2595-2605, Jul. 2018.

[36] A. Burnham et al., "Enabling fast charging—Infrastructure and economic considerations," *J. Power Sources*, vol. 367, pp. 237-249, Nov. 2017.

[37] M. E. Kabir, C. Assi, H. Alameddine, J. Antoun and J. Yan, "Demand Aware Deployment and Expansion Method for an Electric Vehicles Fast Charging Network," in *Proc. IEEE International Conference on Communications, Control, and Computing Technologies for Smart Grids (SmartGridComm)*, 2019.

[38] M. E. Kabir, C. Assi, H. Alameddine, J. Antoun and J. Yan, "Demand-Aware Provisioning of Electric Vehicles Fast Charging Infrastructure," *IEEE Trans. Veh. Technol.*, vol. 69, no. 7, pp. 6952-6963, Jul. 2020.

[39] A. Shukla, K. Verma and R. Kumar, "Planning of Fast Charging Stations in Distribution System Coupled with Transportation Network for Capturing EV flow," in *Proc. 8th IEEE India International Conference on Power Electronics (IICPE)*, 2018.

[40] , V. Radulovic and B. Lutovac, "Efficient placement of electric vehicles charging stations using integer linear programming," *Adv. Electr. Comput. Eng.*, vol. 18, no. 2, pp. 11-16, 2018.

[41] A. A. Iqbal, I. Ashraf, M. Marzband, I. khan, "Optimal location of electric vehicle charging station and its impact on distribution network: A review," *Energy Reports*, vol. 8, pp. 2314-2333, 2022.

[42] A. Shukla, K. Verma and R. Kumar, "Consumer perspective based placement of electric vehicle charging stations by clustering techniques, " in *Proc. National Power Systems Conference (NPSC)*, 2016.

[43] H. Parastvand, V. Moghaddam, O. Bass, M. A. S. Masoum, A. Chapman and S. Lachowicz, "A Graph Automorphic Approach for Placement and Sizing of Charging Stations in EV Network Considering Traffic," *IEEE Trans. Smart Grid*, vol. 11, no. 5, pp. 4190-4200, Sept. 2020.

[44] Y. Xiong, J. Gan, B. An, C. Miao and A. L. C. Bazzan, "Optimal electric vehicle fast charging station placement based on game theoretical framework," *IEEE Trans. Intell. Transp. Syst.*, vol. 19, no. 8, pp. 2493-2504, Aug. 2018.

[45] E. Ucer, I. Koyuncu, M. C. Kisacikoglu, M. Yavuz, A. Meintz and C. Rames, "Modeling and Analysis of a Fast Charging Station and Evaluation of Service

Quality for Electric Vehicles," *IEEE Trans. Transp. Electrif.*, vol. 5, no. 1, pp. 215-225, Mar. 2019

[46] X. Gan, H. Zhang, G. Hang, Z. Qin and H. Jin, "Fast-Charging Station Deployment Considering Elastic Demand," *IEEE Trans. Transp. Electrif.*, vol. 6, no. 1, pp. 158-169, Mar. 2020

[47] C. Li, Y. Shan, L. Zhang, L. Zhang, R. Fu, "Techno-economic evaluation of electric vehicle charging stations based on hybrid renewable energy in China, " *Strategy Reviews*, vol. 41, no. 1, pp. 100850, 2022.

[48] S. Negarestani, M. Fotuhi-Firuzabad, M. Rastegar and A. Rajabi-Ghahnavieh, "Optimal Sizing of Storage System in a Fast Charging Station for Plug-in Hybrid Electric Vehicles," *IEEE Trans. Transp. Electrif.*, vol. 2, no. 4, pp. 443-453, Dec. 2016.

[49] P. Fan, B. Sainbayar and S. Ren, "Operation Analysis of Fast Charging Stations With Energy Demand Control of Electric Vehicles," *IEEE Trans. Smart Grid*, vol. 6, no. 4, pp. 1819-1826, Jul. 2015.

[50] L. Liu, F. Kong, X. Liu, Y. Peng, and Q. Wang, "A review on electric vehicles interacting with renewable energy in smart grid," *Renew. Sust. Energ. Rev.*, vol. 51, pp. 648–661, Nov. 2015.

[51] J. C. Mukherjee and A. Gupta, " Review of Charge Scheduling of Electric Vehicles in Smart Grid," *IEEE Syst. J.*, vol. 9, no. 4, pp. 1541-1553, Dec. 2015.

[52] Z. Xu, W. Su, Z. Hu, Y. Song and H. Zhang, "A Hierarchical Framework for Coordinated Charging of Plug-In Electric Vehicles in China," *IEEE Trans. Smart Grid*, vol. 7, no. 1, pp. 428-438, Jan. 2016.

[53] Z. Xu, Z. Hu, Y. Song, W. Zhao and Y. Zhang, "Coordination of PEVs charging across multiple aggregators," *Appl. Energy*, vol. 136, pp. 582-589, Dec. 2014.

[54] T. Zhao, Y. Li, X. Pan, P. Wang and J. Zhang, "Real-Time Optimal Energy and Reserve Management of Electric Vehicle Fast Charging Station: Hierarchical Game Approach," *IEEE Trans. Smart Grid*, vol. 9, no. 5, pp. 5357-5370, Sept. 2018

[55] D. Wu, C. D. Aliprantis and L. Ying, "Load scheduling and dispatch for aggregators of plug-in electric vehicles," *IEEE Trans. Smart Grid*, vol. 3, no. 1, pp. 368-376, Mar. 2012.

[56] W. Qi, Z. Xu, Z.-J. M. Shen, Z. Hu and Y. Song, "Hierarchical coordinated control of plug-in electric vehicles charging in multifamily dwellings," *IEEE Trans. Smart Grid*, vol. 5, no. 3, pp. 1465-1474, May 2014.

[57] J. Liu, G. Lin, S. Huang, Y. Zhou, Y. Li and C. Rehtanz, "Optimal EV Charging Scheduling by Considering the Limited Number of Chargers," *IEEE Trans. Transp. Electrif.*, vol. 7, no. 3, pp. 1112-1122, Sept. 2021

[58] L. Yao, W. H. Lim and T. S. Tsai, "A Real-Time Charging Scheme for Demand Response in Electric Vehicle Parking Station," *IEEE Trans. Smart Grid*, vol. 8, no. 1, pp. 52-62, Jan. 2017

[59] S. Vandael, B. Claessens, M. Hommelberg, T. Holvoet and G. Deconinck, "A Scalable Three-Step Approach for Demand Side Management of Plug-in Hybrid Vehicles," *IEEE Trans. Smart Grid*, vol. 4, no. 2, pp. 720-728, June 2013, doi: 10.1109/TSG.2012.2213847.

[60] A. Molderink, V. Bakker, M. G. C. Bosman, J. L. Hurink and G. J. M. Smit, "Management and control of domestic smart grid technology," *IEEE Trans. Smart Grid*, vol. 1, no. 2, pp. 109-119, Sep. 2010

[61] L. Gan, U. Topcu and S. H. Low, "Optimal decentralized protocol for electric vehicle charging," *IEEE Trans. Power Syst.*, vol. 28, no. 2, pp. 940-951, May 2013.

[62] J. C. Mukherjee and A. Gupta, "Distributed charge scheduling of plug-in electric vehicles using inter-aggregator collaboration," *IEEE Trans. Smart Grid*, vol. 8, no. 1, pp. 331-341, Jan. 2017.

[63] N. Rahbari-Asr and M. -Y. Chow, "Cooperative Distributed Demand Management for Community Charging of PHEV/PEVs Based on KKT Conditions and Consensus Networks," *IEEE Trans. Industr. Inform.*, vol. 10, no. 3, pp. 1907-1916, Aug. 2014, doi: 10.1109/TII.2014.2304412.

[64] Z. Xu, Z. Hu, Y. Song, W. Zhao and Y. Zhang, "Coordination of PEVS charging across multiple aggregators," *Appl. Energy*, vol. 136, pp. 582-589, Dec. 2014.

[65] C. Jin, J. Tang and P. Ghosh, "Optimizing Electric Vehicle Charging With Energy Storage in the Electricity Market," *IEEE Trans. Smart Grid*, vol. 4, no. 1, pp. 311-320, March 2013.

[66] H. M. Chung, S. Maharjan, Y. Zhang and F. Eliassen, "Intelligent Charging Management of Electric Vehicles Considering Dynamic User Behavior and Renewable Energy: A Stochastic Game Approach," *IEEE Trans. Intell. Transp. Syst.*, vol. 22, no. 12, pp. 7760-7771, Dec. 2021.

[67] S. S. Fazeli, S. Venkatachalam, R. B. Chinnam and A. Murat, "Two-Stage Stochastic Choice Modeling Approach for Electric Vehicle Charging Station Network Design in Urban Communities," *IEEE Transactions on Intell. Transport. Syst.*, vol. 22, no. 5, pp. 3038-3053, May 2021

[68] Y. Zhou, R. Kumar and S. Tang, "Incentive-Based Distributed Scheduling of Electric Vehicle Charging Under Uncertainty," *IEEE Trans. Power Syst.*, vol. 34, no. 1, pp. 3-11, Jan. 2019.

[69] Y. Yu, O. S. Nduka, F. U. Nazir and B. C. Pal, "A Three-Stage Stochastic Framework for Smart Electric Vehicle Charging," *IEEE Access*, vol. 11, pp. 655-666, 2023.

[70] K. M. S. Y. Konara and M. L. Kolhe, " Priority Based Coordinated Electric Vehicle Charging System for Heterogeneous Traffic," in *Proc. 2020* 5^{th} *International Conference on Smart and Sustainable Technologies (SpliTech)*, pp. 1-6

[71] S. Wang, S. Bi, Y. A. Zhang and J. Huang, "Electrical Vehicle Charging Station Profit Maximization: Admission, Pricing, and Online Scheduling," *IEEE Trans. Sustain. Energy*, vol. 9, no. 4, pp. 1722-1731, Oct. 2018

[72] Z. Moghaddam, I. Ahmad, D. Habibi and Q. V. Phung, "Smart Charging Strategy for Electric Vehicle Charging Stations," *IEEE Trans. Transp. Electrif.*, vol. 4, no. 1, pp. 76-88, March 2018

[73] H. M. Abdullah, A. Gastli and L. Ben-Brahim, "Reinforcement Learning Based EV Charging Management Systems–A Review," *IEEE Access*, vol. 9, pp. 41506-41531, 2021.

[74] L. Yan, X. Chen, J. Zhou, Y. Chen and J. Wen, "Deep Reinforcement Learning for Continuous Electric Vehicles Charging Control With Dynamic User Behaviors," *IEEE Trans. Smart Grid*, vol. 12, no. 6, pp. 5124-5134, Nov. 2021.

[75] T. Ding, Z. Zeng, J. Bai, B. Qin, Y. Yang and M. Shahidehpour, "Optimal Electric Vehicle Charging Strategy With Markov Decision Process and Reinforcement Learning Technique," *IEEE Trans. Ind. Appl.*, vol. 56, no. 5, pp. 5811-5823, Sept.-Oct. 2020.

[76] L. Yan, X. Chen, Y. Chen and J. Wen, "A Cooperative Charging Control Strategy for Electric Vehicles Based on Multiagent Deep Reinforcement Learning," *IEEE Trans. Industr. Inform.*, vol. 18, no. 12, pp. 8765-8775, Dec. 2022.

[77] K.M.S.Y. Konara, M.L. Kolhe, "Priority Based Coordinated Electric Vehicle Charging System for Heterogeneous Traffic," in *Proc. 5th International Conference on Smart and Sustainable Technologies (SpliTech)*, Split, Croatia, 23-26 September 2020.

[78] Konara, K.M.S.Y.; Kolhe, M.L. Queue Based Dynamic Charging Resource Allocation and Coordination for Heterogeneous Traffic in an Electrical Vehicle Charging Station, *Energy Sources Part A Recover. Util. Environ. Eff.*, pp. 1-18, 2021, doi.org/10.1080/15567036.2021.1974983

[79] Q. Yang, S. Sun, S. Deng, Q. Zhao and M. Zhou, "Optimal Sizing of PEV Fast Charging Stations With Markovian Demand Characterization," *IEEE Trans. Smart Grid*, vol. 10, no. 4, pp. 4457-4466, July 2019.

[80] Y. -K. Wu, J. -H. Lin and H. -J. Lin, "Standards and Guidelines for Grid-Connected Photovoltaic Generation Systems: A Review and Comparison," *IEEE Trans. Ind. Appl.*, vol. 53, no. 4, pp. 3205-3216, July-Aug. 2017.

[81] H. Fakham, D. Lu and B. Francois, "Power Control Design of a Battery Charger in a Hybrid Active PV Generator for Load-Following Applications," *IEEE Trans. Ind. Electron.*, vol. 58, no. 1, pp. 85-94, Jan. 2011.

[82] M. H. Nehrir et al., "A Review of Hybrid Renewable/Alternative Energy Systems for Electric Power Generation: Configurations, Control, and Applications," *IEEE Trans Sustain Energy*, vol. 2, no. 4, pp. 392-403.

[83] J. Skea, D. Anderson, T. Green, R. Gross, P. Heptonstall, M. Leach, "Intermittent Renewable Generation and Maintaining Power System Reliability," *IET Gener. Transm. Distrib.* vol. 2 no. 1, pp. 82-89, 2008.

[84] S. Mei, R. Li, X. Xue, Y. Chen, Q. Lu, X. Chen, C. D. Ahrens, R. Li, L. Chen, "Paving the Way to Smart Micro Energy Grid: Concepts, Design Principles, and Engineering Practices," *CSEE Journal of Power and Energy Systems*, vol. 3 no. 4, pp. 440-449, 2017.

[85] R. Teodorescu, 470 M. Liserre, P. Rodrguez, Grid Converters for Photovoltaic and Wind Power Systems, John Wiley & Sons, Ltd, 2011.

[86] D. P. Kothari, I. J. Nagrath, Modern Power System Analysis, New Delhi :Tata McGraw-Hill Pub. Co., 2003.

[87] S. Adhikari, F. Li and H. Li, "P-Q and P-V Control of Photovoltaic Generators in Distribution Systems," *IEEE Trans. Smart Grid*, vol. 6, no. 6, pp. 2929-2941, Nov. 2015.

[88] A. N. Azmi, M. L. Kolhe, Photovoltaic Based Active Generator: Energy Control System Using State Flow Analysis, in *Proc. IEEE 11th International Conference on Power Electronics and Drive Systems*, pp. 18-22, 2015.

[89] L. Collins, J. K. Ward, "Real and reactive power control of distributed PV inverters for overvoltage prevention and increased renewable generation hosting capacity," *Renewable Energy* vol. 81, pp. 464-471, 2015.

[90] J. Qiu, K. Sun, T. Wang and H. Gao, "Observer-Based Fuzzy Adaptive Event-Triggered Control for Pure-Feedback Nonlinear Systems With Prescribed Performance," *IEEE Trans. Fuzzy Syst.* , vol. 27, no. 11, pp. 2152-2162, Nov. 2019.

[91] D. Lu, H. Fakham, T. Zhou, B. Francois, Application of Petri nets for the energy management of a photovoltaic based power station including storage units, *Renewable Energy*, vol. 35 no. 6, pp.1117-1124, 2010.

[92] M. A. M. Yassin, M. Kolhe, A. Sharma, S. Garud, Battery Capacity Estimation for Building Integrated Photovoltaic System: Design Study for Different Geographical Location(s), *Energy Procedia*, vol. 142, pp. 3433-3439, 2017.

[93] M. A. M. Yassin, M. L. Kolhe, A. N. Azmi, Battery capacity estimation for tbuilding-integrated photovoltaic system: Design study of a Southern Norway ZEB house, in *Proc. IEEE PES Innovative Smart Grid Technologies Conference Europe (ISGT-Europe)*, pp. 1-6, 2017.

[94] K. M. S. Y. Konara, M. L. Kolhe, A. Sharma, Load Compensator with an Energy Storage for a Grid Connected PV Based Active Generator, IOP Conf. Ser.: Mater. Sci. Eng. 605 2019, pp. 1-8.